EFFICIENT NONLINEAR OPTIMIZATION WITH RIGOROUS MODELS FOR LARGE SCALE INDUSTRIAL CHEMICAL PROCESSES

A Dissertation

by

YU ZHU

Submitted to the Office of Graduate Studies of
Texas A&M University
in partial fulfillment of the requirements for the degree of

DOCTOR OF PHILOSOPHY

May 2011

Major Subject: Chemical Engineering

EFFICIENT NONLINEAR OPTIMIZATION WITH RIGOROUS MODELS FOR LARGE SCALE INDUSTRIAL CHEMICAL PROCESSES

A Dissertation

by

YU ZHU

Submitted to the Office of Graduate Studies of
Texas A&M University
in partial fulfillment of the requirements for the degree of

DOCTOR OF PHILOSOPHY

Approved by:

Chair of Committee,	Carl Laird
Committee Members,	Juergen Hahn
	Mahmoud El-Halwagi
	Mahboohul Mannan
	Sergiy Butenko
Head of Department,	Michael Pishko

May 2011

Major Subject: Chemical Engineering

ABSTRACT

Efficient Nonlinear Optimization with Rigorous Models
for Large Scale Industrial Chemical Processes. (May 2011)
Yu Zhu, B.S., Zhejiang University;
M.S., Zhejiang University;
M.Eng., Texas A&M University
Chair of Advisory Committee: Dr. Carl Laird

Large scale nonlinear programming (NLP) has proven to be an effective framework for obtaining profit gains through optimal process design and operations in chemical engineering. While the classical SQP and Interior Point methods have been successfully applied to solve many optimization problems, the focus of both academia and industry on larger and more complicated problems requires further development of numerical algorithms which can provide improved computational efficiency.

The primary purpose of this dissertation is to develop effective problem formulations and an advanced numerical algorithms for efficient solution of these challenging problems. As problem sizes increase, there is a need for tailored algorithms that can exploit problem specific structure. Furthermore, computer chip manufacturers are no longer focusing on increased clock-speeds, but rather on hyperthreading and multi-core architectures. Therefore, to see continued performance improvement, we must focus on algorithms that can exploit emerging parallel computing architectures. In this dissertation, we develop an advanced parallel solution strategy for nonlinear programming problems with block-angular structure. The effectiveness of this and modern off-the-shelf tools are demonstrated on a wide range of problem classes.

Here, we treat optimal design, optimal operation, dynamic optimization, and parameter estimation. Two case studies (air separation units and heat-integrated

columns) are investigated to deal with design under uncertainty with rigorous models.

For optimal operation, this dissertation takes cryogenic air separation units as a primary case study and focuses on formulations for handling uncertain product demands, contractual constraints on customer satisfaction levels, and variable power pricing. Multiperiod formulations provide operating plans that consider inventory to meet customer demands and improve profits.

In the area of dynamic optimization, optimal reference trajectories are determined for load changes in an air separation process. A multiscenario programming formulation is again used, this time with large-scale discretized dynamic models.

Finally, to emphasize a different decomposition approach, we address a problem with significant spatial complexity. Unknown water demands within a large scale city-wide distribution network are estimated. This problem provides a different decomposition mechanism than the multiscenario or multiperiod problems; nevertheless, our parallel approach provides effective speedup.

To my family

ACKNOWLEDGMENTS

First of all, I would like to express my greatest gratitude to my advisor, Dr. Carl Laird, for providing me a wonderful opportunity to conduct this interesting research. I also thank him for his thoughtful advice throughout the work. He has been my role model for a successful researcher with dedication and passion on both research and teaching. His insights and perception on novel approaches inspired me tremendously. It was my great pleasure to work with him.

I also would like to acknowledge the helpful comments and advice I received from my committee members: Dr. Juergen Hahn, Dr. Mahmoud El-Halwagi, Dr. M. Sam Mannan from the Chemical Engineering (ChE) Department and Dr. Sergiy Butenko from the Industrial and Systems Engineering (ISE) Department.

In addition to my PhD study, I am pursuing my Masters degree in Industrial Engineering. I would like to acknowledge all of the people helping me on transferring between different departments. They are Dr. Daniel Shantz (ChE), Towanna Arnold (ChE), Dr. Guy Curry (ISE), Judy Meeks (ISE), Andrea Reinertson (OGS), and Marisa Ernst(ISS). Without their help, I could not pursue two major degrees simultaneously.

Bill Morrison, Kiran Sheth, Tyler Soderstrom, Yang Zhang, John Hedengren Carl Schwanke, Jitendra Kadam, Tonya Donatto, and Weijie Lin deserve special thanks, as does my boss and my colleagues when I interned at the Core Process Control Department of ExxonMobil Chemicals in Baytown Texas, USA. In particular, I would like to thank Bill and Tonya for their kind help and support. I thank Kiran and Tyler for their technical guidance and advice, and thank Yang, John, Carl, Jitendra and Weijie for our inspiring discussions. They have helped me to understand the many challenges that arise in industrial practice.

During the summer of 2010, I had the opportunity to work for Bayer AG, in Baytown Texas, USA as an intern in the Process Dynamics & Optimization Group. I would like to acknowledge Shoujun Bian, Samrat Mukherjee, David Chen, Xiangmin Hua, Doug Klenke, Randy Garabedian and Ajay Singh for their kind help during my internship. All of them provided me important experience on the application of advanced control solutions in operational plants.

From September 2010 to November 2010, I worked for Modelon AB in Lund, Sweden as a research intern with Hubertus Tummescheit, Johan Åkesson, Katrin Prolss, and Stephane Velut. This internship experience broadened my perspective on the advanced modeling and optimization. I would like to thank them for extensive discussions and strong encouragement on interesting research projects. It was an amazing experience in self improvement.

I would like to acknowledge all of the past and present members of Dr. Laird's group: Ahmed Rabie, George Abbott III, German Oliveros, Jaime Tellez, James Young, Scott Kolodziej, Kristen Young, Derrick Thomas, Angelica Wong, Brandon Barrera, Daniel Word, Sean Legg, Jia Kang, and Gabe Hackebeil. I do cherish the happy time we had together. And thank them for making my office hours so enjoyable. In addition, I am indebted to my peer colleagues, Chuili Sun, Yunfei Chu, Cheryl Qu, Zuyi Huang, Mitch Serpas, Loveleena Bansal, Shreya Maiti, Buping Bao, Fuman Zhao, Nan Shi, Xin Jin, Rongbing Han, Qingqing Wang, Qun Ma, Xin Qu, Peng Lian, Yuan Lu, Xiaole Yang, Ruifeng Qi, Qingsheng Wang, and Peng He. I thank them for providing a stimulating and fun environment where I could learn and grow up.

Finally, and most important, I must thank my parents Benxian Zhu and Jianling Wang, as well as my wife, Yue Wang, for their unflagging love and support. Without their support and encouragement, this dissertation would have simply been impossible

and I could not have come this far. It is to them I dedicate my dissertation.

TABLE OF CONTENTS

CHAPTER Page

CHAPTER Page

Page

LIST OF TABLES

LIST OF FIGURES

FIGURE Page

FIGURE Page

CHAPTER I

INTRODUCTION

The objective of this dissertation is to develop powerful nonlinear programming algorithms and to solve complicated optimization problems arising from large-scale chemical engineering processes. In this chapter, we describe the overall motivation and challenges on when determining optimal decisions of chemical processes with rigorous first-principle models and developing nonlinear programming approach. In addition, we introduce background information and terminology used throughout this dissertation.

A. Nonlinear Optimization with Rigorous Large Scale Models

With growing appreciation of large-scale rigorous models which are based on first principles, nonlinear optimization has also become an effective tool to obtain profit gain through process design and operations in chemical and petroleum industries.

Large scale rigorous nonlinear models are preferred and often required due to three main considerations. The first reason is non-linearity of the chemical process itself. Highly nonlinear behaviors are well known characteristics in most chemical processes. In models of reaction units or separation units, fundamental principles including complex phase and reaction equilibrium, hydraulics, as well as mass and energy balances, are often governed by highly nonlinear equations. In many cases, linear models can not capture process behavior completely and accurately, resulting in large mismatch between the model and plant. Secondly, increasing market competitions drive modern petroleum, chemical and gas companies to pursue the higher

---

The journal model is *IEEE Transactions on Automatic Control.*

profitability of their plants and meet better customer satisfaction. Companies not only focus on stable production and operation as before, but also desire fast, timely response to market changes. Market changes include product demands and prices, material prices and customer satisfaction, and environmental regulations. Therefore, it is necessary to include more and more market information into large scale rigorous models. The third reason concerns the range of model validity. Although data-drive models are still used in many applications, the most important advantage of rigorous first principle models is their large range of validity. For example, the models identified by step or impulse responses can be adopted in dynamic control applications. However, such identified models are not suitable and reliable for optimal design and planning problems.

Optimization (the inverse problem) is more challenging than simulation (the forward problem), and state of the act simulation models are usually more complex than those used for optimization. However, the requirement of optimal decision making for complicated chemical process design and operations seriously pushes the demands to adopt rigorous models in optimization problems, and our desire is to close this gap. With the development of nonlinear optimization algorithms and continuously increasing computing power, it is more and more possible for us to obtain reliable optimal solutions from rigorous mathematical formulations.

B. Chemical Applications of Nonlinear Optimization

There are several important applications of nonlinear optimization in the chemical engineering field. The interaction and relationship among some of these applications is given in Figure 1. Several case studies from these application areas are selected in this dissertation in order to show how to efficiently solve large scale nonlinear

optimization problems with rigorous models.

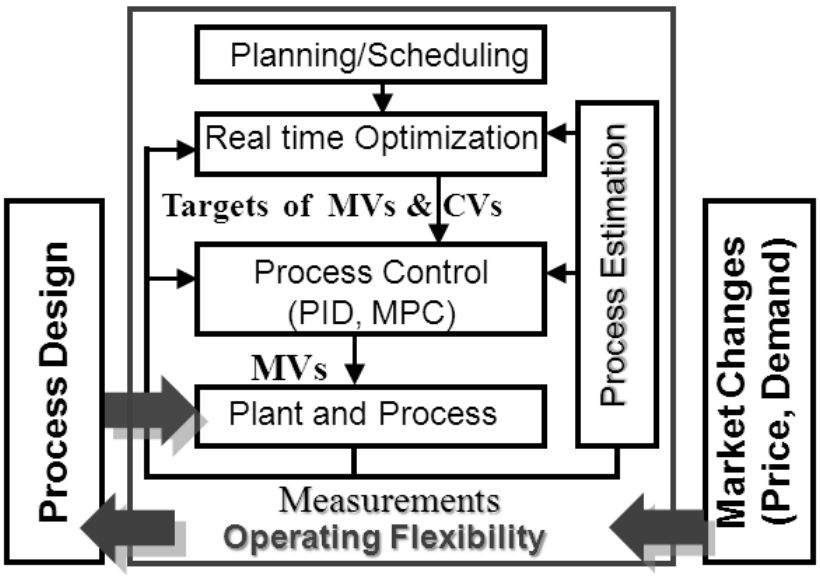

Fig. 1. Nonlinear Optimization Applications in Chemical Engineering

1. Design under Uncertainty

At the design stage, engineers not only focus on the unit structure and cost, must consider how increasing flexibility of operation can affect future operations (especially given significant uncertainty).Before a process design can be started, the design problem must be formulated, which asks for a product specification. After the product design, process design addresses how to transform raw materials into desired chemical products using the most suitable process structures and operating parameters. Traditional process design assumes the process operating capacity stays in a narrow range. However, in modern market-oriented design and operating problems, increased flexibility of the process is required to make fast operating changes. Increasing operating flexibility asks process designers to take market uncertainty into account [1]. Without rigorous consideration of uncertainty at the design stage, process flexibility is limited

and the plant may not effectively handle exogenous disturbances (e.g. changes in products demands and prices as well as raw material prices).

In order to handle potential uncertainties at design stage, the traditional approach is to design the process according to nominal values of the uncertain parameters and then apply empirical overdesign factors. However, this method may not be reliable and can lead to infeasible designs. It is certainly not guaranteed to be optimal. Instead of the traditional overdesign method, nonlinear optimization can be adopted to rigorously treat uncertainties. The main goal of the optimal design problem is to determine optimal values of the desire variables, minimize or maximize the expected value of economic function over the uncertainty space, maintain feasibility over the the uncertainty space, and ensure customer satisfaction. This can be treated with both probabilistic constraints and multiscenario formulations. In the later chapter of this dissertation, we discuss how to deal with different kinds of uncertain factors and obtain optimal design solutions for large scale chemical processes.

2. Optimal Operations with Steady State Models

After the design stage, the structures of processes and some process parameters are fixed during the operation stage. This stage can be separated into several parts. The top part is the planning and scheduling layer, which makes long-term decisions like which products to produce, when and how to produce, then how to control inventory level, in order to earn profit and maintain customer satisfaction. Forecasts of market information like product demands and prices are used to obtain best estimation of the optimal decisions for future operations (years/months/weeks). Because this layer has a strong relationship with market, it is very important for managers and engineers to make planning and scheduling decisions with consideration of various customer satisfactions and uncertain market factors. These high-level decisions are often made

using linear models. However, such linear models can not capture detailed process interactions. Poor planning/scheduling decisions may challenge lower-level practical operation due to both inaccurate market forecast and inaccuracies from linear black-box process models.

Instead of linear black-box process models, rigorous nonlinear models can be adopted to provide more accurate information of process behaviors. All the operational planning and real-time optimization using steady state models are typically imposed. However, prices of raw materials, energy, and products can change frequently. Correspondingly, product demands may also change. Due to external markets, process inputs and requirements are subject to both variability and uncertainty. It is necessary to consider these factors and often multiperiod problem formulations are used.

Furthermore, the conflicts between customer satisfaction and profitability should also be taken into account. if we only focus on high short-term profit and ignore customer satisfaction, nonlinear optimization problems do not need to include constraints from customer satisfactions and the plant profit can be maximized. As time goes by, we may lose customers or violate contracts because their demands can not be adequately satisfied. In order to handle uncertain product demands from customers and guarantee high customer satisfaction, sufficient inventory levels have to be kept. However, it is undesirable from a cost perspective to keep high inventory levels. Therefore, multiperiod optimization formulations can be solved to maximize profits while maintaining contractual obligations. These formulations provide managers with the tools necessary to evaluate the trade-off between short-term profitability and customer satisfaction in this level.

In this dissertation, we adopt nonlinear programming formulations with rigorous models to handle energy cost variability and uncertainty in product demands with

multiperiod inventory planning.

3. Real Time Optimization and Control

Real-time optimization (RTO) is the next layer which follows the planning and scheduling layer. The objective of the RTO is to maximize economic performance of the plant by seeking the detailed optimal operating conditions, based on current process information and decisions from higher level (planning and scheduling level). Therefore, this layer needs to optimize operating conditions in real-time according to the market changes of product price and demands. RTO can be separated into two different kinds of approaches: steady state and dynamic. Traditional steady-state RTO has already been applied widely in the process, and closed-loop steady-state RTO bring increased profits compared with traditional process control alone [2].

However, traditional steady-state RTO has some drawbacks. the first is low frequency. It is normal to run twice or three times per day. second, it does not rigorously consider the cost of transiting from one operating condition to another. Some plants need to respond market changes very quickly, like grade change in polymerization and petroleum process, as well as load changes in cryogenic air separation processes. In these processes, market competition requires the capability to accomodate fast and cost effective transitions so that companies can produce and sell on demand at favorable prices. To provide this capability, dynamic RTO is being developed and implemented in industrial processes. The largest difference between steady state and dynamic RTOs is that traditional RTO only provides optimal operating conditions at one steady state time point, while dynamic RTO provides a trajectory of operating condition changes. As an analogy, traditional GPS only tells us our next location, while advanced GPS can tell us a complete pathway by following the dynamic trajectory it provides. Dynamic RTO does not require steady-state conditions to start

an optimization, and it enables shorter transition times. Shorter transition times generally result in reduction of off-specification material and therefore increased profitability of a plant.

Dynamic RTO is usually formulated using large-scale nonlinear dynamic process model. The resulting optimization problem must be solved quickly and however, computational complexity and efficiency is the largest challenge for the dynamic RTO.

With the set-points or trajectories provided by the RTO layer, the process control layer drives the plant along these optimal operating conditions while keeping the plant safe and stable. Currently, traditional PID controllers are stilled widely applied in practice, because of their cheap price and acceptable performance. When higher control performance is required by fast market changes and smaller operating margins, Model Predictive Control (MPC) has been adopted by a lot of plants because it provides faster process responses and more suitable control actions than traditional PID controllers. The main advantage of MPC, compared with the traditional PID controllers, is that it can handle multi-variable interactions through the model. Currently, the MPC can be separated into two categories: linear and nonlinear. Early MPC strategies like Dynamic Matrix Control (DMC)[3] uses a linear process model and it can provide optimal control actions by on-line minimization of the control objective function. A good review of industrial MPC applications can be found in [4]. However, the control performance of the linear MPC is limited when there is a significant mismatch between the linear models and true process behavior, either because of a highly nonlinear process, or a wide operating range. Therefore, nonlinear MPC using rigorous models has received increasing industrial and academia attention. Rigorous first-principle models are able to significantly reduce the mismatch between process and model. However, as with Dynamic RTO, nonlinear MPC also has significant computational challenges to provide fast solutions and meet on-

line requirements. With development of advanced numerical algorithm and improved hardware, it is a trend to adopt nonlinear MPC and improve control performance.

Both the dynamic RTO and the nonlinear MPC are large scale dynamic optimization problems which have a lot of differential and algebraic equations (DAE) as constraints. There are several methods adopted to solve the DAE optimization problems. In our process industry, main approaches are all based on NLP solvers. These approaches can be separated into three categories, sequential, multiple-shooting, and simultaneous strategies. In the sequential methods, also known as control vector parameterization, only control variables are discretized, and these are typically represented as piece-wise polynomials. A DAE solver is used within an inner loop for integration of DAE system while a NLP solver is adopted at outer loop for solving the optimization. In simultaneous approaches, both the state and control profiles are discretized in time, typically using collocation of finite elements. There is no definitive conclusion about which approach (sequential and simultaneous) is more suitable for large scale dynamic optimization problems since researchers are developing better algorithms to exploit structure and provide computationally cheap approximations for both strategies. In general, simultaneous approaches may be more suitable to deal with DAE optimization problems which include a lot of degrees of freedom. Simultaneous approaches are adopted by this dissertation to deal with rigorous DAE optimization problems, such as Dynamic RTO or nonlinear MPC. In order to obtain more reliable solutions, uncertain disturbances transients are considered.

4. Process Estimation

Both the RTO and the nonliner MPC mentioned above depend on rigorous mathematical models of the industrial process. These models are often developed by repetitive model discrimination and experimental design. After the original model structures

are fixed, model parameters are tuned based on on-line data extracted and measured from the full-scale process. Therefore, whatever on-line or off-line, parameter estimation plays a critical role for further development of reliable models. As an analogy, consider the GPS (the RTO) and the driver (the controller) which need to know the information about weather and traffic conditions provided from the estimation part, in order to make good decisions. Sometimes, the RTO and MPC may provide bad operating decisions due to inaccurate state and parameter estimation.

Nonlinear programming is an effective framework for reliable parameter estimation, by minimizing the objective function associated with differences between estimated and measured variables under rigorous formulations of the process model as constraints. In many cases, the model is very complex and the number of data is so large that the estimation problems are very challenging and require powerful nonlinear programming approaches. Here, in the later chapter of this dissertation, we are interested in exploiting the advantages of modern computing architecture and computational strategies to solve estimation problems incorporating large-scale process models.

C. Challenges of NLP Optimization

In the previous section, several important problem classes for chemical process engineering were discussed in the areas of optimal design, operation, and parameter estimation. The use of rigorous nonlinear models is desired to increase model fidelity and improve solutions, however, this also increases the size and complexity of the NLP formulation. This issue is further intractable with consideration of model variability and uncertainty.

The desire to reduce mismatch between models and processes pushes people to

adopt rigorous first-principle models. Mass and energy balances are required in such rigorous models. Rigorous thermodynamic approaches like activity coefficients and equations of state (EOS) are more frequently adopted in process models for design and operations, compared to previously used relative volatility methods. These complex mathematical descriptions lead to high order implicit equations which are very difficult to solve. As well, the number of variables increases significantly when more complex equations are adopted. In general, rigorous descriptions increase the number of variables by more than a factor of two over simple models [5]. It is a rough estimation that approximately 60% of computational load is resulted from solving rigorous thermodynamic and kinetic equations in simulation and optimization [5]. When all equality and inequality constraints consists of the rigorous model equations (balance equations, thermodynamic and kinetic relationships etc.), the size of problems is very huge, however, the Jacobian of the constraints is typically very sparse.

Besides complexity from the models themselves, rigorous nonlinear optimization problems are very challenging due to other important factors. Here, we want to briefly discuss these factors which increase difficulty when solving rigorous nonlinear optimization problems. Problem sizes continue to grow, and parallel nonlinear optimization algorithms are developed in order to handle these factors well and solve practical nonlinear optimization problems with high computational efficiency.

1. Multiple Units

Because of interactions between highly coupled process units or enterprise activities, both industry and academia are interested in including more of product, process, and enterprise life cycle under the umbrella of a single integrated optimization problem. Enterprise or plant-wide optimization has received an increasing attention during recent decades [6]. The operating condition changes of one unit not only have an impact

on its own energy efficiency and economic performances, but can also significantly affect the performance of its upstream and downstream units. For example, in cryogenic air separation systems, there are three high coupled columns (High-pressure column, HPC, low-pressure column, LPC and crude argon column, CAC). When temperature of the HPC decreases, due to heat integration between the HPC and the LPC, the upward stream rates in LPC also decrease correspondingly. Furthermore, increases in the the nitrogen concentrations in side withdrawal flows to the CAC can lead to unstable operations when producing argon products. Therefore, it is often necessary to consider many units within a simple optimization framework. The optimal solutions from plant-wide optimization can provide more reliable decisions than those obtained from single-unit optimization, and may also avoid dangerous operating situations such as *snowball* effects from recycle operations.

Increasingly, local optimizations over a single unit are replaced by entire plant-wide formulations. If each unit model is developed according to its own first principles, the number of process variables in the rigorous plant-wide optimization problems are close to the sum of all single unit model variables. For instance, the number of variables within cryogenic air separation systems may be several times of a conventional distillation column. Large problem size and strong interactions among different units result in increased difficulty and computational complexity.

2. Uncertainty

Uncertainty always exists in process design and operation.Uncertain process disturbances and market variability affect process performance and profit. In order to make reliable decisions, uncertainty should be rigorously considered within the optimization framework.

There are two main approaches to deal with uncertainty. One is based on a

probabilistic or chance constraints and the other is based on the use of multiscenario formulations. Both these strategies are used to address uncertain in this dissertation, however, the multisecnerio approach causes significant increases in the problem size. Typically, the continuous uncertainty space is discretized into different individual scenario, and the objective function is an expected value over the scenarios. All of these scenarios are included as constraints to ensure feasibility of each scenario. Individual scenarios are coupled by stage-1 variables. When we simultaneously consider multiple uncertain parameters within the same optimization framework, the sizes and complexities of nonlinear optimization problems increase exponentially. For example, there are 3 uncertain parameters we need to focus on in our process. Each parameter has its own uncertain range and we separate each uncertain range by selecting 10 sampling points. So, there are 10^3 scenarios in total. Therefore, considering more uncertainties can increase sizes of nonlinear optimization problems significantly. Furthermore, more scenarios can provide more reliable solution. Of course, increasing the number of scenarios results in larger problem size and heavier computational requirement.

Large problem size creates the need for advanced approaches. In this dissertation, we exploit the structure these problems and develop an internal decomposition approach that allows for efficient parallel solution.

3. Dynamic Systems

Several important problem classes in chemical engineering requires optimization of systems governed by differential-algebraic equations. For design problems, the first-principle models typically consist of all algebraic equations. However, for dynamic operations, the rigorous models are fundamentally described by large sets of Differential and Algebraic Equations (DAEs). Sometimes, partial DAEs may be required

to describe both spatial and time relationships of process variables.

When we solve dynamic optimization problems using simultaneous strategies, the differential equations are discretized th and included as constraints to convert dynamic optimization into a large scale nonlinear optimization problem. The number of elements and the number of collocation points within each element determine the size of the resulting NLP. Implicit Runge-Kutta and Radau collocation methods are often used to keep high order accuracy and excellent stability properties. In this dissertation, we do not decompose these differential problems in the time domain (although this can be done and is the subject of current research). Instead, we address dynamic optimization problems with uncertainty and decompose the multiscenario structure. These problems are particularly challenging because of the large size of each individual scenarios. In this dissertation, we are interested in developing powerful computational strategies and solving rigorous dynamic optimization problems of a multi-unit chemical plant under uncertainties.

4. Multiperiod Problems

A class of problems that can easily be decomposed is multiperiod problems. When we are interested in seeking optimal operating solutions for longer term planning and scheduling, a multiperiod programming approach is often adopted with operating variables within each period and intermediate variables between the periods, such as inventory levels. These may be additional benefit in allowing the start and end of each operating period to change. And these can be considered as variables in the optimization problem. The interaction between additional periods increases the size and complexity of the resulting nonlinear optimization problem. A computational strategy is developed and implemented to efficiently solve a multiple period (weekly) operating problems under uncertain product demands.

5. Spatial Complexity

In regions highly concentrated with chemical and petroleum industries, raw materials and products are often supplied via extensive pipeline networks. Many liquid products, such as gasoline, liquid oxygen and nitrogen, and water, are all delivered from the plant to different customers through pipeline networks. As an example, a middle size oxygen pipeline network is over 50 miles long and has approximately 15 customers and 2 cryogenic air separation plants. Both gasoline and water have more customers, and a city-wide water network can be quite huge, including hundreds of thousands of nodes.

Optimization of large scale water network is just one example of a problem with spatial complexity. This structure can also be decomposed by parallel approach. In this dissertation, we consider the large-scale inverse problem of demand estimation in a city-wide water distribution system. First-principle hydraulic models of all pipes, pumps and other devices need to be included. Spatial complexity imposed by a huge number of nodes and pipes challenges off-the-shelf nonlinear optimization algorithms. In Chapter VII of this dissertation, we are interested in efficiently solving a large scale parameter estimation problem with rigorous process model of a city-wide water pipeline network. Parallel solution is enabled by decomposing the network spatially.

D. Dissertation Outline

While large-scale nonlinear programming (NLP) has seen widespread use within the process industries, the desire to solve larger and more complex problems drives continued improvements in NLP solvers. Because of physical hardware limitations, manufacturers have shifted their focus towards multi-core and other modern parallel computing architectures, and we must focus efforts on the development of parallel computing

solutions for large-scale nonlinear programming. In this dissertation, we develop a parallel nonlinear interior point algorithm for problem with block-angular structure.

With the help of this parallel nonlinear optimization algorithm, we focus on addressing several classes of nonlinear optimization problems including process design and operation under uncertainties, and parameter estimation. We argue that these advanced parallel algorithm can tackle larger problems and allow for solution of previously intractable problems using rigorous nonlinear models. The mentioned challenges, such as uncertainties, dynamics, and spatial complexity, are addressed in the following sections of this dissertation.

Chapter II describes the development of nonlinear programming approaches in chemical process engineering. All problems in this dissertation are solved by the existing nonlinear solver, IPOPT, or by our parallel interior point approach based on IPOPT. A brief introduction of the line-search based interior point approach is introduced and the advantages and disadvantages of this method are discussed. In the later sections of Chapter II, we describe several applications of parallel computing including simulation and optimization in the chemical process engineering area. Our internal decomposition approach based on a schur-complement decomposition of the KKT system is presented.

The main body of this dissertation discusses the application of these approaches to the problem classes discussed earlier. Chapter III focuses on optimal design under uncertainty for large scale cryogenic air separation units (ASU) and internal heat-integrated distillation columns.

Chapter IV addresses the optimal operating problems under uncertain product demands and different customer satisfaction levels in cryogenic air separation units. Chapter V introduces switching time as optimization variables and focuses on obtaining optimal daily operating strategies under various power pricing and uncertain

product demands for large scale cryogenic air separation units. Chapters IV and V focus on optimal multiperiod operation under uncertainty where steady-state models are used with each period. Chapter VI solves a dynamic optimization problem under uncertainty. Using a large-scale differential equation models of an ASU, this chapter focuses on improving dynamic performance during a load change while considering process uncertainty. Chapter VII demonstrates a spatial decomposition by solving a large-scale inverse problem to estimate unknown water demands in a city-wide network. Several of these problems are solved by our parallel nonlinear algorithm, in order to demonstrate scalability and the computational benefit of using parallel computing.

The dissertation closes in Chapter VIII, where general concluding remarks and recommendations for future work are presented.

CHAPTER II

IPOPT ALGORITHM AND ITS PARALLEL DEVELOPMENT

Nonlinear programming (NLP) has proven to be an effective framework for obtaining profit gains through optimal process design and operations in chemical engineering. However, the scale of the NLP problems we wish to solve continues to grow. More and more is being included within a single integrated optimization formulation. Multiple units and products are included in plant-wide and enterprise-wide optimization problems. In order to reduce plant/model mismatch, the development of increasing rigorous models based on first-principles increases both the size and complexity of problem formulations. Large-scale NLP problems result when simultaneous discretization approaches are used to reformulate optimization problems with model behaviour governed by differential and partial differential equations. Furthermore, to improve the robustness of optimization solutions, uncertainties in both design and operations may need to be considered. Multi-scenario problem formulations provide an approach for treating uncertainty, however, these formulations grow with the number of scenarios. Due to the above considerations, as NLP problems grow increasingly large and more complicated, they continue to push the development of nonlinear programming algorithms.

In this chapter, at first, the background of nonlinear programming algorithms is introduced, focusing on the Successive Quadratic Programming (SQP) approach. Then, the interior-point approach is introduced and discussed as an alternative to overcome the large shortcoming of SQP methods. Following this background, we present our implementation of a parallel interior point approach for the solution of large-scale block-angular nonlinear programming problems based on a schur-complement decomposition of the KKT system.

A. SQP Algorithm

The development of nonlinear programming approaches has been very important for effective solution of chemical process problems arising from both design and operations. One of the most important NLP algorithms is Successive Quadratic Programming (SQP), which deals with NLP problems by successively solving a series of quadratic programming (QP) sub-problems in order to obtain a search direction and a step size for next iteration. the constraints of each QP sub-problem are linearizations of the constraints in the original problem, and the objective function of sub-problem is a quadratic approximation of the Lagrangian function. An SQP method was first introduced by Wilson [7] in 1963 for the special case of convex optimization. The approach was popularized mainly Biggs [8], Han [9], and Powell [10] for general nonlinear constraints.

At first, we consider a general nonlinear optimization problems only with equality constraints for easy explanation of fundamental principles of the SQP algorithm.

$$\begin{aligned} \min_{x} \quad & f(x) \\ s.t. \quad & c(x) = 0 \end{aligned} \tag{2.1}$$

Here $x \in \mathbb{R}^n$, $c \in \mathbb{R}^m$ and the functions $f(x)$ and $c_i(x)$, are assumed to have continuous second derivatives.

The relevant Lagrangian function for the problem in Equ. (2.1) is

$$\mathcal{L}(x, \lambda) = f(x) + \lambda^T c(x) \tag{2.2}$$

and the first order optimality conditions are given by,

$$\nabla_x \mathcal{L} = \nabla f(x) + \sum_{i=1}^{m} \lambda_i \nabla c_i(x) = 0 \tag{2.3}$$

$$c(x) = 0 \tag{2.4}$$

Our desire is to find a critical point $\overline{x}$ for the nonlinear optimization problem with optimal multipliers $\overline{\lambda}$. Given an initial estimate (x_0, λ_0) of Equ. 2.3 and 2.4, we can generate a sequence (x_k, λ_k) by,

$$\begin{bmatrix} x_{k+1} \\ \lambda_{k+1} \end{bmatrix} = \begin{bmatrix} x_k \\ \lambda_k \end{bmatrix} + \begin{bmatrix} d_k^x \\ d_k^\lambda \end{bmatrix} \tag{2.5}$$

where the search steps $[d_k^x, d_k^\lambda]$ are obtained by applying Newton's method to the first order optimality conditions.

$$\begin{bmatrix} \nabla_x^2 \mathcal{L}(x_k, \lambda_k) & \nabla c_k^T \\ \nabla c_k & 0 \end{bmatrix} \begin{bmatrix} d_k^x \\ d_k^\lambda \end{bmatrix} = - \begin{bmatrix} \nabla_x \mathcal{L}(x_k, \lambda_k) \\ c_k \end{bmatrix} \tag{2.6}$$

The final optimal values $(\overline{x}, \overline{\lambda})$ can be converged by solving Equ. (2.6) repeatedly with form of line-search to ensure global convergence. In SQP methods, an equivalent formualtion to Equ. (2.6) can be given by the following QP sub-problem.

$$\begin{aligned} \min_d \ & \nabla(x_k)^T d + \frac{1}{2} d^T \nabla_x^2 \mathcal{L}(x_k, \lambda_k) d \\ s.t. \ & c(x_k) + \nabla c(x_k)^T d = 0 \end{aligned} \tag{2.7}$$

As for NLP problems with inequality constraints $g(x) \geq 0$, we can derive the resulting QP with a linear approximation of the inequality constraints

$$\begin{aligned} \min_x \ & \nabla(x_k)^T d + \frac{1}{2} d^T \nabla_x^2 \mathcal{L}(x_k, \lambda_k) d \\ s.t. \ & c(x_k) + \nabla c(x_k)^T d = 0 \\ & g(x_k) + \nabla g(x_k)^T d \geq 0 \end{aligned} \tag{2.8}$$

Historically, most SQP algorithms use a positive-definite quasi-Newton approximation, B, (e.g. BFGS) to replace $\nabla_x^2 \mathcal{L}$, removing the need to calculate the Hessian degrees of freedom. However, enabled by automatic differentiation packages, modern algorithms are making use of full second order information.

When the total number of variables is often larger than the number of variables, reduced space SQP algorithms, termed rSQP, have been developed in order to improve the computational efficiency. There are several available nonlinear software packages based on the SQP methods such as SNOPT [11], filterSQP [12], NLPQL [13], NPSOL [14], and DONLP [15].

However, the main shortcoming of SQP and its variants is that these algorithms require the explicit identification of variable bounds that are active at the solution of the QP. *Barrier methods*, based on earlier work by Fiacco and Mccormick [16], avoid this problem by shifting the bound constraints to the objective function in the form of a logarithmic barrier term.

B. Interior Point Algorithm

Interior-point methods, [17, 18, 19, 20, 21, 22], remove the combinatorial approach of identifying the active-set by moving the variable into the objective in the form of a barrier term. This barrier term penalizes the objective bounds as variable approach their bond. Sequences of barrier sub-problems are solved to converge the original problem. Interior point methods have emerged as highly efficient techniques and are currently considered among the most powerful algorithms for large-scale NLP problems [23].

1. Basic Framework

Here, we briefly introduce the fundamental principles of interior point methods. Consider the NLP problem:

$$\begin{aligned} \min_{x} \;\; & f(x) \\ s.t. \;\; & c(x) = 0 \\ & g(x) \geq 0 \end{aligned} \tag{2.9}$$

where $f : \mathbb{R}^n \to \mathbb{R}$, $c : \mathbb{R}^n \to \mathbb{R}^q$, and $g : \mathbb{R}^n \to \mathbb{R}^m$ are assumed to have continuous second derivatives. With slack variables, s, Equ. (2.9) can be modified to give,

$$\begin{aligned} \min_{x} \;\; & f(x) \\ s.t. \;\; & c(x) = 0 \\ & g(x) - s = 0 \\ & s \geq 0 \end{aligned} \tag{2.10}$$

The problem form, shifting the bounds to the objective function in the form of a log barrier term, gives the barrier sub-problems,

$$\begin{aligned} \min_{x,s} \;\; & f(x) - \mu \sum_{i=1}^{m} \log s_i \\ s.t. \;\; & c(x) = 0 \\ & g(x) - s = 0 \end{aligned} \tag{2.11}$$

where $\mu > 0$ is called the barrier parameter. When μ approaches zero, the barrier problem closely approximates the original problem. This sub-problem is solved for a fixed value of the barrier parameter. then the barrier parameter is decreased as the problem is solved again.

2. Description of IPOPT Solver

The basic interior point method introduced in the last subsection is adopted by the IPOPT solver, which considers the following problem formulation,

$$\begin{aligned} \min_{x} \;& f(x) \\ s.t. \;& c(x) = 0 \\ & d^L \leq d(x) \leq d^U \\ & x^L \leq x \leq x^U. \end{aligned} \tag{2.12}$$

Here, the objective function $f(x)$, the vector-valued equality constraints $c(x)$, and the vector-valued inequality constraints $d(x)$ are all assumed to be twice continuously differentiable. In the general case, not all variables have both upper and lower bounds, and not all functions in $d(x)$ have both upper and lower bounds. Instead of setting these bounds to arbitrarily large positive or negative values, we use permutation matrices, P_x^L, P_x^U, P_d^L, and P_d^U, which allow the dimensions of the bound vectors d^L, d^U, x^L, and x^U to be smaller than the dimension of $d(x)$ and x. Slack variables are added internally to convert the general inequality constraints be equality constraints. This results in the following reformulated problem.

$$\begin{aligned} \min_{x,s} \;& f(x) \\ s.t. \;& c(x) = 0 \\ & d(x) - s = 0 \\ & \left(P_d^L\right) s - d^L \geq 0,\; d^U - \left(P_d^U\right) s \geq 0 \\ & \left(P_x^L\right) x - x^L \geq 0,\; x^U - \left(P_x^U\right) x \geq 0 \end{aligned} \tag{2.13}$$

To simplify the notation, the following definitions are made,

$$s_x^L(x) = \left(P_x^L\right)x - x^L \quad s_x^U(x) = x^U - \left(P_x^U\right)x$$
$$s_d^L(x) = \left(P_d^L\right)s - d^L \quad s_d^U(x) = d^U - \left(P_d^U\right)s$$

The first-order optimality conditions of the barrier sub-problem are given by,

$$\begin{aligned}
\nabla_x f(x) + \nabla_x c(x)\lambda_c + \nabla_x d(x)\lambda_d & \\
-\mu\left(P_x^L\right)^T\left(S_x^L\right)^{-1}e + \mu\left(P_x^U\right)^T\left(S_x^U\right)^{-1}e &= 0 \\
-\lambda_d - \mu\left(P_d^L\right)^T\left(S_d^L\right)^{-1}e + \mu\left(P_d^U\right)^T\left(S_d^U\right)^{-1}e &= 0 \\
c(x) &= 0 \\
d(x) - s &= 0 \qquad (2.14)
\end{aligned}$$

with x and s are restricted to be within bounds.

Here $S_x^L = \mathrm{diag}\left(s_x^L - x\right)$, $S_x^U = \mathrm{diag}\left(s_x^U - s\right)$, $S_d^L = \mathrm{diag}\left(s_d^L - x\right)$, and $S_d^U = \mathrm{diag}\left(s_d^U - s\right)$. Introducing $z^L = \mu\left(S_x^L\right)^{-1}e$, $z^U{=}\mu\left(S_x^U\right)^{-1}e$, $v^L{=}\mu\left(S_d^L\right)^{-1}e$, and $v^U{=}\mu\left(S_d^U\right)^{-1}e$, leads to the primal-dual reformulation of the optimality conditions as,

$$\begin{aligned}
\nabla_x f(x) + \nabla_x c(x)\lambda_c + \nabla_x d(x)\lambda_d - \left(P_x^L\right)^T z^L + \left(P_x^U\right)^T z^U &= 0 \\
-\lambda_d - \left(P_d^L\right)^T v^L + \left(P_d^U\right)^T v^U &= 0 \\
c(x) &= 0 \\
d(x) - s &= 0 \\
\left(S_x^L\right)^T z^L - \mu e &= 0 \\
\left(S_x^U\right)^T z^U - \mu e &= 0 \\
\left(S_d^L\right)^T v^L - \mu e &= 0 \\
\left(S_d^U\right)^T v^U - \mu e &= 0 \qquad (2.15)
\end{aligned}$$

with x and s within bounds, and z^L, z^U, v^L, $v^U \geq 0$.

The Newton step for this system of equations at iteration k is given by,

$$\begin{bmatrix} H^k & 0 & \nabla_x c\left(x^k\right) & \nabla_x d\left(x^k\right) & -\left(P_x^L\right)^T & -\left(P_x^U\right)^T & 0 & 0 \\ 0 & 0 & 0 & -I & 0 & 0 & -\left(P_d^L\right)^T & \left(P_d^U\right)^T \\ \nabla_x c\left(x^k\right)^T & 0 & 0 & 0 & 0 & 0 & 0 & 0 \\ \nabla_x d\left(x^k\right)^T & -I & 0 & 0 & 0 & 0 & 0 & 0 \\ \left(z^L\right)^k P_x^L & 0 & 0 & 0 & \left(S_x^L\right)^k & 0 & 0 & 0 \\ -\left(z^U\right)^k P_x^U & 0 & 0 & 0 & 0 & \left(S_x^U\right)^k & 0 & 0 \\ 0 & \left(v^L\right)^k P_d^L & 0 & 0 & 0 & 0 & \left(S_x^L\right)^k & 0 \\ 0 & -\left(v^U\right)^k P_d^U & 0 & 0 & 0 & 0 & 0 & \left(S_d^U\right)^k \end{bmatrix} \begin{bmatrix} \Delta x \\ \Delta s \\ \Delta \lambda_c \\ \Delta \lambda_d \\ \Delta z^L \\ \Delta z^U \\ \Delta v^L \\ \Delta v^U \end{bmatrix} = \begin{bmatrix} r_x \\ r_s \\ r_c \\ r_d \\ r_z^L \\ r_z^U \\ r_v^L \\ r_v^U \end{bmatrix} \tag{2.16}$$

where $H^k = \nabla_x^2 f\left(x^k\right) + \nabla_x^2 c\left(x^k\right) \lambda_c^k + \nabla_x^2 d\left(x^k\right) \lambda_d^k$ and the right hand side vector is defined by,

$$\begin{aligned} r_x &= -\left[\nabla_x f\left(x^k\right) + \nabla_x c\left(x^k\right) \lambda_c^k + \nabla_x d\left(x\right) \lambda_d^k - \left(P_x^L\right)^T \left(z^L\right)^k + \left(P_x^U\right)^T \left(z^U\right)^k\right] \\ r_s &= \lambda_d^k + \left(P_d^L\right)^T \left(v^L\right)^k - \left(P_d^U\right)^T \left(v^U\right)^k \\ r_c &= -c\left(x^k\right) \\ r_d &= -d\left(x^k\right) + s^k \\ r_z^L &= -\left(S_x^L\right)^k \left(z^L\right)^k + \mu e \\ r_z^U &= -\left(S_x^U\right)^k \left(z^U\right)^k + \mu e \\ r_v^L &= -\left(S_d^L\right)^k \left(v^L\right)^k + \mu e \\ r_v^U &= -\left(S_d^U\right)^k \left(v^U\right)^k + \mu e \end{aligned} \tag{2.17}$$

Rather than solve the above system directly, the smaller symmetric augmented system can be obtained by eliminating the step variables corresponding to the bound multipliers.

Global convergence is ensured through the use of a filter based line search coupled with the fraction-to-the-boundary rule to make sure x and s stay within bounds and z^L, z^U, v^L, v^U remain positive. The line search requires that the calculated step is a descent direction. This can be guaranteed by checking the inertia of the augmented system (available from the linear solver). If the inertia is not correct, the linear system is modified with the addition of $\delta_1 I$ in the upper left corner and/or the addition of $-\delta_2 I$ in the following linear system that must be solved (at least once) at each iteration of the algorithm.

$$\begin{bmatrix} H^k + \delta_1 I & 0 & \nabla_x c\left(x^k\right) & \nabla_x d\left(x^k\right) \\ 0 & \delta_1 I & 0 & -I \\ \nabla_x c\left(x^k\right)^T & 0 & -\delta_2 I & 0 \\ \nabla_x d\left(x^k\right)^T & -I & 0 & -\delta_2 I \end{bmatrix} \begin{bmatrix} \Delta x \\ \Delta s \\ \Delta \lambda_c \\ \Delta \lambda_d \end{bmatrix} = \begin{bmatrix} \bar{r}_x \\ \bar{r}_s \\ c\left(x\right) \\ d\left(x\right) - s \end{bmatrix} \tag{2.18}$$

where,

$$\begin{aligned} \bar{r}_x &= r_x + \left(P_x^L\right)^T \left(\left(S_x^L\right)^k\right)^{-1} r_z^L - \left(P_x^U\right)^T \left(\left(S_x^U\right)^k\right)^{-1} r_z^U \\ \bar{r}_s &= r_s + \left(P_d^L\right)^T \left(\left(S_d^L\right)^k\right)^{-1} r_v^L - \left(P_d^U\right)^T \left(\left(S_d^U\right)^k\right)^{-1} r_v^U \end{aligned}$$

The solution of this linear system is the dominant computational expense of this algorithm and is the focus of the discussion here. Further details about the IPOPT algorithm can be found in [20] and the website: https://projects.coin.org/.

C. Parallel Computing Applications in Chemical Process Engineering

For many optimization problems encountered in chemical engineering general off-the-shelf solvers are sufficient for timely solutions. However, because observed factors the size of problems we want to solve continues to increase, often outstripping the capabilities of a single workstation and a serial algorithm.

Furthermore, computer chip manufacturers are no longer focusing on increasing clock speeds and instruction throughput, but rather on hyper-threading and multi-core architectures [24]. This means that free performance improvements that we have enjoyed as a result of increased clock speed will no longer be possible unless we develop algorithms that are capable of utilizing parallel architectures efficiently.

In fact, parallel computing has long been used as a means to address large-scale problems in chemical engineering. In regards to simulation of nonlinear process models, Vegeais and Stadtherr [25] focus on providing a parallel computing strategy for chemical flowsheets. Mallya et al. [26, 27] present a parallel block frontal solver for large-scale process simulation. For dynamic systems, Paloshi [28, 29] shows a parallel dynamic simulation strategy for industrial chemical engineering problems based on the dynamic simulator SPEEDUP, and Borchardt [30] presents a Newton-type decomposition strategy. In addition, there are a number of important contributions related to parallel solution strategies for nonlinear optimization [31, 32, 33, 34]. Several methods have been developed based on inducing separation through an augmented Lagrangian approach [35, 36]. Biegler and Tjoa [37] study a parallel strategy for parameter estimation with implicit models, and Jiang et al. [38] parallelize the sensitivity calculation in the dynamic optimization of pressure swing adsorption systems. Zavala, Laird and Biegler [39] apply schur-complement decomposition strategy into solving large-scale parameter estimation problems.

While there are a number of approaches that can be implemented for parallel solution of NLP problems, very large-scale optimization problems are almost always inherently structured since they are necessarily formulated from a repeating set of mathematical expressions [40], and algorithms that specifically exploit this structure show significant promise.

D. Internal Decomposition

Traditional approaches for parallel solution of structured optimization problems depend on problem-level decomposition methods such as Bender's decomposition [41, 42] and Lagrangian [43] decomposition. These problem-level methods have been extremely powerful on particular problem classes. However, for the general non-convex NLP case, they can exhibit several drawbacks, including poor convergence rates and overall convergence difficulties[44]. An alternative to these problem-level methods is internal decomposition, which is adopted in this work. Internal decomposition is based on the principle that a structured optimization problem will induce structure in the internal data required by the solver. The fundamental linear algebra operations in the algorithm can be modified to exploit this structure. Since the fundamental steps performed by the host algorithm remain unchanged, this approach has the primary benefit that it enables parallel solution while retaining all the convergence properties of the host solver.

The major computational expense in serial IPOPT is the solution of large linear system at each iteration resulting from a Newton step on Primal-dual optimality conditions. To solve these large linear systems efficiently, there are mainly two general approaches: iterative and direct. Currently, several sparse parallel direct linear solvers have been interfaced with IPOPT. MUMPS [45] is a distributed-memory parallel

direct solver based on a multifrontal method. PARDISO [46] is a well-known shared-memory parallel direct solver based on a multifrontal method. WSMP [47] has a hybrid distributed and shared-memory architecture based on multifrontal algorithm. As an extension of PARDISO on distributed-memory, the new parallel linear system solver, PSPIKE, has been used and combined with IPOPT to solve large scale PDE-constrained optimization problem for cancer treatment planning [24]. PSPIKE is developed from basic SPIKE algorithm [48].

While several parallel linear solvers have been interfaced with IPOPT, these linear solvers are general in nature and not tailored to a specific, predetermined problem structure. Significantly improved scalability is possible using a specifically tailored approach. In this work, we develop an internal linear decomposition approach based on the IPOPT algorithm that is tailored to problems with block angular structure.

E. Development of Parallel Interior Point Algorithm with Internal Decomposition

Since the dominant computational expense in the algorithm, is the solution of the augmented system, any internal linear decomposition strategy must be able to solve this system efficiently. Here, we develop a schur-complement decomposition approach for this linear system that allows efficient solutions of problems with specialized block angular structure. The problem formulation considered is,

$$
\begin{aligned}
\min_{z_q, y} \ & \sum_{q \in Q} \Gamma_q \left(z_q \right) \\
s.t. \ & \Omega_q \left(z_q \right) = 0 \\
& \phi_q^L \leq (P_{\phi_q}^L) \Phi_q \left(z_q \right) \\
& \phi_q^U \geq (P_{\phi_q}^U) \Phi_q \left(z_q \right) \\
& z_q^L \leq (P_{z_q}^L) z_q \\
& z_q^U \geq (P_{z_q}^U) z_q \\
& L_{z_q} z_q - L_{y_q} y = 0
\end{aligned} \tag{2.19}
$$

where z_q are the all local variables corresponding to block q, and y is a vector of common variables coupling the blocks. The matrices L_{z_q} and L_{y_q} define the linking relationship between local variables within each block and the common variables. The equations Ω_q contains all local equality constraints corresponding to block q. Note that Ω_q need not have the same structure in each block. The permutation matrices, $P_{\phi_q}^L$, $P_{\phi_q}^U$, $P_{z_q}^L$, $P_{z_q}^U$ and Φ_q form the inequality constraints for each block. Note that common variables, y, are not included in any local equality or inequality constraints.

Rather than deriving the augmented system for this problem formulation, we simply define the mapping between the problem in Equ. 2.12 and the problem in Equ. 2.19. The primal variables, and their bounds are given by

$$x = \left[z_1, \ \ldots, \ z_{n_q}, \ y \right]^T ; \tag{2.20}$$

$$x^L = \left[z_1^L, \ \ldots, \ z_{n_q}^L, \right]^T ; \tag{2.21}$$

$$x^U = \left[z_1^U, \ \ldots, \ z_{n_q}^U, \right]^T ; \tag{2.22}$$

with the corresponding permutation matrices,

$$P_x^L = \begin{bmatrix} P_{z_1}^L & 0 & 0 & 0 \\ 0 & \ddots & 0 & \vdots \\ 0 & \cdots & P_{z_{n_q}}^L & 0 \end{bmatrix} \tag{2.23}$$

$$P_x^U = \begin{bmatrix} P_{z_1}^U & 0 & 0 & 0 \\ 0 & \ddots & 0 & \vdots \\ 0 & \cdots & P_{z_{n_q}}^U & 0 \end{bmatrix} \tag{2.24}$$

The objective function, equality constraints, inequality constraints, and bounds s defined as,

$$f(x) = \sum_{q \in Q} \Gamma_q \left(z_q \right), \tag{2.25}$$

$$c(x) = \left[\Omega_1 \left(z_1 \right),\ L_{z_1} z_1 - L_{y_1} y,\ \cdots,\ , \Omega_{n_q} \left(z_{n_q} \right),\ L_{z_{n_q}} z_{n_q} - L_{y_{n_q}} y \right]^T, \tag{2.26}$$

$$d(x) = \left[\Phi_1(z_1),\ \ldots,\ \Phi_{z_{n_q}}(z_{n_q}) \right]^T; \tag{2.27}$$

$$d^L = \left[\phi_1^L,\ \ldots,\ \phi_{n_q}^L, \right]^T; \tag{2.28}$$

$$d^U = \left[\phi_1^U,\ \ldots,\ \phi_{n_q}^U, \right]^T; \tag{2.29}$$

with the corresponding permutation matrices,

$$P_d^L = \begin{bmatrix} P_{d_1}^L & 0 & 0 & 0 \\ 0 & \ddots & 0 & \vdots \\ 0 & \cdots & P_{d_{n_q}}^L & 0 \end{bmatrix} \tag{2.30}$$

$$P_d^U = \begin{bmatrix} P_{d_1}^U & 0 & 0 & 0 \\ 0 & \ddots & 0 & \vdots \\ 0 & \cdots & P_{d_{n_q}}^U & 0 \end{bmatrix} \tag{2.31}$$

Using this mapping, the augmented system of Equ. 2.18 can be rearranged to a

block-bordered structure as,

$$\begin{bmatrix} K_1 & & & & A_1 \\ & K_2 & & & A_2 \\ & & \ddots & & \vdots \\ & & & K_{n_q} & A_n \\ A_1^T & A_2^T & \cdots & A_{n_q}^T & \delta_1 I \end{bmatrix} \begin{bmatrix} \Delta t_1 \\ \Delta t_2 \\ \vdots \\ \Delta t_{n_q} \\ \Delta y \end{bmatrix} = \begin{bmatrix} r_1 \\ r_2 \\ \vdots \\ r_{n_q} \\ r_y \end{bmatrix} \tag{2.32}$$

where

$$K_q = \begin{bmatrix} H_{z_q} + \delta_1 I & \cdot & \nabla_{z_q}\Omega_q & L_{z_q}^T & \nabla_{z_q}\Phi_q \\ \cdot & \delta_1 I & \cdot & \cdot & -I \\ \nabla_{z_q}\Omega_q^T & \cdot & -\delta_2 I & \cdot & \cdot \\ L_{z_q} & \cdot & \cdot & -\delta_2 I & \cdot \\ \nabla_{z_q}\Phi_q^T & -I & \cdot & \cdot & -\delta_2 I \end{bmatrix}, \tag{2.33}$$

$$A_q^T = \begin{bmatrix} \cdot & \cdot & \cdot & L_{y_q}^T & \cdot \end{bmatrix}, \tag{2.34}$$

$$\Delta_{t_q} = \left[\Delta_{z_q},\ \Delta_{s_q},\ \Delta\lambda_{\Omega_q},\ \Delta\lambda_{L_{z_q}},\ \Delta\lambda_{\Phi_q}\right]^T, \tag{2.35}$$

$$r_q = \left[\bar{r}_{z_q},\ \bar{r}_{s_q},\ r_{\Omega_q},\ r_{L_{z_q}},\ r_{\Phi_q}\right]^T, \tag{2.36}$$

Given the structure of Equ. (2.32), we can separate the problem by eliminating each of the A^T matrices in the bottom block of rows and solve the linear system with the schur-complement approach,

$$\left[\delta_1 I - \sum_{q\in Q} A_q^T K_q^{-1} A_q\right] \Delta y = r_y - \sum_{q\in Q} A_q^T K_q^{-1} r_q \tag{2.37}$$

$$K_q \Delta t_q = r_q - A_q \Delta y, \forall q \in Q. \tag{2.38}$$

Therefore, instead of solving the complete system with a single direct solver,

the linear system is solved in 3 steps: (1) form the Schur-complement, (2) solve the Schur-complement linear system for the step in the common variables, and (3) solve for the steps in the remaining primal and dual variables.

The Schur-Complement in Equ. (2.37) is square, possibly dense, and has the same dimension as the number of common variables. The computational cost of solving this Schur-complement is cubic in the number of common variables, therefore, here it is desirable to keep the number of common variables few (less than a few hundred). The reason to do this decomposition is because step 1 and 3 can be easily parallelized. The summations in Equ. (2.37) can be parallelized using a separate processor for each q in Q. Furthermore, the linear solver in Equ. (2.38) are independent and can be solved in parallel. The complete serial algorithm is shown below.

Step 1: Form the Schur-complement and the right hand side

for each q in Q

factor K_q (using MA27 from Harwell Subroutine Library)

let $S = [-\delta_1 I]$, $r_{sc} = r_y$

for each q in Q

for each column j in A_q

solve the system $K_q d_q^{<j>} = [A_q]^{<j>}$

let $S^{<j>} = S^{<j>} + A_q^T d_q^{<j>}$

solve the system $K_q p_q = r_q$

let $r_{sc} = r_{sc} - A_q^T p_q$

Step 2: Solve the Schur-complement for step in common variables

solve $S\ \Delta y = r_{sc}$ using dense linear solver from LAPACK

Step 3: Solve for steps in remaining variables

for each q in Q

solve $K_q \Delta t_q = r_q - A_q \Delta y$ for Δt_q

In this algorithm, there are two potential levels of parallelism. On the first level, each for loop overall q in Q can be parallelized. This requires one processor for each block in Q. This level of parallelized has been implemented in the work in this dissertation. The second potential for parallelism occurs in step 1. If enough processors are available, then the for loop over all columns j in A_q can also be parallelized. This level of parallelism is not implemented in this dissertation.

This section describes the algorithm for parallel solution of the augmented system since this is the dominant computational expense. Nevertheless, all scale dependent operations need to be parallelized for an efficient algorithm. This means that all required linear operations, including all matrix-vector and vector-vector operations much be parallelized. This is discussed further in the next section.

Our parallel implementation is based on the nonlinear optimization package, IPOPT. A recent reimplementation of the IPOPT code focused on a design that allows straightforward customization of all the linear operations for structure specific problems. A high-level illustration of the design is shown in Figure 2. The fundamental algorithm code is separated from both the problem specification and the details of the implementation of all linear operations. This means that the algorithm code itself never accesses individual elements in any matrix or vector, but rather performs all operations through the base-class interfaces of the linear algebra library. With this approach the algorithm code is completely independent from the linear solver and the implementation of the linear operations. This is extremely valuable since custom linear operations can be developed that exploit the problem structure without any

necessary changes to the algorithm code itself. Furthermore, all the theoretical benefits of the IPOPT algorithm are retained since the parallel implementation performs the same mathematical operations - it just performs them more efficiently, in parallel.

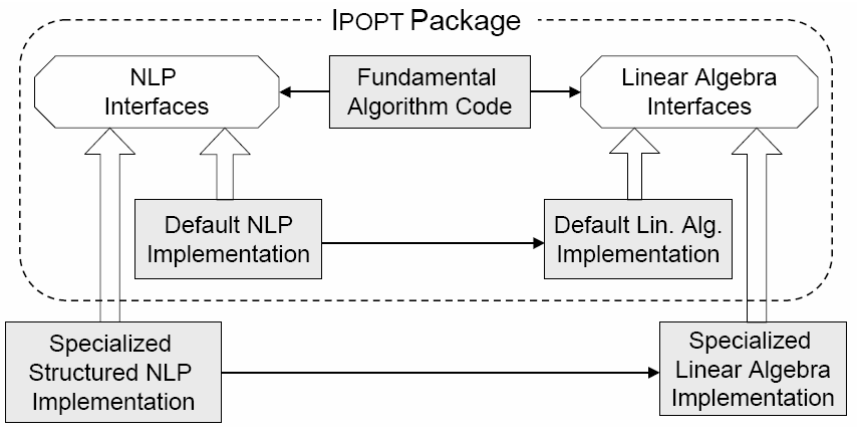

Fig. 2. Redesign IPOPT Structure with Specialized NLP and Linear Algebraic Implementation

In our implementation, the structure of the problem must be specified so it can be recognized within the linear operations. On the problem formulation side, we have implemented a composite NLP that forms the block-angular problem from separate NLP instances. The overall objective function is built up as the summation of the individual contributions from each of the blocks, and the constraints from each individual NLP is included as independent blocks in the composite NLP. A secondary specification is used to describe the linking constraints between the variables within each block and the common variables. This was a very flexible interface that allowed straightforward specification of the entire block-angular problem with individual pieces. Our specific implementation supports the use of individual AMPL models to represent each block. In parallel, a separate instance of the AMPL Solver Library (ASL) exists for each block. Therefore, the objective function, constraint evaluations, and derivatives could all be evaluated in parallel at the block level.

In addition, a specialized set of linear algebra classes were developed that were specific to the structure of the block angular problem. This includes both vectors and matrices. All scale-dependent operations on both the vectors and the matrices (mat-vec products, dot products, linear solves, etc.) were implemented to allow parallel solution across individual blocks. Given this approach, it is important to note that data corresponding to an individual block (all variables, Jacobian, and Hessian information) is only ever stored with one process. The entire problem never exists on one machine or needs to be analyzed on one machine. This is a tremendous benefit that allows parallel solution of very large-scale problems with much improved scalability. All of the required parallel communication is performed using the MPICH implementation of the Message Passing Interface (MPI).

The next four chapters of this dissertation address several challenging problems in chemical engineering. Each of these problem classes is amenable to parallel solution using the algorithm previously discussed. In each chapter, the rigorous nonlinear models, problem formulations, and solution results are discussed.

CHAPTER III

DESIGN UNDER UNCERTAINTY

Design with unknown information is an important problem in chemical process engineering area. As mentioned in the Chapter I, taking uncertain information into account at the design phase can increase the robust operating performance and process flexibility.

To handle potential uncertainties in the design phase, the traditional approach is to design the process according to nominal values of the uncertain parameters and then overdesign based on empirical factors. However, this approach may result in infeasible or conservative design decisions. The development of systematic design methods that explicitly consider process uncertainty has been an important research topic for many years [49, 50]. The two dominant approaches for rigorous consideration of uncertainty in optimization are the stochastic programming approach and the chance-constrained approach. Grossmann and Guillén-Gosálbez [51] recently discussed the opportunities for the use of these approaches in the syndissertation and planning of sustainable processes.

In the stochastic programming approach, individual scenarios are included in the optimization formulation for each discrete realization of the uncertain parameters. Continuous uncertainty spaces are usually approximated by appropriate sampling. The problem can be formulated using multiple stages with potential for decisions (or recourse) at each stage. Several good textbooks describe this approach in detail [52].

In chance-constrained programming, constraints need not be satisfied over the entire uncertainty space, but instead they are required to be satisfied with a given probability. While this explicit description is often desirable, these formulations can be very difficult to solve in the general case.

In optimal design under uncertainty, multi-scenario programming problem formulations adopted in this work. Compared with chance-constrained programming, multi-scenario formulations requires feasibility over all discrete scenarios.

A. Multi-scenario Programming Approaches

Multi-scenario optimization is a popular approach for design of chemical processes under uncertainty. Several researchers have investigated effective formulation and solution strategies for this class of problems [53, 54, 55, 56, 57, 58, 59, 60, 61], and several well known reviews are available [62, 63, 64]. Two stages are typically considered in these formulations: the design stage and the operation stage. Values for the design variables must be determined, whereas values of the control variables can be determined during the operational stage when some uncertainties may have been resolved.

Rooney and Biegler [60] generalize the multi-scenario approach and classify the uncertainties into process variability and process uncertainty. Process uncertainty refers to quantities that are unknown at both the design stage and the operation stage. The design itself should ensure feasibility across these uncertainties. Process uncertainty includes, for example, unmeasured disturbances and uncertain model parameters. Process variability refers to quantities that are uncertain at the design stage but measurable during operation. Process control variables are allowed to change in order to compensate for this variability. While multi-scenario programming is a popular approach, challenges still include efficient solution of these large-scale problems, especially in the general nonlinear case.

The multi-scenario approach is generally viewed as focusing on reliability more than profitability since it requires feasibility of all scenarios. However, when the

uncertainty space is continuous, the discrete scenarios represent only a sample of the continuous space. Recent research has demonstrated that this approach represents an approximation of the probabilistic approach and, in special cases, rigorous confidence intervals can be established [65, 66]. These developments, coupled with improvements in optimization tools and computational capability, serve to increase the importance of this approach and its practical applicability.

In conceptual design, unknown information can be classified into two categories [60, 67]. *Process uncertainty* includes values that are unknown at the design stage and the operation stage. These include, for example, unmeasured disturbances, and unknown model parameters. *Process variability* includes values that are not known at the design stage, but can be measured during operation. This variation may be compensated by control variables.

The multi-scenario formulation can be expressed in general form as:

$$\begin{aligned} \min_{d,u} \;\; & f_0(d) + \sum_{k \in K} \sum_{m \in M} \omega_{mk} f_{mk}\left(d, u_k, l_{mk}, \theta_k^{\nu}, \theta_m^{u}\right) \\ s.t. \;\; & h_{mk}\left(d, u_k, l_{mk}, \theta_k^{\nu}, \theta_m^{u}\right) = 0 \\ & g_{mk}\left(d, u_k, l_{mk}, \theta_k^{\nu}, \theta_m^{u}\right) \leq 0, \; k \in K, \; m \in M \end{aligned} \tag{3.1}$$

Where the design variables are given by d, control variables are given by u, and the state variables are given by l. Inequality and equality constraints are given by g and h respectively. In the multi-scenario formulation, the uncertainty space is separated into discrete points. The index set K is defined for discrete values of variable parameters, θ^{ν}, and the index set M is defined for discrete values of unknown parameters, θ^{u}. The objective function includes fixed costs related to the design variables and a weighted sum arising from a quadrature representation of the expected value of the objective over the uncertainty space. Discretization points are selected for

this quadrature, however realizations can be added to enforce feasibility at additional points. This gives a large-scale nonlinear multi-scenario problem with significant coupling or interaction induced by both the control and design variables. We assume that the control variables u can be used to compensate for measured variable parameters, θ^{ν}, but not the uncertainty associated with unknown parameters, θ^{u}. Thus, the control variables are indexed over k in the multi-scenario design problem, while the state variables, determined by the equality constraints, are indexed over m and k. There are two case studies which are investigated for design under uncertainty in this chapter.

B. Case Study 1: Design under Uncertainty for Cryogenic Air Separation Units

Cryogenic air separation systems are widely utilized for providing significant quantities of high purity nitrogen, argon, and oxygen products in many industries including the steel, chemical, refining, semiconductor, and aeronautical industries. Methods of air separation include cryogenic and non-cryogenic approaches [68]. Although non-cryogenic processes such as pressure swing adsorption and membrane separation have become more competitive, cryogenic distillation technology is still the dominant choice for producing large quantities of very high-purity and liquefied air products [69]. However, cryogenic air separation is an energy-intensive process consuming large amounts of electricity to compress air for separation and liquefying gas products. The industrial gas industry consumed approximately 31,460 million kilowatt hours (over $ 700 million/year) in the USA in 1998, which accounts 3.5% of the total electricity purchased by the manufacturing industry [70, 71]. In 2002, the industrial gas industry consumed approximately 35,000 million kilowatt hours of electricity in the USA [72], which is an increase of 11.3% compared with the amount in 1998.

1. Current Research about Air Separation Systems

Optimizing the design of the cryogenic air separation system has the potential to significantly affect not only the capital investment, but also the future economic performance. In practice, most current design schemes focus on specialized column structures and opportunities for energy and mass integration. Agrawal and coworkers simulate and analyze various thermal coupling methods [73], structured packing on packed columns for argon production [74], and multiple component distillation sequences [75, 76] in order to improve energy efficiency and separation performance. Egoshi, Kawakami, and Asano [77] address the problem of predicting practical separation performance and obtaining the optimal design of cryogenic air separation plants using a rigorous transport model for structured packing. Regardless of the design strategy used, in order to retain future process flexibility it is important to consider potential uncertainties during the design phase. These include uncertainty in process performance, uncertainty in product demands and pricing, and uncertainty in availability and pricing of process inputs.

In addition to design problems, current research on cryogenic air separation columns includes process optimization and control. Here, we briefly review the relative literature. Optimization of cryogenic air separation systems also includes high level planning and scheduling. Dynamic optimization strategies, linear model predictive control, and nonlinear model predictive control techniques have all been applied to cryogenic air separation systems [78, 79, 80, 81, 82, 83, 84, 79, 85]. These studies have focused primarily on the use of rigorous models for improving controller performance, and on determining optimal operating profiles targeting specific load changes. However, formulations like these, with detailed process models, typically do not consider high level operating concerns like uncertainty in product demands. On the other

hand, planning and scheduling studies [86, 87, 88, 71, 89] do consider market uncertainty and product inventory when planning operating strategies. To enable efficient solution of these challenging problems, simplified or linearized models are often used, which may ignore the integrated nature of the system and the nonlinear interactions between multiple products.

In the following chapters, we investigate optimization and control under uncertainty of cryogenic air separation columns. In this chapter, we discuss the design of integrated air separation units considering both process uncertainty and process variability.

2. Uncertainties in Air Separation Process

There are several uncertainties affecting optimal solutions of design and operating problems. One example of uncertainty in the model arises in the selection of thermodynamic methods and parameters. The primary components are separated under extremely low temperatures, and standard packages may not adequately describe the behavior of the system under these conditions. Indeed, many companies specializing in air separation have spent significant resources developing specialized thermodynamic methods for their systems.

A second form of uncertainty relates to unknown demands on the process. Air separation systems can produce three component products of various grades in both vapor and liquid phases. Different customers have different product and purity demands, and these demands can change with seasons and other external factors. It is important to consider this product demand uncertainty during the design phase and develop a process that is flexible enough to meet future product demands.

A third form of uncertainty comes from unknown or varying availability of process inputs and pricing. The dominant operating expense in cryogenic air separation

systems is the electricity required by the process. Peak versus off-peak costs and real-time pricing changes, can significantly affect the economic performance of the process. This uncertainty is well studied in a number of articles [87, 71, 89].

3. Process Description

Considering cryogenic air separation systems, uncertainty can arise from several sources. Process uncertainty (which is unknown during operation) can arise from unknown physical properties. For example, activity coefficient models for N2–Ar–O2 systems contain binary interaction parameters that are sensitive to argon purities and pressures [90]. Process variability (or measurable uncertainty) can arise because of changing product demands. In order to satisfy variable product demands, the cryogenic air separation system may be required to switch among different operating conditions. The argon product variability is often ignored; however, it can affect the optimal design significantly.

A typical cryogenic air separation system includes a double-effect heat integrated distillation column with a side column of crude argon. The double distillation column is the common part of all cryogenic air separation systems, while a crude argon column (CAC) is adopted in some systems for coproduction of argon. Addition of the argon column increases the complexity of the system significantly through additional coupling and recycling, and makes operation more difficult than the system with a double-effect distillation column alone. Figure 3 shows the process flowsheet for the system studied in this paper. The crude air feed stream is compressed and primary impurities such as water and carbon dioxide are removed. After cooling, a portion of the air feed stream is expanded and introduced into the low-pressure distillation column (LPC) containing 70 theoretical stages. The remaining feed air stream enters the bottom of the high-pressure distillation column (HPC) with 36 theoretical stages.

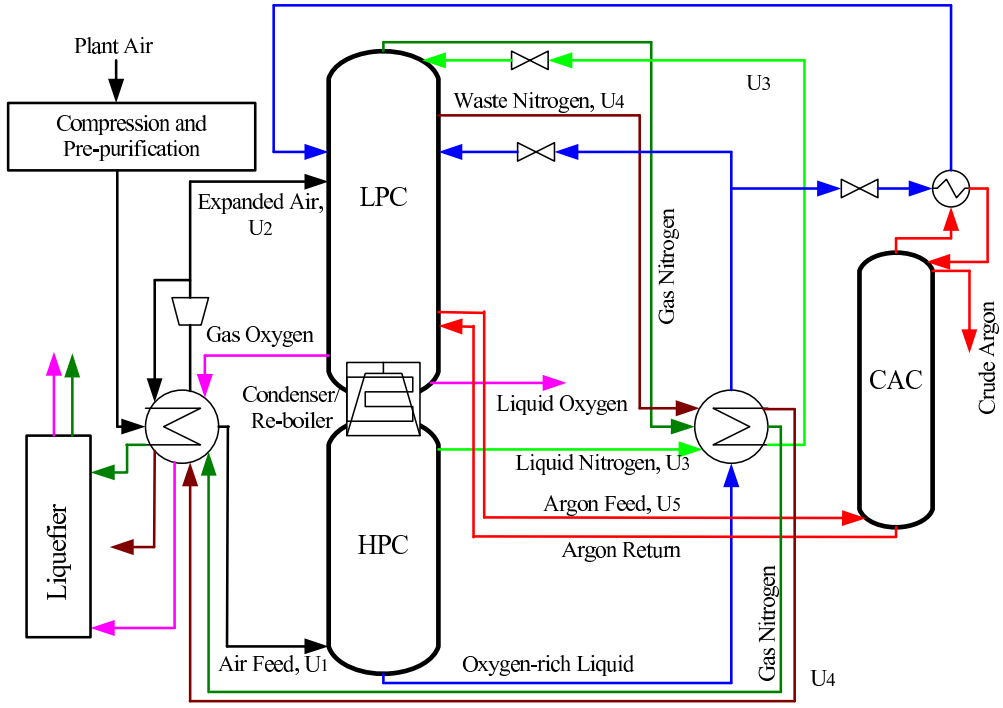

Fig. 3. Simplified Structure of the Cryogenic Air Separation Process

In the combined condenser/reboiler, the partially liquefied stream in the bottom of the LPC is vaporized, while the nitrogen vapor stream in the top of the HPC is condensed. A liquid nitrogen stream from the top of the HPC is introduced into the top of the LPC as the reflux stream. A portion of the oxygen-rich liquid from the bottom of the HPC is introduced into the 17th tray of the LPC in order to produce oxygen product with high purity. The remainder of the oxygen-rich liquid is used by the condenser at the top of the CAC to condense the argon-rich stream and produce the reflux for the CAC. A side vapor stream primarily composed of oxygen and argon is withdrawn at the 28th tray of the LPC and separated in the CAC. Liquid oxygen product is directly taken from combined condenser/reboiler and gas oxygen product is taken from the bottom of the LPC. Liquid nitrogen product is taken from the top of the HPC while gas nitrogen product is from the top of LPC. Crude argon product

is withdrawn from the top of CAC.

This is a highly integrated system that can be very difficult to design and operate. Typically, there are a large number of design variables which need to be determined in the detailed design phase of a cryogenic air separation plant. However, this study mainly focuses on conceptual design under uncertainty. Therefore all valves are assumed to be throttle expansion valves, the mass loss in pipelines are assumed to be negligible, and constant heat transfer area and coefficients are used in the heat exchanger calculations. Based on process dynamics of the cryogenic air separation system, five main control variables, $u = [U1, U2, U3, U4, U5]$, are selected to compensate for variability of argon product demands. These variables are defined as the feed air stream of the HPC ($U1$), the feed air stream of the LPC ($U2$), the reflux flow from the HPC to the LPC ($U3$), the waste nitrogen stream ($U4$), and the side withdrawal from the LPC to the CAC ($U5$). The five main design variables are the diameters of the three distillation columns (the HPC, LPC and CAC), the heat transfer area of the combined condenser/reboiler, and the brake horsepower of the compressor. Table I shows the nominal operating conditions of the plant used in the case study.

4. Mathematical Steady State Model of Air Separation Columns

The detailed air separation model is derived using the following four assumptions: (1) complete mixing on each tray and 100% tray efficiency; (2) negligible heat losses in the tray; (3) constant pressure drop on each tray; (4) uniform pressure and temperature on each tray.

The model includes mathematical expressions for the three distillation columns, two main heat exchangers, two integrated exchangers (one between the HPC and the LPC, another between the CAC and the HPC), and several throttle valves. The model contains mass and energy balances for all the exchangers and throttle valves.

Table I. Nominal Operating Conditions for Design of the Air Separation Unit

Process variable	Values
Gas oxygen product, mol/s	2.44
Liquid oxygen product, mol/s	0.64
Oxygen product purity	≥98%
Gas nitrogen product, mol/s	13.13
Nitrogen product purity	≥99.99%
Argon product purity	≥96%
Pressure of the LPC, MPa	0.13-0.14
Pressure of the HPC, MPa	0.68-0.69
Pressure of the CAC, MPa	0.12-0.13

We assume that there is no energy loss in the exchangers, and that the pressure drops are constant across these units. The three distillation columns are all modeled using the following tray-by-tray equations, physical property expressions, and phase equilibrium.

The mass balances for each tray are given by,

$$F_j^V + F_j^L + V_{j+1} + L_{j-1} - V_j - S_j^V - L_j - S_j^L = 0, \tag{3.2}$$

where j is the index of each tray from the top of each column. F_j^V and F_j^L are the vapor and liquid molar feed flows entering into the j^{th} tray. S_j^V and S_j^L are the vapor and liquid molar side flows out of the j^{th} tray. The vapor and liquid flow rates are given by V_j and L_j, respectively. Component mass balances are given by,

$$\begin{aligned} &V_{j+1}y_{i,j+1} + L_{j-1}x_{i,j-1} + F_j^V z_{i,j}^V + F_j^L z_{i,j}^L \\ &\quad -\big(V_j + S_j^V\big)y_{i,j} - \big(L_j + S_j^L\big)x_{i,j} = 0 \end{aligned} \tag{3.3}$$

where $i \in \mathcal{CP}$ is the index of each component(1-Nitrogen, 2-Argon, 3-Oxygen), the liquid and vapor compositions are given by $x_{i,j}$ and $y_{i,j}$ respectively. $z^V_{i,j}$ and $z^L_{i,j}$ are the vapor and liquid compositions of feed flows entering the j^{th} tray.

The model includes tray by tray energy balances, expressed by,

$$\begin{aligned} V_{j+1}H^V_{j+1} + L_{j-1}H^L_{j-1} + F^V_j H^{FV}_j + F^L_j H^{FL}_j \\ -\left(V_j + S^V_j\right)H^V_j - \left(L_j + S^L_j\right)H^L_j = 0, \end{aligned} \tag{3.4}$$

where H^{FV}_j and H^{FL}_j are the vapor and liquid enthalpies of feed flows entering into the j^{th} tray. The vapor and liquid enthalpies of the j^{th} tray are given by H^V_j and H^L_j respectively. $H^{FV}_{i,j}$, $H^{FL}_{i,j}$, $H^V_{i,j}$ and $H^L_{i,j}$ are calculated by,

$$H^V_j = \sum_{i\in\mathcal{CP}} y_{i,j}\underline{H}^V_{i,j}\left(T_j, \mathbf{P}_j\right) + \Delta H^V_{mix}\left(T_j, \mathbf{P}_j\right) \tag{3.5}$$

$$H^L_j = \sum_{i\in\mathcal{CP}} x_{i,j}\underline{H}^L_{i,j}\left(T_j, \mathbf{P}_j\right) + \Delta H^L_{mix}\left(T_j, \mathbf{P}_j\right) \tag{3.6}$$

$$H^{FV}_j = \sum_{i\in\mathcal{CP}} y_{i,j}\underline{H}^{FV}_{i,j}\left(T^F_j, \mathbf{P}^F_j\right) + \Delta H^{FV}_{mix}\left(T^F_j, \mathbf{P}^F_j\right) \tag{3.7}$$

$$H^{FL}_j = \sum_{i\in\mathcal{CP}} x_{i,j}\underline{H}^{FL}_{i,j}\left(T^F_j, \mathbf{P}^F_j\right) + \Delta H^{FL}_{mix}\left(T^F_j, \mathbf{P}^F_j\right) \tag{3.8}$$

where $\underline{H}^{FV}_{i,j}$, $\underline{H}^{FL}_{i,j}$, $\underline{H}^V_{i,j}$ and $\underline{H}^L_{i,j}$ are the vapor and liquid enthalpies of each component in each tray respectively, while these enthalpies are calculated based on relevant bubble point temperatures (T) and pressures ($\mathbf{P}$). ΔH_{mix} is mixture enthalpies and calculated with relevant compressibility factors and binary interactive parameters. The temperature and pressure dependence of the enthalpies were represented using a high-order polynomial fit to simulation data.

Summation equations in the j^{th} tray are written by

$$\sum_{i\in\mathcal{CP}} y_{i,j} = 1 \tag{3.9}$$

The vapor-liquid equilibrium expressions for each tray are given by,

$$y_{i,j} = \kappa_j \gamma_j K_{i,j} x_{i,j} + (1 - \kappa_j)\, y_{i,j+1} \tag{3.10}$$

where κ_j is the Murphee tray efficiency of the j^{th} tray, K is the ideal vapor-liquid equilibrium constant calculated using Antoine equations (3.12) and γ is the activity coefficient calculated with Margules equations (3.13-3.15). The tray efficiency is assumed to be 100% in this study, giving (3.11) from (3.10).

$$y_{i,j} = \gamma_j K_{i,j} x_{i,j} \tag{3.11}$$

$$K_{i,j} = \exp\left[A_i - \left(B_i / \left(T_j + C_i\right)\right)\right] / \mathbf{P}_j \tag{3.12}$$

$$\log \gamma_{1,j} = \left(\frac{A_{1,3} x_{3,j}^2 + A_{1,2} x_{2,j}^2 + \left(A_{1,3} + A_{1,2} - A_{2,3}\right) x_{3,j} x_{2,j}}{RT_j} \right) \tag{3.13}$$

$$\log \gamma_{2,j} = \left(\frac{A_{1,2} x_{1,j}^2 + A_{2,3} x_{3,j}^2 + \left(A_{1,2} + A_{2,3} - A_{1,3}\right) x_{1,j} x_{3,j}}{RT_j} \right) \tag{3.14}$$

$$\log \gamma_{3,j} = \left(\frac{A_{1,3} x_{1,j}^2 + A_{2,3} x_{2,j}^2 + \left(A_{1,3} + A_{2,3} - A_{1,2}\right) x_{1,j} x_{2,j}}{RT_j} \right) \tag{3.15}$$

where R is the ideal gas constant and Margules constants, $a_{i,k}$ describe the liquid phase interactions between components i and k. Margules constants can be found in [90] while Antoine constants are reported in http://webbook.nist.gov/chemistry/.

The combined condenser/reboiler is modeled as an additional normal tray for both the HPC and the LPC, which is given by (3.16).

$$\begin{aligned} Q_1 = UA_1 \left(T_1^{HPC} - T_{70}^{LPC}\right) &= V_1^{HPC} \left(H_1^{V,HPC} - H_1^{L,HPC}\right) \\ &= \left(V_{70}^{LPC} + S_{70}^{V}\right) \left(H_{70}^{V,LPC} - H_{70}^{L,LPC}\right) \end{aligned} \tag{3.16}$$

where Q_1 is the energy transfer from the HPC to the LPC. UA_1 is the heat transfer coefficients in the condenser/reboiler. T_1^{HPC} is the temperature at the first tray of the HPC and T_{70}^{LPC} is the temperature at the last tray of the LPC. V_1^{HPC} is the vapor

flow of the first tray in the HPC, which is fully condensed by Q_1. The heat Q_1 is released to the vapor flow V_{70}^{LPC} and oxygen product flow S_{70}^{V} at the last tray of the LPC.

Similarly, the heat-integrated condenser of the CAC is modeled using (3.17). The energy, Q_2, is extracted from the condensing vapor stream at the top of the CAC and released to a portion of the liquid oxygen-rich stream so that this stream is partially vaporized.

$$\begin{aligned} Q_2 = UA_2\left(T_1^{CAC} - T_{O_{2-rich}}\right) &= V_1^{CAC}\left(H_1^{V,CAC} - H_1^{L,CAC}\right) \\ &= \Delta V_{O_{2-rich}}\left(H_{O_{2-rich}}^{V} - H_{O_{2-rich}}^{L}\right) \end{aligned} \tag{3.17}$$

where T_1^{CAC}, $H_1^{V,CAC}$ and $H_1^{L,CAC}$ are the temperature, vapor and liquid enthalpies at the first tray of the CAC, respectively. V_1^{CAC} is the vapor flow at the first tray of the CAC. $T_{O_{2-rich}}$ and $\Delta V_{O_{2-rich}}$ are temperature and the partially vaporized amount in the oxygen-rivh stream, respectively. $H_{O_{2-rich}}^{V}$ and $H_{O_{2-rich}}^{L}$ are the vapor and liquid enthalpies for vaporization in the oxygen-rich stream.

5. Mathematical Formulation for Conceptual Design under Uncertainty

The following expressions are used to capture design relationships [91, 92]. Column diameters are given by,

$$D_{m,j} = \left(0.0164 V_{m,j}^{0.5}\left[378 M_g\left(\frac{T_{m,j}}{520}\right)\left(\frac{14.7}{P_{m,j}}\right)\right]^{\frac{1}{4}}\right) \tag{3.18}$$

where P_m is the tray pressure of each column, and M_g is the molecular weight of distillate.

$$D_m = max(D_{m,j}), m \in (LPC, HPC, CAC) \tag{3.19}$$

The height of each column is,

$$H_m = 2.4 n_m, \tag{3.20}$$

where nm is the number of stages in each column and the heat transfer area in the combined condenser/reboiler can be described by,

$$A = \frac{Q}{U \Delta T}, \tag{3.21}$$

where ΔT is the temperature driving force. Q_I is the transferred heat between the LPC and the HPC, and U is the heat transfer coefficient. The capital costs of column shells and trays (CSC and CTC) are estimated with the following equations:

$$CSC_m = \left(\frac{M\&S}{280}\right) 102 D^{1.066} H^{0.802} \left(c_{in} + c_m c_p\right) \tag{3.22}$$

$$CTC_m = \left(\frac{M\&S}{280}\right) 4.7 D^{1.55} H \left(c_s + c_t + c_m\right) \tag{3.23}$$

Here, $M\&S$ is the Marshall and Swift index. The parameters c_p, c_m and c_{in} are the pressure range, construction material and installation cost coefficients. The parameters c_s and c_t are the tray spacing and design cost coefficients, respectively. The capital cost of heat exchanger (HEC) in combined condenser/reboiler is,

$$HEC = \left(\frac{M\&S}{280}\right) 102 A^{0.65} \left(c_{in} + c_m \left(c_t + c_p\right)\right) \tag{3.24}$$

and the capital cost of the main compressor (CPC) is,

$$BHP = \left(\frac{(U1 + U2)}{1 - \Delta F_l} \frac{\kappa}{\kappa - 1} R T_{in} \left(\left(\frac{P_{out}}{P_{in}}\right)^{\frac{\kappa - 1}{\kappa}} - 1\right)\right) \tag{3.25}$$

$$CPC = \left(\frac{M\&S}{280}\right) 518 \left(BHP\right)^{0.82} \left(c_{in} + c_t\right) \tag{3.26}$$

where BHP is the brake horsepower of the compressor. The entrance and exit pressures of the compressor are P_{in} and P_{out}, and ΔF_l is the loss amount of the feed flow

in the compressor. The adiabatic index number of the gas is given by k.

Because the major operating cost of cryogenic air separation processes is required electrical power, we assume the other operating costs can be ignored. Here, we also assume that a liquefier is not installed in the system. The power price is assumed to be constant in this study, however, more complex formulations considering uncertain power prices will be investigated in future work.

The electricity cost (EC) is given by,

$$EC = C_{ele}\frac{BHP}{\eta} \tag{3.27}$$

where C_{ele} is electricity price (\$0.0574/(kWh)), and η is the efficiency of the compressor (0.75). The total annual cost (TAC) of our air separation process is given by the following form,

$$TAC = \frac{(CSC + CTC + HEC + CPC)}{t_p} + \sum_{k\in K}\sum_{q\in Q}(\omega_{qk}EC_{qk}) \tag{3.28}$$

where t_p is the payback time, which is assumed to be 3 years. The last term in Eq. (3.28) is a numerical integration for the expected value of the operating cost. In the case studies, we assume that variability and uncertainty are both uniformly distributed. Therefore, the weights ω_{qk} are all equal. More accurate quadrature rules could be used along with other distributions. Other costs such as pipelines and valves are not included in this study.

6. Numerical Results

The base formulation described in the previous subsection is used to find the optimal design for the nominal case. In addition, a multi-scenario formulation is developed

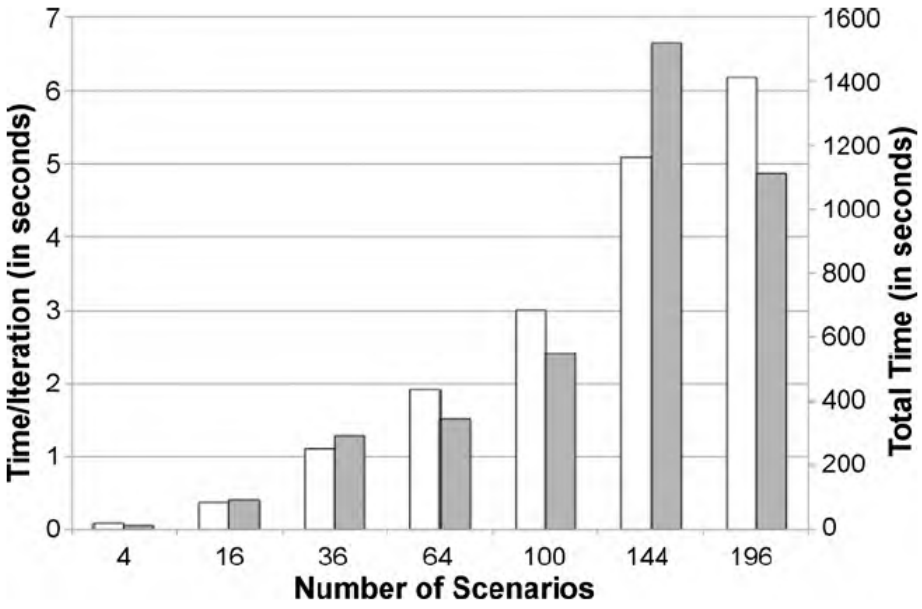

Fig. 4. Timing Results for Multi-Scenario Approach (Default options)

that considers uncertainty in argon product demands and the thermodynamic parameter α_{12}, and evaluates the objective using the expected value of the operating costs. Before discussing the optimization results in detail, we first present the timing results showing the scalability of the multi-scenario approach with IPOPT.

Argon product demands are assumed to be uniformly distributed between 0.1063 (-20%) mol/s and 0.1595 (+20%) mol/s, and the binary interaction parameter, α_{12}, is assumed to be uniformly distributed between 7.0 and 9.5. Figure 4 shows the IPOPT solution times using the default options. The same number of discretizations is used for each uncertain parameter, and the category labels give the total number of scenarios considered for each run. The white bars on the left list the average CPU time for each iteration. The grey bars on the right list the total CPU time in seconds. Note that the number of iterations need not be the same for each case. Furthermore, by default IPOPT uses exact first and second derivative information, and the number

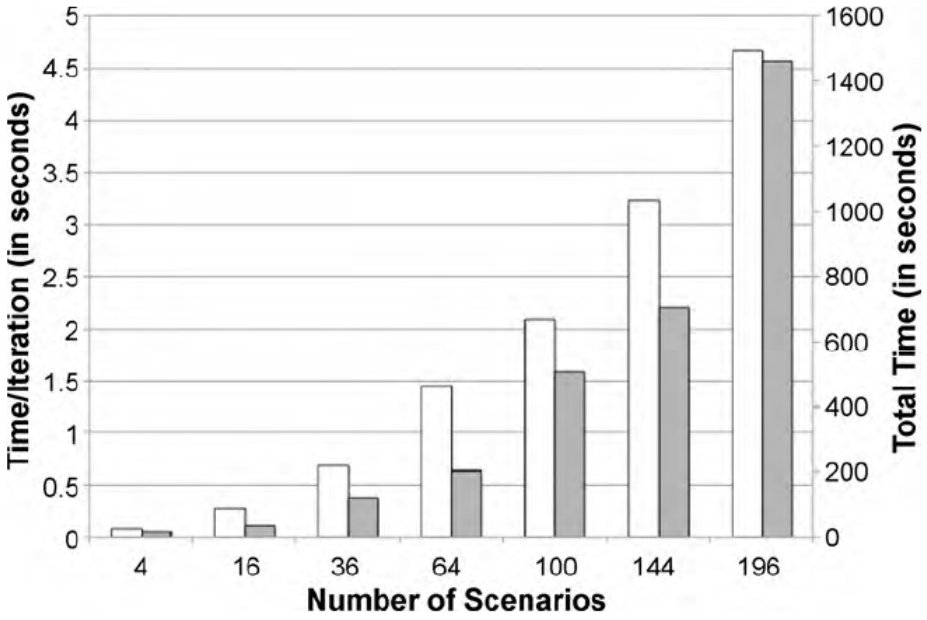

Fig. 5. Timing Results for Multi-Scenario Approach (L-BFGS)

of iterations remains relatively constant as the size of the problem increases.

Figure 5 shows the timing information using the quasi-Newton approach within IPOPT. With this option, the Hessian information is approximated using a limited memory BFGS update. Similar scaling is seen for this approach. The number of variables in the 4 scenario case is approximately 8,000, while the number of variables in the 196 scenario case is approximately 675,000. These results demonstrate that off-the-shelf nonlinear programming tools are able to scale effectively to reasonably large problems, even when the models are highly coupled and nonlinear.

Taking the largest number of scenarios (196 scenarios), optimal results from the multi-scenario formulations are compared with optimal results for the nominal case in Table II. As expected, the design is more conservative when uncertainty is considered. The optimal diameter of the HPC is the least sensitive to the uncertainty considered here.

The diameter of the CAC and the brake horsepower are significantly affected.

Table II. Optimal Design for the Nominal and Multi-scenario Formulation of the Air Separation Unit

Variables	Nominal Case	Multi-scenario Case	Difference
Diameter of LPC (m)	0.66	0.76	15.65%
Diameter of HPC (m)	0.88	0.95	8.24%
Diameter of CAC (m)	0.44	0.54	23.42%
BHP (KW)	90	113	25.57%
Heat exchanger area (m^2)	24	26	11.45%
TAC ($\$10^6$)	1.412	1.586	12.35%

This is reasonable, since the variability in argon demands will require greater process flexibility. This result also shows that it is not optimal (and may not be feasible) to absorb potential argon variability by operational changes alone. Both design and operation changes should be considered. The effects of these uncertainties on the diameter of the LPC are more dramatic than on the diameter of the HPC. This is expected given the variability in argon production and the integration between the LPC and the CAC. Increased withdrawal from the LPC to the CAC, coupled with variability in recycle from the CAC, requires increased flexibility in the LPC. In contrast, the CAC is less tightly integrated with the HPC.

Figure 6 shows how the optimal design changes as a function of the number of scenarios considered. The values for the argon demand and the uncertain binary interaction parameter were selected randomly from the ranges given previously. While it is difficult to guarantee that the scenarios sufficiently span the space of variability and uncertainty, it can be seen that the multi-scenario design solution converges as we increase the number of scenarios.

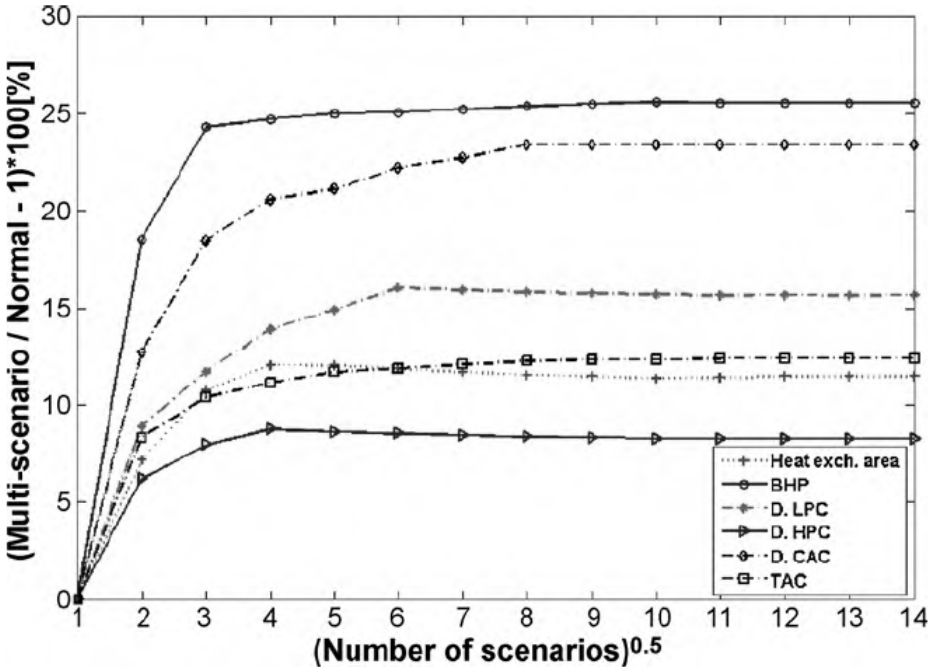

Fig. 6. Dependence between Multi-scenario Design and Increasing Scenario Number

7. Conclusions and Future Work

a. Summary and Conclusions

This work uses a multi-scenario approach to determine the optimal design of a cryogenic air separation process considering two classes of uncertainty. Process variability is describes uncertainty that is measurable during operation, and control variables can be used to compensate for this uncertainty. Process uncertainty represents unmeasurable quantities like uncertain model parameters or unmeasured disturbances. In this paper, argon product demands were selected as an example of process variability, and unknown activity coefficients were selected as an example of process uncertainty.

As expected, the optimal design is more conservative when uncertainties are considered. However, the multi-scenario approach provides a more rigorous treatment of uncertainty than applying traditional overdesign factors. The approach allows for a

more efficient design by capturing the potential for operational changes in the control variables as a function of process variability. Furthermore, nonlinear interactions between the uncertainties, the design decisions, and these potential control possibilities are rigorously captured.

While multi-scenario programming is a popular approach for treatment of uncertainty in optimization, it can be challenging to find efficient solution strategies for these large-scale problems, especially in the general nonlinear case. Nevertheless, there have been significant advancements in nonlinear programming algorithms, and the capabilities of general off-the-shelf solvers (e.g. IPOPT) have increased dramatically. The largest multi-scenario problem considered in this paper includes 196 scenarios and more than 675,000 variables. Nevertheless, this formulation solves in under 20 minutes on a standard desktop computer. These results show that recent algorithm improvements, coupled with continued increases in computational capability, allow practical application of the multi-scenario approach with rigorous, large-scale nonlinear models. This will be even more evident as we continue to develop algorithms that can exploit modern computing architectures to promote efficient solution in parallel.

b. Future Work

In this study, a rigorous model of an air separation process was developed that considered three highly integrated columns. The two uncertainties considered were a thermodynamic interaction parameter and the argon product demand. Future work is needed to include treatment of additional uncertainties. A key variability during operation is the price of electricity, which is the dominant operating cost for the process. A careful analysis will help engineers further quantify the impact of this and other uncertainties on design and operation.

This work used a steady-state model and assumed that perfect control was possible. Given the potential control challenges with such a highly integrated process, these optimization formulations should consider integrated design and control.

Finally, the main challenge in multi-scenario optimization is still efficient solution of the large-scale problem. The dominant computational expense of the IPOPT algorithm is the solution of the augmented linear system resulting from a Newton iteration of the primal-dual equations. Given a problem with a specialized structure, decompositions are possible that can exploit this structure and produce efficient solutions in parallel. We have developed a package, SCHUR-IPOPT, that uses an internal decomposition approach for the parallel solution of structured nonlinear programming problems based on the serial IPOPT algorithm. For the general design under uncertainty formulation, previous results on a large distributed cluster have demonstrated that the solution time is almost constant as scenarios and processors are added [93, 39, 85]. In the general multi-scenario formulation considering both process variability and process uncertainty, there is additional structure. If the problem is decomposed with a single scenario for each processor, then the common variables in the parallel decomposition include both the control variables and the design variables. However, there is no restriction that each individual block needs to consider only a single scenario. If the problem is decomposed over the process variabilities only, then the number of common variables considered in the parallel decomposition includes only the design variables. With this scheme, the coupling induced by the control variables is handled internally by the serial linear solver. Furthermore, nested decomposition strategies are possible to promote further parallelization. Future work will include the development of specialized decomposition strategies for this nested structure.

C. Case Study 2: Design under Uncertainty for Internal Heat-integrated Distillation Columns

1. Process Description

In this subsection, we determine optimal design solutions under uncertainty with consideration of controllability for an internal heat-integrated distillation column. Here, on schur-complement decomposition approach is used for parallel solution. Internal heat-integrated distillation column has received increased attention in recent years due to its high efficiency and potential for energy saving [94, 95, 96, 97, 98, 99, 100, 101]. Figure 7 shows the structure of this process. The rectifying section and the stripping section in this process are separated into two columns operating at the different pressures. To adjust the pressures, a compressor and a throttling valve are installed between the two sections. Unlike the case of the conventional columns, the condenser and reboiler are not required in this process. Most previous research on this

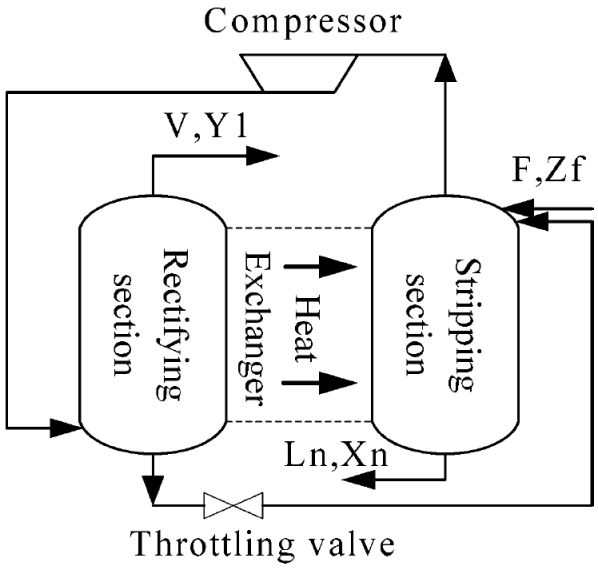

Fig. 7. Simplified Structure of Internal Heat-integrated Distillation Column

process focuses on two areas: conceptual design [95, 97, 98, 99] and dynamic con-

trol [97, 100, 101]. However, little existing research in this area considers potential uncertainties during the design phase. Adopting deterministic values of operating parameters without considering the impact from unknown information may produce a design that does not perform as expected. Conceptual design under uncertainty can provide more reliable performance in practical scaleup processes, compared to nominal design parameters that do not consider uncertainty.

2. Mathematical Model of the Process

In order to minimize the total annual cost, a rigorous mathematical model of internal heat-integrated distillation column is built in the modelling language, AMPL, based on the mass and energy balances coupled with the equilibrium relationships. The number of total trays and the feed tray are fixed to 30 and 16, respectively, while the stripping section pressure is assumed to be 0.1013MPa. Detailed model information can be found in references [94, 96].

$$0 = V_2Y_2 - V_1Y_1 - L_1X_1 \tag{3.29}$$

$$0 = V_{j+1}Y_{j+1} - V_jY_j + L_{j-1}X_{j-1} - L_jX_j, j = 2, .., n-1 \; and \; j \neq f \tag{3.30}$$

$$0 = V_{f+1}Y_{f+1} - V_fY_f + L_{f-1}X_{f-1} - L_fX_f + FZ_f \tag{3.31}$$

$$0 = -V_nY_n + L_{n-1}X_{n-1} - L_nX_n \tag{3.32}$$

$$0 = L_j - \sum_{k=1}^{j} Q_k/\lambda, \; j = 1, .., f-1 \tag{3.33}$$

$$0 = L_{f+j-1} - L_{f-1} - Fq + L_j, \; j = 1, .., f-2 \tag{3.34}$$

$$0 = L_n - F - V_1 \tag{3.35}$$

$$0 = V_1 - F\,(1-q) \tag{3.36}$$

$$0 = V_{j+1} - V_1 - L_j, \; j = 1, .., f-1 \tag{3.37}$$

$$0 = V_{f+j} - V_f + F\,(1-q) - L_j,\ j = 1, .., f-2 \tag{3.38}$$

$$0 = Y_j - \alpha X_j((\alpha - 1)\,X_j + 1)^{-1} \tag{3.39}$$

$$0 = Q_j - UA\,(T_j - T_{j+f-1})\,,\ \ j = 1, .., f-1 \tag{3.40}$$

$$0 = T_j - b/\big(a - \log\left(P_j^{sat}\right)\big) + c \tag{3.41}$$

$$0 = P_j^{sat} - P\,(X_j - (1 - X_j)\,/\alpha)^{-1} \tag{3.42}$$

where V and L are vapor and liquid flow rates; T, P, and F are temperature, pressure, and feed flow rate; X and Y are the mole fraction of the liquid and vapor in each tray; f is the feed tray, and Q is the heat transfer amount of each tray. UA is the heat transfer rate and α is the relative volatility. The variables q and Z_f are the feed thermal condition and mole fraction of the feed respectively, and n is the number of total trays indexed by j. P_r is pressure of the rectifying section.

In addition, some inequality constraints are given by,

$$V_1 Y_1 - F Z_f \leq 0 \tag{3.43}$$

$$Y_1 \geq 97\% \tag{3.44}$$

$$X_n \leq 4\% \tag{3.45}$$

$$0.1013\text{Mpa} \leq P_r \leq 0.7091\text{Mpa} \tag{3.46}$$

$$0 \leq q, X_j, Y_j \leq 1 \tag{3.47}$$

a. Conceptual Design Formulation

The design formulas for installation and operating cost are given briefly and detailed information can be found in references [99, 97, 91, 92].

$$D = \max\left(0.0164 V_j^{0.5}\left[379 M_{G,j}\left(\frac{T_{b,j}}{520}\right)\left(\frac{14.7}{P_{T,j}}\right)\right]^{\frac{1}{4}}\right) \tag{3.48}$$

$$H = 2.4n \tag{3.49}$$

$$A = \frac{Q}{U\Delta T} \tag{3.50}$$

$$CSC = \left(\frac{M\&S}{280}\right) 102 D^{1.066} H^{0.802}\left(c_{in} + c_m c_p\right) \tag{3.51}$$

$$CTC = \left(\frac{M\&S}{280}\right) 4.7 D^{1.55} H\left(c_s + c_t + c_m\right) \tag{3.52}$$

$$HEC = \left(\frac{M\&S}{280}\right) 102 A^{0.65}\left(c_{in} + c_m\left(c_t + c_p\right)\right) \tag{3.53}$$

$$BHP = \left(\frac{F}{1-\Delta F_l}\frac{\kappa}{\kappa-1} R T_{in}\left(\left(\frac{P_{out}}{P_{in}}\right)^{\frac{\kappa-1}{\kappa}} - 1\right)\right) \tag{3.54}$$

$$CPC = \left(\frac{M\&S}{280}\right) 518\left(BHP\right)^{0.82}\left(c_{in} + c_t\right) \tag{3.55}$$

$$EC = C_{ele}\frac{BHP}{\eta} \tag{3.56}$$

$$TAC = \frac{\left(CSC + CTC + HEC + CPC\right)}{t_p} + \sum_{k\in K}\sum_{m\in M}\left(\omega_{mk} EC_{mk}\right) \tag{3.57}$$

where D are the diameters of the distillation column, H are the heights of the distillation columns, A is the heat transfer area, and ΔT is the temperature driving force. The capital costs of column shells and trays as estimated are given by CSC and CTC, respectively. The c_p, c_m, and c_{in} are the pressure range, construction material, and installation cost coefficients. The variables c_s and c_t are the tray spacing, and design cost coefficients. The capital costs of heat exchanger and a main compressor

are given by HEC and CPC, respectively. The major operating cost is given by EC. C_{ele} is electricity price and η is the efficiency of the compressor. The total annual cost, (TAC), is minimized in our optimization problem.

The three main design variables selected include: the diameter of distillation columns, D, the heat transfer area, UA, and the brake horsepower, BHP. Again, two types of uncertainty are considered in this work, unmeasurable and measurable uncertainty. The relative volatility of benzene and toluene, which may vary from 2.517 to 2.117 is selected as an unmeasurable uncertainty. The range is discretized by selecting 7 points assuming a normal distribution. Measurable uncertainties include the concentration of the feed flow, Z_f, which varies from 0.55 to 0.45, and the feed flow rate, F, which varies from 90 to 110 (mol/s). Both of them are measurable during operation and may be compensated by two control variables: the rectifying section pressure, P_r, and the thermal condition in the feed flow, q. Here, we discretize the uncertainty in Z_f and F by selecting 15 points with normally distributed assumptions. In this large-scale structured problem, there are 1575 scenarios and approximately $300,000$ total variables including 453 common variables (the design and control variables common across the scenarios).

3. Controllability Constraints

In the previous subsection, it is assumed that the control variables are able to compensate process variability caused from the measurable uncertainties Z_f and F. However, the above assumption is not easily satisfied. Inherent conflicts between process design and control are present in a lot of chemical processes. The design solution that results in challenging control problems should be avoided even if this design provides low capital and operating cost. Therefore, this work considers controllability constraints on the conceptual design in order to avoid potential serious control problems.

Here, we only select the rectifying section pressure, P_r, and thermal condition in the feed flow, q as control variables to reject disturbances from both mole fraction of feed flow and feed flow rate, based on our previous dynamics research [100, 101]. The work does not attempt to test all potential control pairings. A relative gain array (RGA) is employed for interaction analysis. The 2×2 RGA matrix is defined by:

$$RGA = \begin{bmatrix} \lambda_{11} & 1-\lambda_{11} \\ 1-\lambda_{11} & \lambda_{11} \end{bmatrix} \tag{3.58}$$

The RGA value λ_{11} of the internal heat integrated distillation column is limited greater than 0.65, to avoid difficult control interactions during dynamic operation. In addition to RGA, the condition number (γ) is also adopted here as an index of loop interaction, which is the ratio between the maximum singular value (σ_{max}) and the minimum singular value (σ_{min}) of the process shown in 3.59. The condition number of internal heat integrated distillation column is limited to be less than 9.

$$\gamma = \sigma_{max}/\sigma_{min} \tag{3.59}$$

4. Optimal Results

The objective function of the above problem focuses on how to minimize the total annual cost. In order to obtain comprehensive design information, the results with and without uncertain parameters and controllability, are compared and listed in the Table III. As expected consideration o uncertainty and controllability leads to more conservative designs.

To demonstrate the scaleup properties of Schur-IPOPT on a multi-core parallel machine, we solve problems with an increasing number of scenarios (225 scenarios for each block). The timing results are shown in Figure 8. With each additional

Table III. Design Results with/without Considering Uncertainties and Controllability (HIDiC)

Variables	Nominal Case	Multi-scenario Case	difference
Diameter, ft	2.1	3.0	42.8%
Horsepower, KW	22.5	39.4	75.1%
Heat exchanger area, ft^2	210	245	16.7%

block, we utilize an additional processor. These results show that there is significant performance improvement possible with the parallel approach. Furthermore, this approach scales favourably as we increase the number of processors used. These results were obtained on an 8-core, 3.2Ghz Intel Xeon architecture.

We also tested the scalability of our approach against the general purpose, shared-memory linear solver PARDISO [46]. We do not have a version of the solver interfaced with the IPOPT. Therefore, to compare the computational time for PARDISO to perform the numerical factorization and backsolve of the same linear system arising from a particular iteration of the Schur-IPOPT solver is measured. It is important to note that PARDISO performs a symbolic factorization prior to performing the numerical factorization. However, within an optimization context, the symbolic factorization would only need to be performed once, at the beginning of the optimization, therefore this time was not included in the results. For this reason, coupled with the fact that PARDISO is simply solving the linear system and not performing the other serial operations required by Schur-IPOPT, the comparison is conservative (that is the comparison favors PARDISO somewhat). Figure 8 and Figure 9 show the normalized wall clock time for the two techniques. The x-axis shows the number of blocks, with an additional thread or process added along with each block.

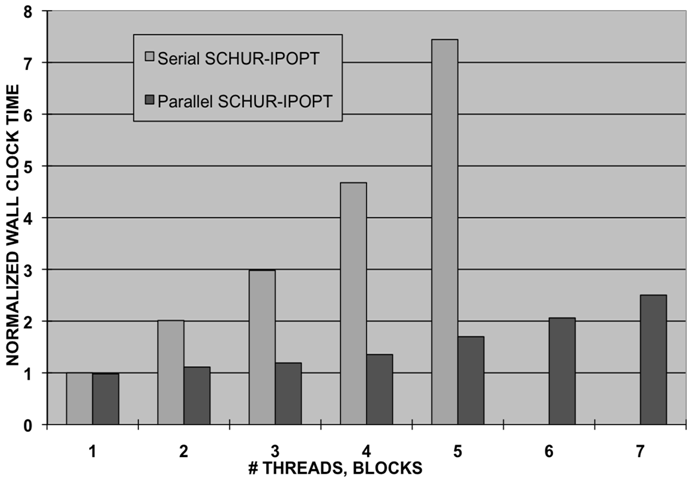

Fig. 8. Parallel Scalability Results of Schur-IPOPT on a Multi-core System

We can see that, in both cases, the scalability as we increase the size of the problem is impressive. We see a slight increase in the wall clock time as we increase the size of the problem, which is primarily due to memory bandwidth issues. The Schur-IPOPT approach does scale better than the general purpose solver PARDISO due to the fact that it is tailored to the specific problem structure. Furthermore, Schur-IPOPT shows even better scalability on distributed architectures to many processors, whereas PARDISO is available for shared-memory machines only.

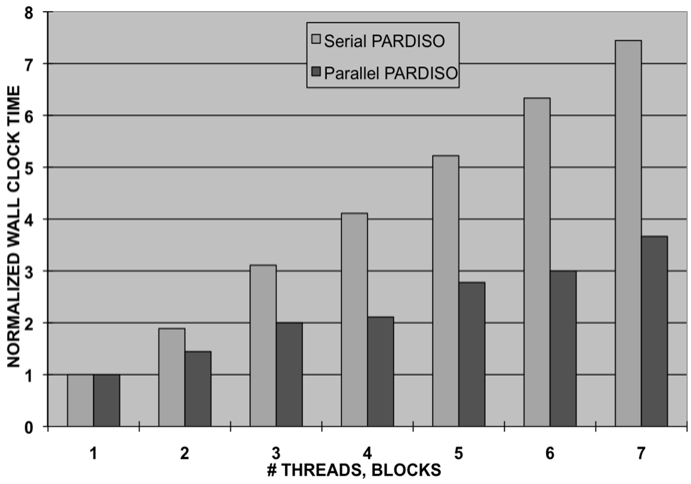

Fig. 9. Parallel Scalability Results of PARDISO on a Multi-core System

CHAPTER IV

OPTIMAL OPERATION: UNCERTAIN DEMANDS AND CONTRACTUAL CONSTRAINTS

In Chapter III, optimal design under uncertainty is studied for cryogenic air separation columns and internal hear-integrated distillation columns. In this chapter, we instead focus on optimal operation under uncertainty. Specially, we address optimal operation of cryogenic air separation processes with uncertain product demands and constraints on customer satisfaction levels.

A. Previous and Proposed Research on Operation of Air Separation Units

Optimal operation and control of cryogenic air separation processes has received significant attention, with the primary goal of reducing energy consumption and improving economic performance during operation. Load switching in air separation columns are analyzed by [78], and multivariable control schemes for cryogenic air separation are developed in [79] and [80]. Trierweiler and Engell [81] investigated the selection of an appropriate control structure based on dynamic behavior analysis. Seliger, Hanke, Hannemann, and Sundmacher [82] integrated an air separation process model with an IGCC power plant and analyzed the combined process dynamics. Control strategies such as nonlinear model predictive control (NMPC) are difficult to implement for these systems because of the high computational cost associated with optimization of a large, complex dynamic model. Approaches have been developed that promote efficient NMPC for these systems by reducing the size and complexity of the model. Bian, Henson, Belanger, and Megan [83] developed a strategy for nonlinear model predictive control by adopting a dynamic wave model for the single nitrogen column. The advanced step NMPC controller [102], an alternative approach

based on NLP sensitivity, has also been used in [84] to perform efficient nonlinear model predictive control of a cryogenic air separation column as a part of an IGCC. Considering off-line dynamic optimization, Zhu and Laird [85] proposed an effective parallel nonlinear solution to deal with optimal control and operation under uncertainty for two highly coupled cryogenic air separation columns. These studies have focused primarily on the use of rigorous models for improving controller performance, and on determining optimal operating profiles targeting specific load changes. However, formulations like these, with detailed process models, typically do not consider high level operating concerns like uncertainty in product demands. On the other hand, planning and scheduling studies [86, 87, 88, 71, 89] do consider market uncertainty and product inventory when planning operating strategies. To enable efficient solution of these challenging problems, simplified or linearized models are often used, which may ignore the integrated nature of the system and the nonlinear interactions between multiple products.

Several of these formulations directly address uncertainty in product demand. Multi-scenario approaches are often adopted in stochastic programming to deal with problems that contain uncertainties in the objective function or constraints [63, 60]. While previous research using this approach has been successful for optimal planning and operation of air separation systems [87, 88], adopting a purely multi-scenario approach that requires the satisfaction of customer demands over all the scenarios can lead to solutions that are too conservative [103, 104, 105]. To relax the constraints, the feasible region can be expanded and the objective function can be modified to penalize failure to satisfy all scenarios. However, the exact formulation and penalty parameter values may be difficult to determine or tune. As an alternative, probabilistic approaches [106, 105] have been used. Coupled with known probability density distributions, probabilistic constraints can be reformulated as equivalent determinis-

tic forms. Since the original constraints are only required to be satisfied with a given probability, solutions using these approaches can be significantly less conservative [105].

This chapter addresses the problem of determining optimal operating strategies to maximize the total profit of a cryogenic air separation system while considering rigorous nonlinear process models, uncertain product demands, and contractual obligations in the form of probabilistic fill rate constraints. A first principles model of an air separation system is developed for three coupled columns to capture the nonlinear interactions in this highly integrated flowsheet. This model includes the necessary mass and energy balances as well as rigorous phase equilibrium and physical property expressions. In this chapter, we adopt the probabilistic loss function developed in [103] and [104] to address the uncertainty associated with product demands. Uncertain demands are assumed to be normally distributed with known mean and variance, and the loss function is used to evaluate the expected revenue in the objective function.

To include contractual obligations, two types of service levels are typically considered [103, 104]. The Type 1 service level only focuses on the number of scenarios that fail to satisfy demands. It it does not consider the magnitude of the demand deficit in stock-out scenarios. In contrast, the Type 2 service level explicitly considers the amount of the demand that is not satisfied by plant. The *fill rate*, or customer satisfaction level, provides a lower bound on the ratio of the expected product sales to the expected product demand. The Type 2 service level is used in this work to capture contractual obligations since it is typically more consistent with actual contracts [104].

The complete nonlinear programming formulation can be used to identify optimal operating strategies for a particular facility with given contractual obligations in the

form of fill rate constraints. As well, solving the optimization problem repeatedly over the complete space of fill rate values for different products provides valuable planning information. In particular, three regions can be identified. In the first region, the *Profit Defined Region* (PDR), all the fill rate constraints are inactive and the operating conditions are determined by profit considerations alone. As the required fill rates are increased, at least one of these constraints becomes active. Profits begin to deteriorate since the operating strategies are now constrained by contractual obligations. This region is called the *Fill rate Constrained Region* (FCR). The third region, the *Infeasible Region* (IR), identifies the space of fill rates that cannot be met by the plant without the use of inventory. These figures can be generated for a particular facility and used to assist management in analyzing the tradeoffs between contractual obligations and expected profit.

B. Optimization Formulation and Case Studies

The steady state mathematical model of air separation units is the same as the one we used in the subsection 4 of Chapter III. However, the nominal operating conditions are different. The nominal operating conditions for planning under product demands and various customer satisfactions are listed in the Table IV.

1. Formulation of Uncertain Demands and Customer Satisfactions

Using the process model presented in the Chapter III, a nonlinear programming formulation is developed to determine optimal operating strategies (eg. production rates and operating loads). The formulation presented first is for a single period with no inventory. It will later be extended to a multiperiod formulation with inventory. Uncertain product demands are considered in both the objective function and in

Table IV. Nominal Operating Conditions for Planning with Customer Satisfaction of the Air Separation Process

Process Variable	Values
Air input of the HPC, mol/s	25.9
Expanded air feed of the LPC, mol/s	2.18
Waste Nitrogen stream, mol/s	4.38
Side stream from the LPC to the CAC, mol/s,	3.02
Gas oxygen product, mol/s	4.787
Liquid oxygen product, mol/s	0.65
Oxygen product purity	$\geq$98%
Gas nitrogen product, mol/s	18.13
Nitrogen product purity	$\geq$99.99%
Argon product output, mol/s	0.133
Argon product purity	$\geq$96%
Pressure of the LPC, MPa	0.13-0.14
Pressure of the HPC, MPa	0.68-0.69
Pressure of the CAC, MPa	0.12-0.13

probabilistic fill rate constraints. These are both formulated using the loss function while assuming normally distributed demands. The objective function is written as,

$$\max \quad profit = \left(\sum_{i \in \mathcal{CP}} R_i \right) - C^{op} \tag{4.1}$$

where R_i is the expected revenue from selling the i^{th} product, and is calculated by

$$R_i = \mathrm{E}_{\varphi_i} \left[C_i \left(\min(P_i, \varphi_i) \right) \right]. \tag{4.2}$$

Here C_i is the price of each product, P_i is the production rate, and φ_i is the uncertain product demand. We assume that the product prices are constant and known and that the air compressor can successfully switch to meet the requirements of different operating loads. The prices of nitrogen, argon and oxygen products are assumed to be \$0.113/liter, \$0.286/liter, and \$0.176/liter, respectively [107, 108]. The expected revenue from product i can be written as [104]

$$\begin{aligned} R_i &= C_i \int_0^{+\infty} \min\left(P_i, \varphi_i\right) d\varphi_i \\ &= C_i \int_0^{P_i} \varphi_i \rho\left(\varphi_i\right) + C_i \int_{P_i}^{+\infty} P_i \rho\left(\varphi_i\right) d\varphi_i \\ &= C_i \mu_i - C_i \int_{P_i}^{+\infty} \left(\varphi_i - P_i\right) \rho\left(\varphi_i\right) d\varphi_i, \end{aligned} \tag{4.3}$$

where $\rho(\varphi_i)$ is the density function of the uncertain demand and $\mu = \int_0^{\infty} \varphi\rho\left(\varphi\right) d\varphi$ is the mean of the uncertain demand. When the demand is normally distributed with the mean μ and standard deviation, σ, the integral in (4.3) is written as,

$$\begin{aligned} \int_P^{\infty} \left(\varphi - P\right) \rho\left(\varphi\right) d\varphi &= \sigma \int_{\frac{P-\mu}{\sigma}}^{\infty} \left(\tau - \frac{P-\mu}{\sigma}\right) \frac{1}{\sqrt{2\pi}} e^{\frac{-\tau^2}{2}} d\tau \\ &= \sigma L\left(\frac{P-\mu}{\sigma}\right) = \sigma L\left(\underline{z}\right) \end{aligned} \tag{4.4}$$

where $L(\underline{z})$ is defined as the standardized loss function and $\underline{z} = (P-\mu)/\sigma$ is defined as the standardized variate. Therefore, the expression for the expected revenue becomes,

$$\begin{aligned} R_i &= C_i \left(\mu_i - \sigma_i L\left(\frac{P_i - \mu_i}{\sigma_i}\right)\right) \\ &= C_i \left(\mu_i - \sigma_i L\left(\underline{z}_i\right)\right), \end{aligned} \tag{4.5}$$

where the expected amount of product i sold to customers is $S_i = \mu_i - \sigma_i L(\underline{z}_i)$.

Note that Taguchi loss functions have been used to express the loss in product quality when a variable deviates from its desired values[109, 110, 111], providing an

economic penalty for quality deviation.

The loss function used in this chapter is not a quadratic penalty, but the expected value of the lost demand that cannot be met by the current production rate and inventory.

Product storage can be added to the facility to increase flexibility and allow for higher expected product sales. The corresponding revenue from each product including available production P_i and inventory I_i is given by,

$$R_i = C_i \left(\mu_i - \sigma_i \int_{\frac{P_i+I_i-\mu_i}{\sigma_i}}^{\infty} \left(\tau - \frac{P_i + I_i - \mu_i}{\sigma_i} \right) \frac{1}{\sqrt{2\pi}} e^{\frac{-t^2}{2}} d\tau \right), \tag{4.6}$$

which gives the resulting objective function for a single period,

$$\max\ profit = (\sum_{i \in \mathcal{CP}} R_i) - C^{op} - C_i I_i - \frac{C_i^{inv,install} I_i}{t_{i,payback}}. \tag{4.7}$$

Here, $C_i I_i$ is operating cost associated with keeping inventory. $C_i^{inv,Install}$ is the capital cost of storage equipment for product i, and $t_{i,payback}$ is the desired payback time.

The mean of the uncertain demands for nitrogen, argon, and oxygen are assumed to be 18.13, 0.133, and 5.44 mol/s respectively, and the standard deviation values are assumed to be 6, 0.04, and 1.4 mol/s respectively.

In this process, the dominant operating cost is the electrical power required to operate the air compressor and the liquefier. The operating cost is given by,

$$C^{op} = C_{ele} \left(V_{fe} \frac{\kappa_c}{\kappa_c - 1} R T_{in} \left(\left(\frac{\mathbf{P}_{out}}{\mathbf{P}_{in}} \right)^{\frac{\kappa_c - 1}{\kappa_c}} - 1 \right) \eta^{-1} + W_{liq} \right). \tag{4.8}$$

This expression assumes adiabatic compression and constant compression efficiency, given by η. The price of electricity is assumed to be constant at $C_{ele} = 0.0574/(\text{kWh})$ [87, 89] in this study, however more complex formulations that consider time-varying electricity costs will be investigated in future work. The entrance and exit pressures

of the compressor are $\mathbf{P}_{in}$ and $\mathbf{P}_{out}$ respectively, and V_{fe} is the feed flow rate to the compressor, which is equal to the sum of the feed air flows of the HPC and the LPC.

The adiabatic index number of the gas is given by κ and the W_{liq} is the energy consumed by the liquifier. Note that we assume that the capital investment for the air compressor, the liquifier, and three distillation columns has already been made, and this cost is not considered here.

The optimal operating conditions are not dictated by expected profit alone. Contractual obligations may further constrain the operation. Given uncertainty in product demand, probabilistic constraints can be formulated to capture these contractual obligations. There are two general approaches for handling feasibility in optimization under uncertainty problems. The multi-scenario approach [56, 112, 60] considers a discrete set of possible realizations and can be formulated with a single stage or with multiple stages containing recourse. These formulations usually require feasibility at all discrete scenarios, however, scenario specific control variables or recourse decisions can allow for more aggressive solutions. Infeasibility can also be allowed through relaxed formulations where constraint violations are penalized in the objective, however, in many cases it can be difficult to determine appropriate penalty terms for complex processes. Probabilistic or chance-constrained programming offers an alternative approach where constraints containing uncertain parameters are only satisfied with a given probability. In this chapter, we consider a probabilistic fill rate constraint as described in [103] and [104].

Considering customer satisfaction as a measure of whether or not the actual customer demands are met in a given time interval, two types of service levels are typical considered [103, 104]. The Type 1 service level (also called confidence level) has been adopted in the application of chance-constrained programming [113, 103],

and can be written as,

$$Pr_{\varphi}\{\Psi^{i}(\varphi_{i}) \geq 0\} \geq \alpha_{i} \tag{4.9}$$

where α is the confidence level decided by managers. This type of formulation ensures that all customer demand will be satisfied with a given probability, however it does not consider the magnitude of the deficit when the demand is not met. This Type 1 service level is appropriate when any failure to meet product demand has the same consequence, independent of its time or amount [103, 104].

The Type 2 service level (also called the fill rate) provides a lower bound on the ratio of expected sales to expected demand. A Type 2 service level is typically more consistent with actual contracts [104] and is captured through the following constraint [103],

$$\frac{S_i}{\mu_i} = \frac{\mu_i - \sigma_i L(\underline{z}_i)}{\mu_i} \geq \beta_i. \tag{4.10}$$

Here, S_i is the expected value for the sales of product i and μ_i is the expected value for the demand. The fill rate or customer satisfaction level β_i is the lower bound on S_i/μ_i. For the assumption of normally distributed product demands with the mean μ_i and standard deviation σ_i, the above constraint on service level can be written using the standard loss function from Eq. (4.4). Since the actual sales are always less than or equal to the actual demand, $S_i \leq \mu_i$.

Available inventory can be used to significantly improve customer satisfaction levels, and the fill rate constraints with inventory variables I_i can be written as,

$$S_i = \mu_i - \sigma_i L\left(\frac{P_i + I_i - \mu_i}{\sigma}\right) \geq \beta_i \mu_i. \tag{4.11}$$

For a multiperiod formulation, the following changes in the inventory level can be considered,

$$I_{t,i} \;=\; I_{t-1,i} + P_{t,i} - S_{t,i}, \tag{4.12}$$

where t is the index for the period, $I_{t,i}$ is the inventory level of product i in period t, and $P_{t,i}$ is the production volume of product i in period t. $S_{t,i}$, the expected sales of product i in period t is given by,

$$S_{t,i} = \mu_{t,i} - \sigma_{t,i} L\left(\frac{P_{t,i} + I_{t-1,i} - \mu_{t,i}}{\sigma_{t,i}}\right). \tag{4.13}$$

This gives rise to the following multiperiod objective function,

$$\begin{aligned} \max \ profit &= \sum_{t=1}^{N}\left(\sum_{i\in\mathcal{CP}} R_{t,i} - C_t^{op}\right) \\ &- \sum_{i\in\mathcal{CP}} \frac{C_i^{inv,install}\max_i\left(I_{t,i}\right)}{t_{i,payback}}. \end{aligned} \tag{4.14}$$

Following the approach of [103], the loss function $L(\underline{z})$ is represented using piecewise high-order polynomials. The whole range of the standardized variates, $\underline{z}$ of $L\left(\underline{z}\right)$, is divided into four continuous parts: $(-\infty, -3]$, $(-3, 0]$, $(0, 3]$, $(3, +\infty)$. The relevant coefficients are reported in [103].

2. Case Study 1: Optimal Single Period Operation with a Single Fill Rate Constraint

In this first case study, we consider only a single operating period. Five manipulated variables are selected (the same manipulated variables are selected in the all case studies): the feed air flow of the HPC (U_1), the feed air flow of the LPC (U_2), the reflux flow from the HPC to the LPC (U_3), the waste nitrogen flow (U_4) and the side withdrawal from the LPC to the CAC (U_5). U_1, U_2, and U_3 are the variable symbols for relevant tray feed flow rates (F) in the equations listed in subsection 4 of Chapter III, while the variables symbols U_4 and U_5 are used for relevant tray side withdrawal flow rates (S) in the equations in subsection 4 of Chapter III.

While we would prefer to meet customer demands where possible, enforcing a

high fill rate can significantly reduce expected profits over the planning period. Both the short-term economic profit goals and the long-term economic consideration associated with various customer satisfaction levels need to be considered within the optimization framework. For existing facilities with fixed fill rates, individual problem formulations can be solved to find the optimal operating conditions while respecting customer satisfaction constraints. However, profiles can also be created to show the expected profit and optimal operating conditions as a function of the fill rate. These profiles can be used as a tool for evaluating future contract alternatives.

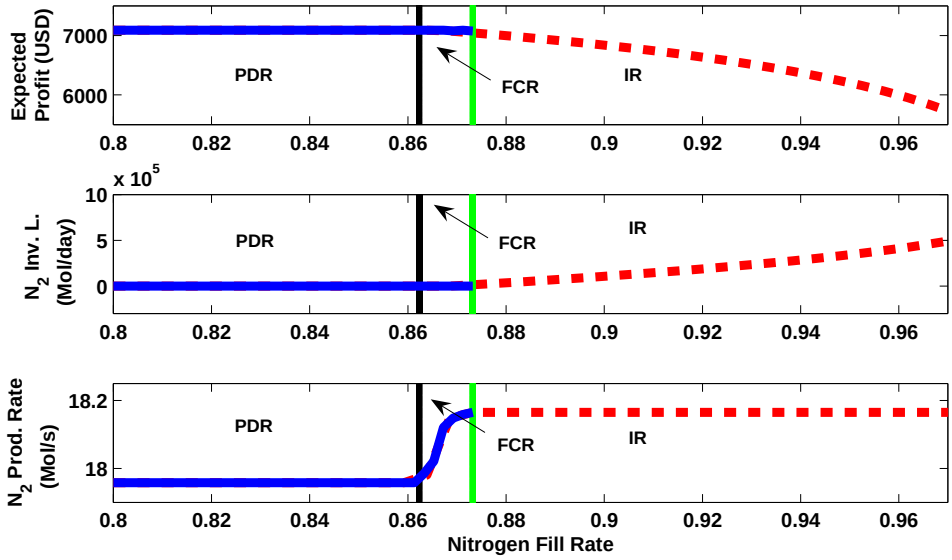

Fig. 10. Optimal Operating Strategies as a Function of N_2 Fill Rate (Solid Line: without Inventory, Dash Line: with Inventory)

Figures 10 - 12 show the expected profit and optimal operating conditions as a function of the fill rate for constraints on nitrogen (N_2), oxygen (O_2), and argon (Ar) respectively. The first region is the Profit Defined Region (PDR). Within this region, the fill rate constraint is inactive and operating conditions are determined solely by profit considerations. This is the ideal region for operation since the expected profit

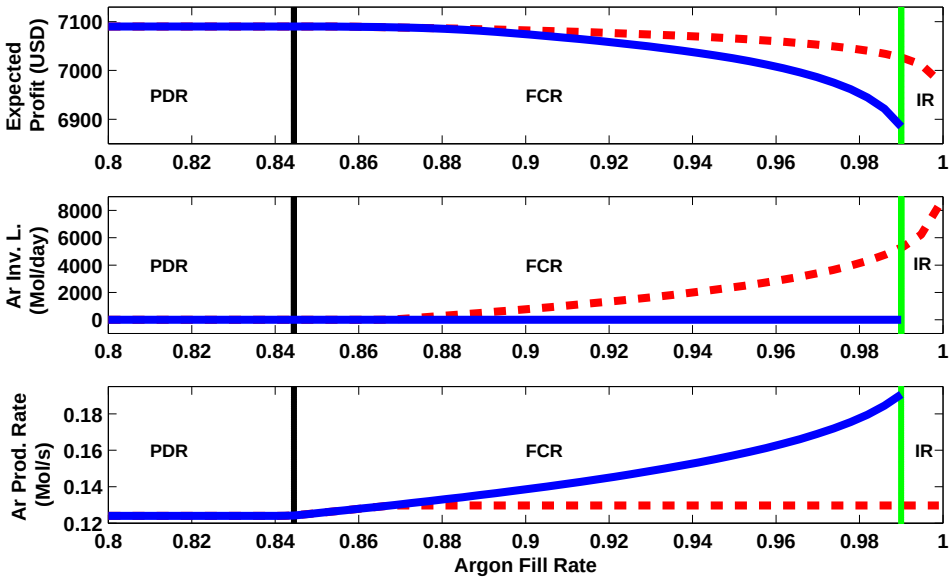

Fig. 11. Optimal Operating Strategies as a Function of *Ar* Fill Rate (Solid Line: without Inventory, Dash Line: with Inventory)

is maximized.

The second region is the Fill rate Constrained Region (FCR). Within this region, the fill rate constraint becomes active and the expected product sales are forced to be higher than the optimal value dictated by profit considerations alone. Within this region, profits decrease as the bound on expected fill rate is increased.

The third region is the Infeasible Region (IR). This region identifies the values of the fill rate that cannot be met with the existing facility. Adding inventory or purchasing additional product are potential techniques to achieve higher fill rates with existing process equipment.

The solid lines in Figures 10 - 12 show the optimal operating conditions and expected profit for the process with no inventory. For this particular case study, the profits are most sensitive to variation in the O_2 fill rate. Both gas and liquid oxygen products are generated at the bottom of the LPC where it is coupled with

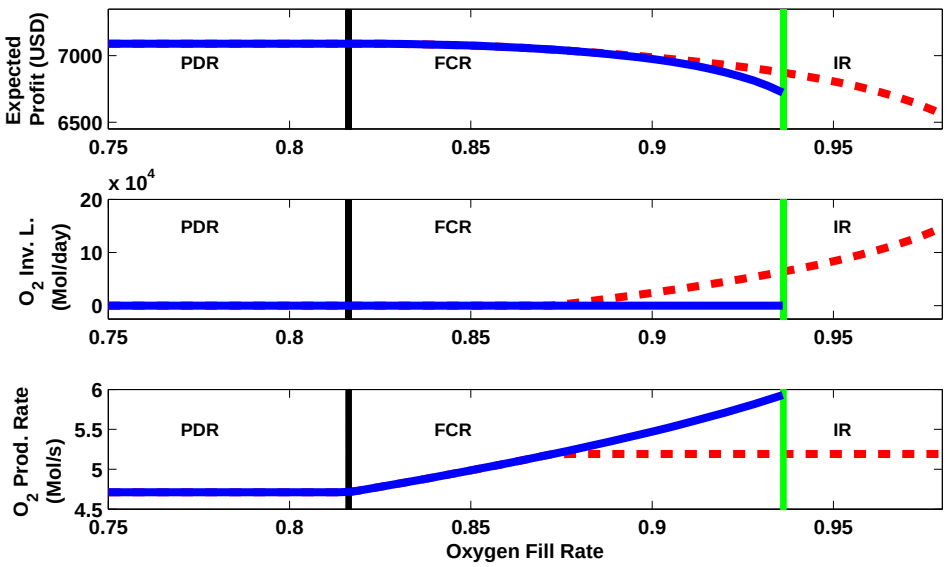

Fig. 12. Optimal Operating Strategies as a Function of O_2 Fill Rate (Solid Line: without Inventory, Dash Line: with Inventory)

the top of the HPC by the combined condenser/reboiler. The oxygen production rate affects not only the LPC, but also the HPC through the combined condenser/reboiler. Furthermore, the oxygen production rate affects the purity and flowrate to the argon column. In order to meet an increasing fill rate for oxygen, the optimal solution contains significant changes in all five manipulated variables (U_1 through U_5).

By contrast, meeting an increased fill rate for nitrogen requires significant changes to U_4 (waste N_2 side withdrawal rate) and U_3 (reflux rate from the HPC to the LPC) only. Argon production is primarily affected by the feed flow to the argon column (U_5).

The dashed lines in Figures 10 through 12 show the optimal profit and operating conditions when inventory is allowed. Including the potential for product storage allows much higher fill rates to be achieved. The curve of inventory level as a function of the fill rate shows the point at which inventory should be used. Of course, in all

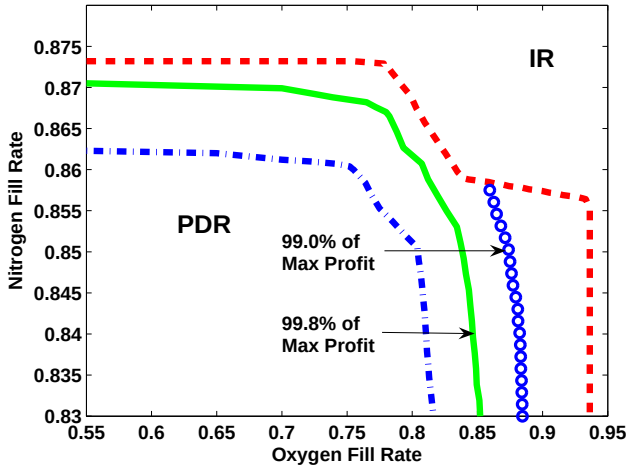

Fig. 13. Feasible Region and Profit Changes as a Function of Nitrogen and Oxygen Fill Rates without Considering Inventory

three cases, inventory is required to meet fill rate values within the Infeasible Region. However, in this case study it is more economical to use inventory before this point when fill rate constraints exist on oxygen or argon alone.

3. Case Study 2: Optimal Single Period Operation with Multiple Fill Rate Constraints

The previous subsection considered case studies with a fill rate on a single product only. However, the cryogenic air separation process is highly coupled and the production rates cannot be manipulated independently. For example, increasing the oxygen production rate reduces the production of argon considerably. Therefore, fill rate constraints across multiple products need to be considered simultaneously.

Figures 13 - 15 show the feasible and infeasible operating regions as a function of fill rates for two products. For values within the Profit Defined Region, the fill rate constraints are inactive and the operating conditions are determined by profit and safety considerations alone. As the fill rate values are increased into the Fill rate

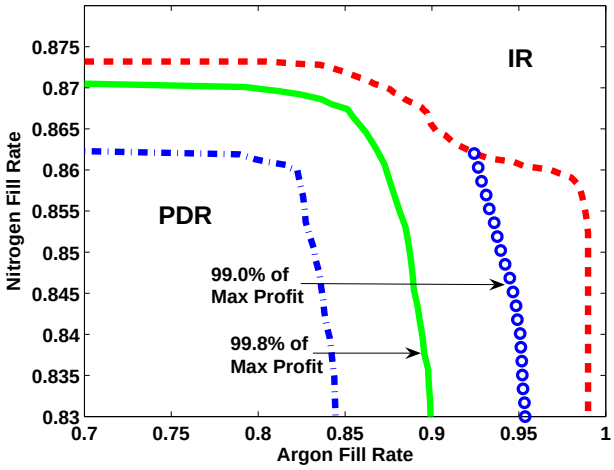

Fig. 14. Feasible Region and Profit Changes as a Function of Nitrogen and Argon Fill Rates without Considering Inventory

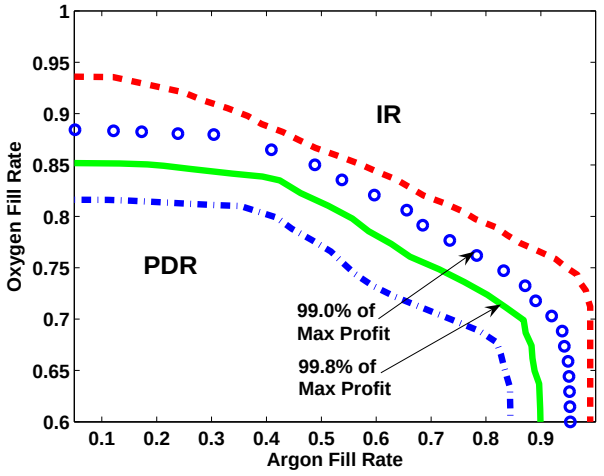

Fig. 15. Feasible Region and Profit Changes as a Function of Oxygen and Argon Fill Rates without Considering Inventory

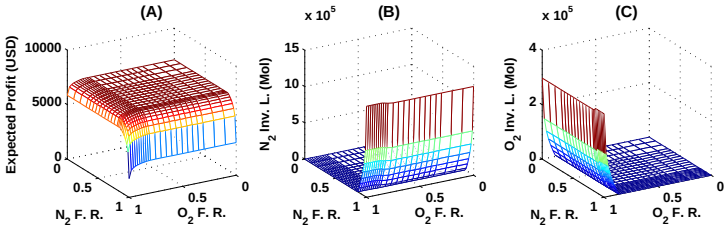

Fig. 16. Optimal Expected Profit and Inventory under Nitrogen-Oxygen Fill Rate Constraints with Product Storage

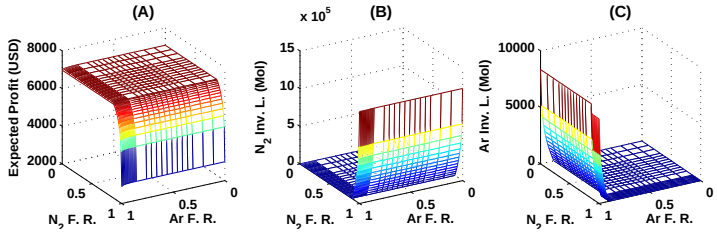

Fig. 17. Optimal Expected Profit and Inventory under Nitrogen-Argon Fill Rate Constraints with Product Storage

Constrained Region (FCR), the constraints become active and profits begin to suffer. While not shown in these figures, the optimal operating strategy can be found for any point within the feasible region.

Extending the fill rate values into the infeasible region will again require changes to the process, the addition of product storage capability, or the purchase of additional product. In the next case study, we consider the addition of product inventory.

Figure 16 shows the expected profit as a function of nitrogen and oxygen fill

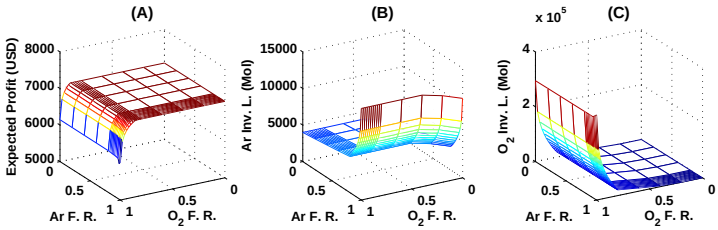

Fig. 18. Optimal Expected Profit and Inventory under Oxygen-Argon Fill Rate Constraints with Product Storage

rate values. Figure 16 also shows when it is economical to consider inventory. Profits decrease quickly as fill rates approach 100% and increased product storage is required. These same results are shown for the remaining two product pairings in Figures 17 and 18.These figures show that expected profits are more sensitive to fill rate constraints on nitrogen and oxygen than on argon. However, even with no fill rate constraint on argon, the optimal solution may include the addition of argon inventory since it increases process flexibility and allows greater freedom for adjusting nitrogen and oxygen production rates. Optimal analysis of this situation requires that we consider all three demand satisfaction constraints simultaneously.

4. Case Study 3: Optimal Multiperiod Operation with Multiple Fill Rate Constraints

This subsection addresses the more complex multiperiod formulation with fill rate constraints on each of the three products. Use of inventory is necessary when high fill rates are required. The formulation seeks to find the optimal operating conditions for each period. Individual periods are coupled by the product inventory levels at the start and end of each period. In this case study, we consider a seven day operating cycle where demands and operating conditions can change daily. Product pricing and power costs are assumed to be constant. However, this formulation allows for their variation.

For this seven day multiperiod formulation with rigorous models, the nonlinear programming problem contains over one million variables and constraints. This large-scale nonlinear programming problem is very challenging for general purpose optimization tools. Instead, we make use of our tailored NLP solver, Schur-IPOPT to allow for efficient solution in parallel. A brief overview of the internal decomposition approach used in this algorithm was presented in Chapter II.

Table V. Standard Deviations of Uncertain Product Demands of ASU planning

Day	1	2	3	4	5	6	7
σ_{N_2}	6	6	6	6	6	6	6
σ_{Ar}	0.04	0.046	0.05	0.054	0.05	0.046	0.04
σ_{O_2}	1.4	1.4	1.4	1.4	1.4	1.4	1.4

Each period in this formulation is treated as a single block $q \in Q$ from equations (2.19). The inventory levels link different periods and form the common variables, l, that couple individual blocks. Therefore, 24 common variables appear in the seven-day planning strategy. Seven processors from an 8-core 2.8 GHz Intel Xeon workstation are used, with one core dedicated to each period. The mean values for the product demands are assumed to be constant and the same as in the single period case. The fill rates for each product are set to 88.8%. It is assumed that no additional purchased product can be used to refill inventory. The assumed values of the standard deviations for the product demands are given in Table V. In practice, this information would come from historical data.

In this particular case study, the standard deviations on the demand of nitrogen and oxygen are assumed to be constant, while the standard deviation on argon change throughout the week. The optimal inventory levels for all seven days are shown in Figure 19. This figure shows the increase in argon inventory levels corresponding to the increase in the standard deviation of the demands. This figure also shows the interaction of multiple products. While the means and standard deviations of the demands for both nitrogen and oxygen did not change, the optimal solution shows changes in these inventory levels, demonstrating the significance of nonlinear interactions between the different products. This multiperiod formulation provides an

optimal operating strategy that considers demand uncertainty in both the objective function and in the required contractual obligations formulated as a probabilistic fill rate constraint.

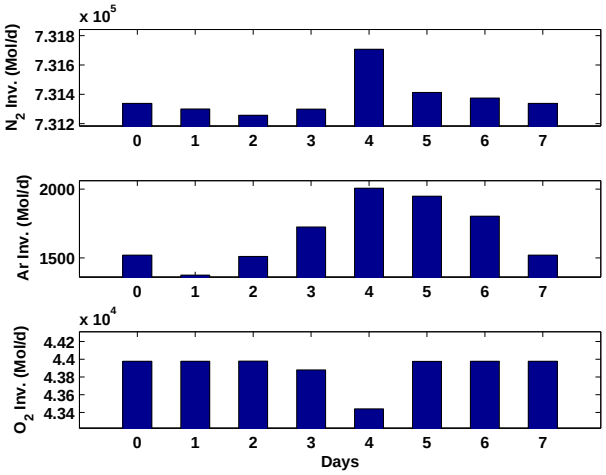

Fig. 19. Optimal Inventory Levels for all Seven Days

The full seven day multiperiod problem contains over one million variables and constraints. Using a serial implementation, this problem requires over 40 minutes of CPU time to solve. With the parallel approach using seven processors, however, solution requires only 6 minutes to solve. The complete set of timing results are shown in Figure 20. Here, we progressively consider two through seven periods, using one processor for each period. The figure shows the wall clock time per iteration for each of these problems. These results clearly show the significant benefit using the parallel approach when scaling to larger problems.Using additional processors, optimal operating strategies for larger multiperiod problems could be obtained.

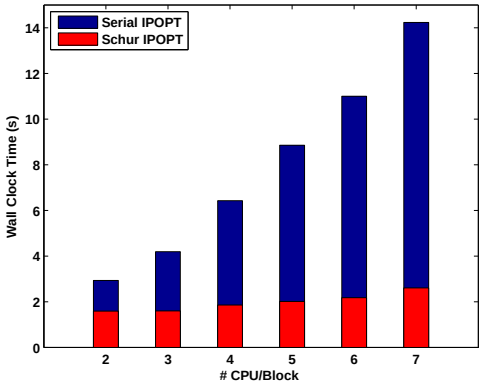

Fig. 20. Wall Clock Time per Iteration for Serial and Parallel Approaches

C. Summary and Conclusions

Effective operation of complex air separation systems can be challenging, especially in the face of uncertainty on key variables such as product demands. There are often competing short term goals. It is desirable to select an operating strategy that maximizes profit.This specific strategy may not be feasible, however, given particular contractual obligations. Therefore, it is important to consider the trade-off between profitability and customer satisfaction levels. This work addresses the problem of determining optimal operating strategies for a complex air separation process under uncertain product demands while considering contractual obligations.

Complex cryogenic air separation processes contain highly integrated flowsheets and can exhibit strong nonlinear interactions between different process variables and resulting production rates. A rigorous nonlinear model is developed for three highly coupled distillation columns. This model is included in a nonlinear programming formulation to maximize expected profit. The Type 2 service level (fill rate) is used as a measure of the customer satisfaction levels. Here, the loss function is adopted to describe the expected value of the product sales as well as the probabilistic constraints

on the fill rate.

This formulation is used for determining the optimal operating conditions for a particular facility under given fill rate based contractual obligations. As well, considering the full space of fill rate values on multiple products, management can effectively determine the trade-off between expected profits and customer demand satisfaction levels. Ideally, facilities would like to operate within the Profit Defined Region (PDR) where operating conditions are determined by profit considerations alone. The three case studies presented include both single and multiple operating periods with fill rate constraints on multiple products.

As the complexity of the problem is increased, and multiple planning periods are considered, the size of the nonlinear programming formulation can become prohibitive. The largest case study considered here is a seven day multiperiod formulation with over a million variables.Here, we use an internal decomposition approach to exploit the structure of the multiperiod problem and enable efficient solution in parallel. Schur-IPOPT is a parallel implementation of the nonlinear interior-point method IPOPT. This tailored approach uses a Schur-complement decomposition to induce separation in the linear system solved at each iteration of the algorithm. The case study demonstrates the computational efficiency of the algorithm. Furthermore, this approach scales very effectively as the problem size is increased, and shows how additional processors allow efficient solution of larger, more complex problems.

The use of rigorous optimization tools to determine operating strategies is important to improve profitability and to enable effective decision making for any complex chemical process. However, efficient solution of problem formulations addressing uncertainty is difficult, and the solution of optimization problems including rigorous nonlinear models and uncertainty remains a significant challenge. Here, we demonstrate that rigorous nonlinear models can be used to determine optimal operating

conditions while addressing demand uncertainty and contractual obligations consistent with Type 2 service levels.

CHAPTER V

OPTIMAL OPERATIONS: UNCERTAIN DEMANDS, CONTRACTUAL CONSTRAINTS, AND VARIABLE POWER PRICES

As discussed earlier, cryogenic air separation processes consume a large amount of electricity producing significant quantities of high purity gases. Rather than operating at a fixed steady state, it may be profitable to switch among different operating conditions because of variability of electrical prices and product demands. This chapter addresses the problem of determining the optimal daily multiperiod operating conditions for an air separation process under variable electricity pricing and uncertain product demands. The multiperiod nonlinear programming formulation includes a rigorous nonlinear model of the highly-coupled process, and decision variables include the operating conditions within each period, as well as the transition times. Demand uncertainty is treated using the loss function included in the objective function and constraints on customer satisfaction levels. Solutions are obtained with high computational efficiency, allowing management to make informed decisions regarding operating strategies while considering the trade off between profitability and customer satisfaction levels.

A. Introduction

Previously, Ierapetritou et al. [87] adopted a two stage stochastic programming approach to seek optimal operating strategies under varying power prices. Three different operating modes are defined and a mixed-integer linear programming formulation is used to solve for the optimal operating schedule by transitioning among these three modes. Karwan and Keblis [71] developed a similar mixed-integer programming formulation to obtain operating strategies under real time pricing, considering the impact

of the forecast horizon length on operating cost. Miller and Luyben [89] used ideal thermodynamic work to analyze operating strategies under peak and off-peak power prices. The ratio of peak and off-peak power prices is used to determine when intermittent operation of air separation systems is economically feasible. The above research contributions assume instantaneous switching among different operating conditions and typically adopt a simplified or linearized model to capture the process behavior of the complex air separation plant. When changing operation conditions, interactions among several highly-coupled distillation columns and other chemical units must be considered along with safety limits. Therefore, it is preferable to use rigorous nonlinear models that can capture this interaction and reduce plant-model mismatch. In previous work (Chapter IV), we developed a nonlinear programming formulation and solution approach to determine optimal operating strategies that considered uncertain demands with probabilistic constraints for contractual obligations. While this work demonstrated that rigorous nonlinear models of the air separation process could be included within this probabilistic optimization formulation, it also assumed that the switching time between different operating conditions was instantaneous. Furthermore, it assumed that electricity prices were constant across the operating cycle.

This chapter extends previous research and addresses the problem of determining an optimal 24-hour multiperiod operating strategy considering varying power prices, uncertain product demands, and non-zero transition times. The optimization is performed using a rigorous model of an air separation process based on first principles. This model includes the double-effect columns (coupled high and low pressure columns), as well as two crude argon columns for providing high purity argon. Focusing on multiperiod operation, a single day is separated into four different time periods based on the peak/off-peak power prices, and the rigorous nonlinear process model is included within each period. A typical air separation process can take over several

hours to reach desired product purities following a complete shutdown. In practice, it is not reasonable to assume instantaneous transition between different operating conditions. Instead, this chapter assumes a linear relationship between the required load change and the transition time.

In addition to power pricing variability, a probabilistic approach is used in this chapter to handle uncertain demand requirements from customers. Multi-scenario formulations are widely used to deal with uncertainty in design and operation. However, this method typically requires feasibility of each scenario, regardless of scenario probability. Furthermore, the problem size can grow prohibitively large as the number of scenarios is increased. As in our previous work, we have adopted the loss function developed in Li et al. [103] and Nahmias et al. [104] to quantify the expected profit in terms of production rates and uncertain customer demands. To model contractual obligations, a Type 2 service level, as described in Li et al. [103] and Nahmias et al. [104], is assumed, and the fill-rate expression is used to constrain customer satisfaction levels. This treatment allows decision makers to quantify the interaction between demand uncertainty levels and fill-rate constraints.

B. Multiple Period Operation Formulation

The steady state mathematical model of air separation units is similar to the one used in Chapter III and Chapter IV, except that this model includes four coupled distillation columns while the previous chapters only consider three columns. The model in this chapter contains two crude argon columns rather than one argon column. Figure 21 shows the structure of four highly coupled distillation columns in air separation systems. The operating conditions are also different. Table VI gives the studied operating conditions of air separation columns in this chapter.

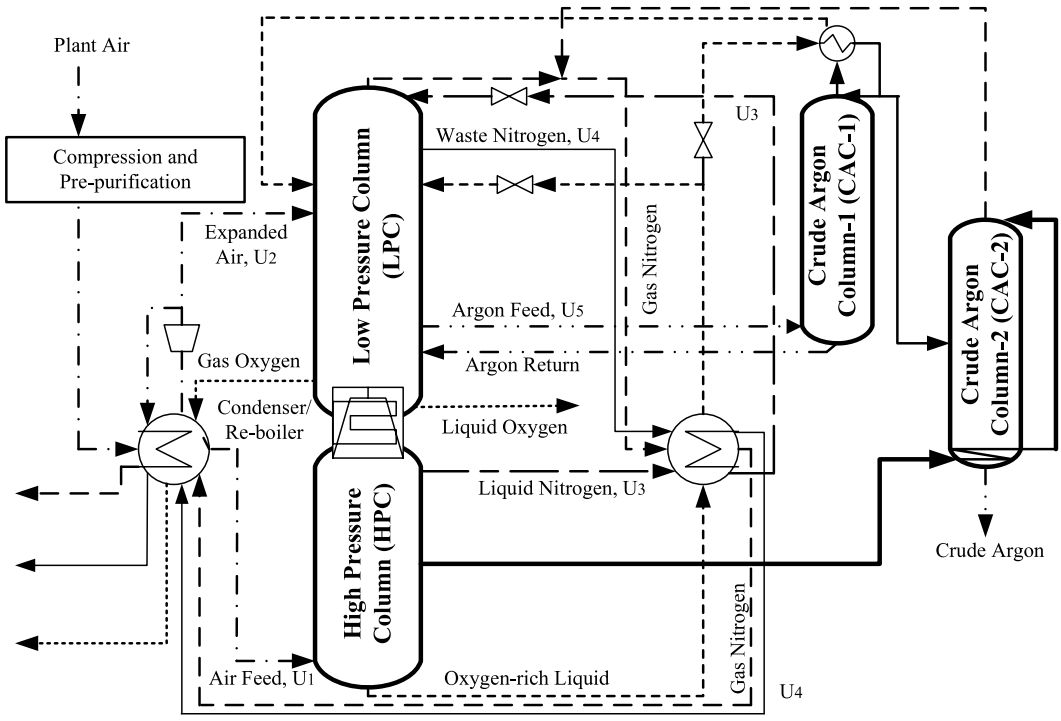

Fig. 21. Simplified Structure of Cryogenic Air Separation Systems with Four Coupled Columns

Products from an air separation plant may be available as both a gas and a liquid. All liquids in our process are liquefied gas products. Therefore, the dominant operating cost is the energy consumed by the air compressors and liquefiers. We assume the pressure drop through pipelines, throttle valves, heat exchangers and other units are constant during the transient operation. The main air compressor is an integral gear centrifugal compressor. Assuming an adiabatic compression process, the work is given by,

$$W_n^C = \frac{\Phi_n^F}{1-\Delta V_{loss}} \frac{\kappa}{\kappa-1} RT_n^C \left(\left(\frac{P_{out}^C}{P_{in}^C} \right)^{\left(\frac{\kappa-1}{\kappa}\right)} - 1 \right) {\eta_1}^{-1}, \tag{5.1}$$

where adiabatic index number of gas, κ, and compression efficiency, η_1, are 1.4 and 0.686, respectively. Φ_n^F is the total amount of air feed flow into the air separation system during the n^{th} period. P_{in}^C and P_{out}^C are the entering and exiting flow pressures

Table VI. Column Pressures and Product Specifications

Oxygen product output, kmol/h	1306
Oxygen product purity	≥98%
Nitrogen product output, kmol/h	4520
Nitrogen product purity	≥99.99%
Argon product output, kmol/h	33
Argon product purity	≥97
Pressure of LPC, MPa	0.13-0.14
Pressure of HPC, MPa	0.68-0.69
Pressure of CAC-1, MPa	0.12-0.13
Pressure of CAC-2, MPa	0.13-0.14

of the compressor. The flow loss ratio of the air compressor, ΔV_{loss}, is 0.04. The liquefier consists of a makeup compressor and a recycle system including the warm and cold expanders.

The liquefier work is given by,

$$W_n^L = \left(\sum_{i \in \mathcal{P}} V_{i,n}^L \Delta H_{i,n}^L \right) {\eta_2}^{-1} \tag{5.2}$$

where the liquifier efficiency $\eta_2 = 0.5$, and $\mathcal{P}$ is the set of products, namely nitrogen, argon, and oxygen. $V_{i,n}^L$ and $\Delta H_{i,n}^L$ are liquefied product flows and corresponding enthalpy changes, respectively.

In this section, we develop a multiperiod formulation that allows for different steady state operating conditions within each period. Variability of power prices is one of the main reasons for switching between different operating conditions. The example pricing schedule used in the case studies is shown in Figure 22. In the multiperiod

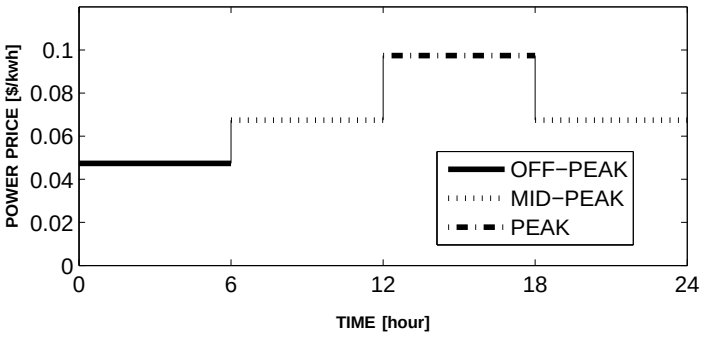

Fig. 22. Four Periods of Daily Operation Associated with Peak/Off-Peak Power Pricing

formulation, the daily operation of the air separation process is separated into four periods according to this schedule. In our case studies, the peak, off-peak, and mid-peak prices are assumed to be 0.0974, 0.0474, and 0.0674 \$/kWh. $T^M = [0, 6, 12, 18]$ are the time points between consecutive periods. Note that the time period could easily be reduced to smaller units such as one hour if the resolution of the power pricing or other inputs warrant. Unequal intervals can be also formulated in our approach, by changing the values of T^M.

Equations (5.1-5.2), coupled with the mass and energy balances for all recycle streams and piping equipment form the rigorous, steady state model for the air separation process. These equations are included in the multiperiod formulation as constraints describing the process model for each period n. In this work, we do not consider the possibility of shutting down the crude argon columns since the process may require very long periods of time to recover normal argon production in the event of a shutdown. Other practical issues need to be considered when switching between different operating conditions. These factors include the operating range of the compressor, pressure control in the distillation columns, and performance of the expanders. Therefore, in order to prevent hazardous risks like compressor surge, large

pressure ramps, and nitrogen block in the crude argon columns, we do not assume instantaneous transition, but rather restrict the rate of transition between periods. Here, we assume a linear relationship between the transition time and the change in the air feed flow rate. Furthermore, we allow the start time of the transition to be an optimization variable. It is assumed that increasing the load values from 65% to 115% requires 126 mins, while decreasing the load values from 115% to 65% also requires the same 126 mins, giving a transition slope of 0.4%/min. The air feed flow rate in period n is defined by V_n^A. $\overline{V}_n^A$ is the feed flow rate at the start of the n^{th} period (i.e. at time T_n^M during the transition). V_n^A and $\overline{V}_n^A$ are given by,

$$V_n^A = U_{1,n} + U_{2,n},\ n \in (1,2,3,4) \tag{5.3}$$

$$\overline{V}_n^A = V_n^A - b_n\left(T_n^F - T_n^M\right),\ n \in (1,2,3,4) \tag{5.4}$$

where b_n represents the transition slope defined previously. T_n^F is the final time of the transition into time period n, while T_n^S is the start time of the transition out of time period n. Their relationship is defined by,

$$T_1^F = T_4^S + \frac{\left(V_1^A - V_4^A\right)}{b_1} - 24 \tag{5.5}$$

$$T_n^F = T_{n-1}^S + \frac{\left(V_n^A - V_{n-1}^A\right)}{b_n}, n \in (2,3,4) \tag{5.6}$$

$$T_n^M \le T_n^F \le T_n^S \le T_{n+1}^M, n \in (1,2,3,4)\,. \tag{5.7}$$

The variables relating to the transition are all described in Figure 23. The value of the slope b_n is positive if the process is transitioning from a period of low feed flow rate to a period of high feed flow rate, and negative for the opposite case. Note that the transition from positive slope to negative slope is smooth since it occurs when the difference between V_n^A and V_{n-1}^A (and hence the transition time) is zero. The total

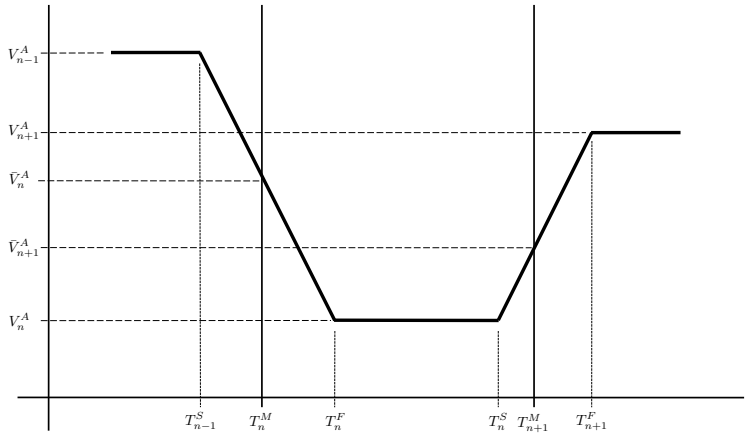

Fig. 23. Air Feed Flow Load Change under Peak vs. Off-peak Power Pricing

amount of air feed flow compressed in each period, Φ^F_n, is described by,

$$\begin{aligned}\Phi^F_n &= \frac{1}{2}\left(V^A_n + \overline{V}^A_n\right)\left(T^F_n - T^M_n\right) + V^A_n\left(T^S_n - T^F_n\right) \\ &+ \frac{1}{2}\left(V^A_n + \overline{V}^A_{n+1}\right)\left(T^M_{n+1} - T^S_n\right), n \in (1,2,3) \qquad (5.8)\\ \Phi^F_4 &= \frac{1}{2}\left(V^A_4 + \overline{V}^A_4\right)\left(T^F_4 - T^M_4\right) + V^A_4\left(T^S_4 - T^F_4\right) \\ &+ \frac{1}{2}\left(V^A_4 + \overline{V}^A_1\right)\left(T^M_1 - T^S_4\right). \qquad (5.9)\end{aligned}$$

Similarly, the total amount of each liquefied product at the n^{th} period, $\Phi^L_{i,n}$, is

given by,

$$\begin{aligned}\Phi_{i,n}^{L} &= \frac{1}{2}\left(S_{i,n}^{P}+\overline{S}_{i,n}^{P}\right)\left(T_{n}^{F}-T_{n}^{M}\right)+S_{i,n}^{P}\left(T_{n}^{S}-T_{n}^{F}\right)\\ &+ \frac{1}{2}\left(S_{i,n}^{P}+\overline{S}_{i,n+1}^{P}\right)\left(T_{n+1}^{M}-T_{n}^{S}\right), i\in\mathcal{P}, n\in(1,2,3) \qquad (5.10)\\ \Phi_{i,4}^{L} &= \frac{1}{2}\left(S_{i,4}^{P}+\overline{S}_{i,4}^{P}\right)\left(T_{4}^{F}-T_{4}^{M}\right)+S_{i,4}^{P}\left(T_{4}^{S}-T_{4}^{F}\right)\\ &+ \frac{1}{2}\left(S_{i,4}^{P}+\overline{S}_{i,1}^{P}\right)\left(T_{1}^{M}-T_{4}^{S}\right), i\in\mathcal{P} \qquad (5.11)\end{aligned}$$

where $S_{i,n}^{P}$ are the production rates in the n^{th} period, as defined by the process model. $\overline{S}_{i,n}^{P}$ are the production rates at the front boundary of the period ($t=T_{n}^{M}$) given by,

$$\begin{aligned}\overline{S}_{i,n}^{P} &= S_{i,n}^{P}-\left(\frac{S_{i,n}^{P}-S_{i,n-1}^{P}}{T_{n}^{F}-T_{n-1}^{S}}\right)\left(T_{n}^{F}-T_{n}^{M}\right), i\in\mathcal{P},\\ &\quad n\in(2,3,4) \qquad (5.12)\\ \overline{S}_{i,1}^{P} &= S_{i,1}^{P}-\left(\frac{S_{i,1}^{P}-S_{i,4}^{P}}{24+T_{1}^{F}-T_{4}^{S}}\right)\left(T_{1}^{F}-T_{1}^{M}\right), i\in\mathcal{P}. \qquad (5.13)\end{aligned}$$

In order to satisfy the product demands, product storage is included and the following constraints can be added,

$$\begin{aligned}I_{i,n-1}+\Phi_{i,n}^{L}-I_{i,n} &= D_{i,n}, i\in\mathcal{P}, n\in(2,3,4) \qquad (5.14)\\ I_{i,4}+\Phi_{i,1}^{L}-I_{i,1} &= D_{i,1}, i\in\mathcal{P}, \qquad (5.15)\end{aligned}$$

where $I_{i,n}$ is the inventory level of the i^{th} product in the n^{th} period. $D_{i,n}$ are the product demand amounts of the i^{th} product in the n^{th} period. The variables, $\Phi_{i,n}^{L}$, are the total amounts of each product liquefied at the n^{th} period.

C. Optimal Operating Strategy under Constant Product Demands

In this section, we present a case study assuming that the product demands are known and constant throughout day so that the only variation is in peak and off-peak power

pricing. The revenues generated by supplying product to customers are the same in each period, and the objective minimizes operating costs associated with power usage as given by,

$$\min \mathbb{O} \quad = \quad \sum_{n=1}^{4} P_n^E \left(W_n^C + W_n^L \right) \tag{5.16}$$

where P_n^E is the price of electricity in the n^{th} period. Note that other costs associated with delivery and transportation could be included in the above function; however, they do not directly affect the optimal operating strategy of the process.

Two different operating strategies are compared. In the first strategy, the operating conditions are assumed to be constant over the entire day. The second strategy is the multiperiod formulation where the operating conditions are allowed to change. This case study demonstrates that transitioning among different operating conditions can reduce the operating costs compared with constant operation.

These two cases are formulated using the AMPL modeling language [114] and solved using IPOPT [20]. It is assumed that the constant product demands in each period for nitrogen, argon, and oxygen are 25920 kmol, 187 kmol, and 6843 kmol, respectively. Five main manipulated variables are selected for optimization: the feed air stream of the HPC, U_1, the feed air stream of the LPC, U_2, the reflux flow from the HPC to the LPC, U_3, the waste nitrogen stream, U_4, and the side withdrawal from the LPC to the CAC-1, U_5. Figure 24 shows the profiles of the air feed flow and production rates for both the constant case (solid line) and the multiperiod case (dashed line). As expected, the desired feed flowrate (and hence the load on the plant) is lowest when the price of electricity is the highest and vice versa. The optimal transition times over the four periods are (5:49-7:21, 10:49-12:00, 18:00-18:18, and 21:54-0:19). Given the high cost of electricity in the third period, the optimal transition times are such that the lowest feed flow rate is utilized over this entire

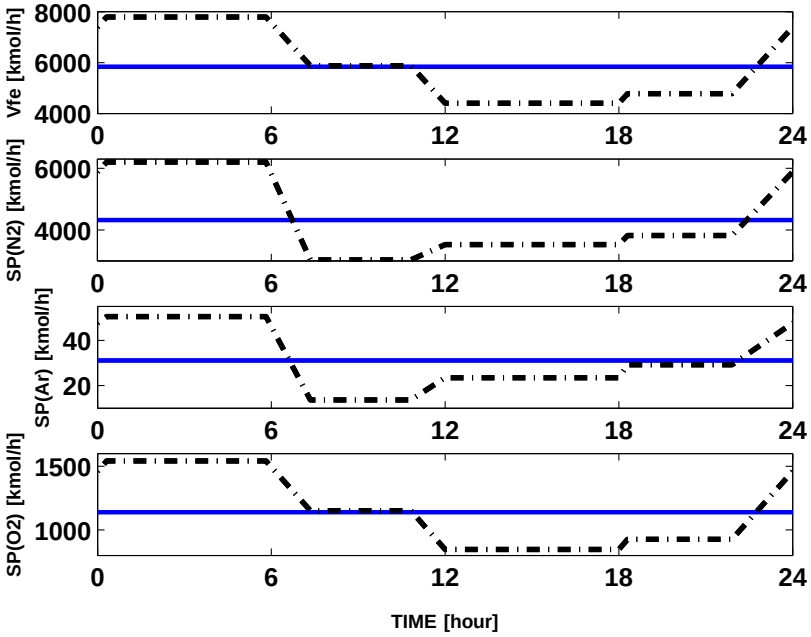

Fig. 24. Profiles for Total Air Feed Flow Rate (Vfe) and Production Rates of Each Component (SP). The Solid Lines Represent the Optimal Values When Operating Conditions Are Forced to Be Constant, and the Dashed Lines Represent the Multiperiod Solution

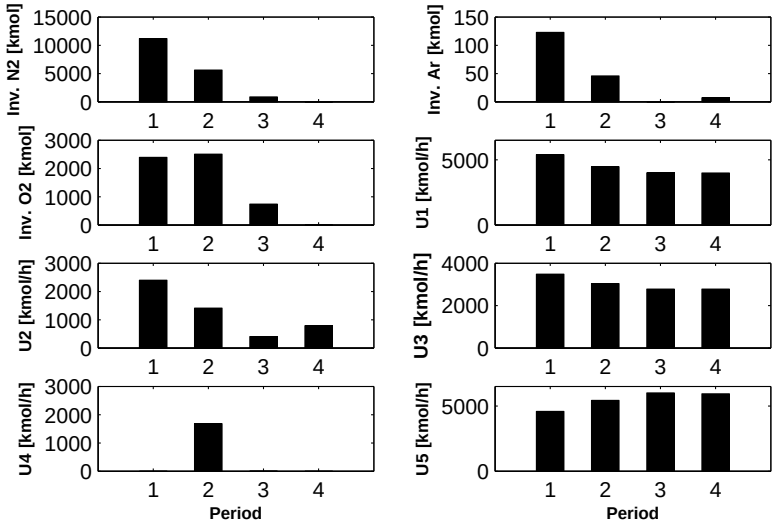

Fig. 25. Optimal Results for Inventory Levels (inv) and Manipulated Variables (U) in the Multiperiod Case

period. The optimization has effectively determined, not only the operating conditions within each period, but also the specific time to start and end each transition. The variation in these times demonstrates the importance of including these degrees of freedom instead of specifying fixed transition points. For the multiperiod case, Figure 25 shows the inventory levels at the end of each period and the values for the manipulated variables. In this case study, the product demands were kept constant. Therefore, to meet these demands throughout the day, the optimal inventory levels for each of the three products are highest before their lowest production rate. Comparing these two test cases, there is an overall savings of 5.11% in the total operating costs if we allow multiperiod operation instead of operating at a fixed steady state. This represents a significant savings for an air separation plant where operating costs can be very high. Furthermore, the possible savings are a direct function of the gap between high and low electricity prices. There is potential for increased savings in cases where variability in electricity pricing is higher.

D. Optimal Operating Strategy under Uncertain Product Demands

In addition to variability in power prices, in certain gas product markets air separation plants may need to switch operating conditions to satisfy variable product demands from different customers. Furthermore, the actual demand for specific products may not be known a priori. In this section, we focus on a multiperiod problem formulation that considers optimal operating plans for air separation processes with variable (but known) electricity prices and uncertain product demands.

Uncertainty in product demands has a direct effect on expected revenue and, hence, profits. Furthermore, contractual obligations may place constraints on the amount of demand that must be met. As described by Li et al [103] and Nahmais et

al [104], we use the loss function to evaluate the expected revenue and, assuming a Type 2 service level, formulate probabilistic fill-rate constraints on customer demands. In this section, we describe the necessary changes to the multiperiod formulation and show how the solution is affected by increasing demand uncertainty.

In any given time period, the actual amount of product sold to customers is the minimum of the customer demand and the available product (production plus available inventory). Therefore, the objective function includes the expected revenue from sale of product i in time period n, and the operating costs, as given by,

$$\max \mathbb{P} \quad = \quad \sum_{n=1}^{4} \sum_{i \in \mathcal{P}} Rev_{i,n} - \sum_{n=1}^{4} P_n^E \left(W_n^C + W_n^L \right), \tag{5.17}$$

where the expected revenue is,

$$Rev_{i,n} \quad = \quad \mathbf{E}_{\hat{D}_{i,n}} \left[P_i^P \cdot \mathbf{min} \left(\hat{S}_{i,n}, \hat{D}_{i,n} \right) \right], i \in \mathcal{P}, n \in (1,2,3,4). \tag{5.18}$$

The available supply of product i in period n is given by,

$$\hat{S}_{i,n} = \begin{cases} \Phi_{i,n}^L + I_{i,n-1} & n \in (2,3,4) \\ \Phi_{i,1}^L + I_{i,4} & n = 1. \end{cases} \tag{5.19}$$

The parameters, P_i^P, are the known prices for the i^{th} product, which are assumed constant throughout the day. Here, we assume that the prices of nitrogen, argon, and oxygen products are \$0.113/L, \$0.286/L, and \$0.176/L, respectively [107, 108]. The variables, $\hat{D}_{i,n}$, are the uncertain demands of the i^{th} product in the n^{th} period.

Defining $\rho\left(\hat{D}_{i,n}\right)$ as the density function of the uncertain demand, the revenue

can be written as,

$$\begin{aligned} Rev_{i,n} &= P_i^P \int_0^{+\infty} \rho\Big(\hat{D}_{i,n}\Big) \cdot \mathbf{min}\left(\hat{S}_{i,n}, \hat{D}_{i,n}\right) d\hat{D}_{i,n} \\ &= P_i^P \left(\int_0^{\hat{S}_{i,n}} \rho\Big(\hat{D}_{i,n}\Big) \hat{D}_{i,n} d\hat{D}_{i,n} + \int_{\hat{S}_{i,n}}^{+\infty} \rho\Big(\hat{D}_{i,n}\Big) \hat{S}_{i,n} d\hat{D}_{i,n} \right) \\ &= P_i^P \left(\theta_{i,n} - \int_{\hat{S}_{i,n}}^{+\infty} \left(\hat{D}_{i,n} - \hat{S}_{i,n}\right) \rho\left(\hat{D}_{i,n}\right) d\hat{D}_{i,n} \right), \\ i &\in \mathcal{P}, n \in (1,2,3,4) \end{aligned} \tag{5.20}$$

where the mean of the uncertain product demand, $\theta_{i,n}$, is equal to $\int_0^{+\infty} \rho\Big(\hat{D}_{i,n}\Big) \hat{D}_{i,n} d\hat{D}_{i,n}$. The expression, $\int_{\hat{S}_{i,n}}^{+\infty} \rho\Big(\hat{D}_{i,n}\Big) \left(\hat{D}_{i,n} - \hat{S}_{i,n}\right) d\hat{D}_{i,n}$ is called the loss function. If the demands are assumed normally distributed with the mean, $\theta_{i,n}$, and the deviation, $\sigma_{i,n}$, the loss function can be expressed by

$$\begin{aligned} &\int_{\hat{S}_{i,n}}^{+\infty} \rho\Big(\hat{D}_{i,n}\Big) \left(\hat{D}_{i,n} - \hat{S}_{i,n}\right) d\hat{D}_{i,n} \\ &= \sigma_{i,n} \int_{\frac{\hat{S}_{i,n} - \theta_{i,n}}{\sigma_{i,n}}}^{\infty} \left(\tau - \frac{\hat{S}_{i,n} - \theta_{i,n}}{\sigma_{i,n}} \right) \frac{1}{\sqrt{2\pi}} e^{\frac{-\tau^2}{2}} d\tau \\ &= \sigma_{i,n} \mathcal{L}\left(\frac{\hat{S}_{i,n} - \theta_{i,n}}{\sigma_{i,n}} \right), i \in \mathcal{P}, n \in (1,2,3,4), \end{aligned} \tag{5.21}$$

and finally the expected revenue is written as,

$$Rev_{i,n} = P_i^P \left(\theta_{i,n} - \sigma_{i,n} \mathcal{L}\left(\frac{\hat{S}_{i,n} - \theta_{i,n}}{\sigma_{i,n}} \right) \right), i \in \mathcal{P}, n \in (1,2,3,4). \tag{5.22}$$

Here, $\mathcal{L}(\cdot)$ is defined as the standardized loss function. From equation (5.22), the expected amount of product i sold to customers in period n is $\theta_{i,n} - \sigma_{i,n} \mathcal{L}\left(\frac{\hat{S}_{i,n} - \theta_{i,n}}{\sigma_{i,n}}\right)$. The numerical integration of the standardized loss function can be expressed by piecewise polynomial functions [103].

Since we are now considering the expected value for product sales, the inventories

are expected values as well, as defined by,

$$I_{i,n} = \hat{S}_{i,n} - \left(\theta_{i,n} - \sigma_{i,n}\mathcal{L}\left(\frac{\hat{S}_{i,n} - \theta_{i,n}}{\sigma_{i,n}}\right)\right), i \in \mathcal{P}, n \in (1,2,3,4). \tag{5.23}$$

In addition to the impact on expected profit, uncertain demands may have an impact on customer satisfaction levels if the plant is not able to deliver the desired product amounts. Two types of customer service levels have been described[103, 104], where customer satisfaction is measured by whether or not actual customer demands are met in a given interval. The Type 1 service levels (called confidence levels) have been adopted in the application of chance-constrained programming [103, 105], and can be written as

$$Pr_{\varphi}\{\Psi^{i}(\varphi_i) \geq 0\} \geq \alpha_i \tag{5.24}$$

where α is the confidence level decided by managers. This type of formulation ensures that customer demand will be satisfied with a given probability; however, it does not consider the magnitude of the deficit when the demand is not met.

In this paper, we consider Type 2 service levels. The Type 2 service level (also called the fill-rate) measures the expected fraction of demand that can be met by a plant. The Type 2 service level is typically more consistent with actual contracts [104]. Here, the expected sales of product i is constrained to be at least some fraction of the expected demand [103], as given by,

$$\theta_{i,n} - \sigma_{i,n}\mathcal{L}\left(\frac{\hat{S}_{i,n} - \theta_{i,n}}{\sigma_{i,n}}\right) \geq \beta_{i,n}\theta_{i,n} \tag{5.25}$$

where β is the fill-rate specified in the contract.

To handle demand uncertainty, the original multiperiod formulation is modified as follows. The fill-rate constraints (5.25) are added, the original inventory constraints (5.14) and (5.15) are replaced with (5.23), and the objective function is changed to

Table VII. Mean Product Demands and Fill-rate over Four Time Periods

	Period 1	2	3	4
θ_{N_2}, kmol	20736	25920	33696	25920
θ_{Ar}, kmol	150	187	243	187
θ_{O_2}, kmol	5474	6843	8896	6843
$\beta_{N_2,n}$,	60%	70%	90%	70%
$\beta_{Ar,n}$,	60%	70%	90%	70%
$\beta_{O_2,n}$,	60%	70%	90%	70%

that described in equation (5.17). Assuming a known distribution for the product demands, this probabilistic formulation can be solved to maximize expected profits while maintaining contractual obligations.

Here, we assume that the product demands are normally distributed with known mean and standard deviation obtained from statistical analysis of historical data. In this section, we demonstrate that the multiperiod formulation can be solved efficiently while considering this demand uncertainty. Table VII shows the values for the mean demands and the fill-rates.

Table VIII. Results for Different Standard Deviations in Argon Demand

	$\sigma_{N_2}/\theta_{N_2}$	$\sigma_{O_2}/\theta_{O_2}$	σ_{Ar}/θ_{Ar}	Optimal Obj.
Case 3	20%	20%	15%	\$ $5.42 \cdot 10^5$
Case 4	20%	20%	17.5%	\$ $5.42 \cdot 10^5$
Case 5	20%	20%	18%	\$ $5.39 \cdot 10^5$

In the next three case studies, the standard deviation in the uncertain demand

of argon is varied from 15% to 18% while nitrogen and oxygen are kept constant at 20%, as seen in Table VIII.

Table VIII also shows the optimal objective value for each of these case studies. There is almost no difference in the optimal objective value between case study 3 and 4. This implies that the fill-rate constraint for argon is not active and that the process is able to meet the customer satisfaction constraints with optimal operating conditions based on profit considerations alone. As seen in case study 5, increasing the standard deviation of argon from 17.5% to 18% causes a reduction in the optimal objective value. Here, the fill-rate constraint for argon in period 3 becomes active and profits suffer because of the need to meet customer satisfaction levels. Solving different case studies and examining the values of the constraint multipliers corresponding to the fill-rate constraints allows managers to effectively evaluation the contractual obligations and their impact (at least locally) on profits. In addition to this analysis, the formulation also provides an optimal multiperiod operating strategy, including operating conditions and transition times.

In this example, if we increase the standard deviation on the argon demand to 20%, the optimization problem becomes infeasible, indicating that the current plant is not able to meet the customer satisfaction constraints with this level of uncertainty. This is important information for managers, showing the challenges associated with increased uncertainty. At this point, management has few choices to deal with the increased uncertainty. They can try to find additional resources or seek to increase facility capacity in order to meet customer requirements. Management may also choose to negotiate different contracts, guaranteeing lower uncertainty in product demands or reducing required fill-rates. Detailed case studies addressing the effect of varying fill-rates have been discussed in our previous work (Chapter IV). Of course, selection of values for fill-rates needs to account for multiple product interactions. In

this particular case study, reducing the fill-rate for argon in period 3 from 90% to 80% makes the problem feasible again, with an optimal objective value of $\$ 5.30 \cdot 10^5$.

This case study illustrates the potential tradeoffs between profit and customer satisfaction levels in the face of uncertainty and variable power pricing. More importantly, this multiperiod formulation gives engineers an effective tool to analyze these tradeoffs using a rigorous model of their facility.

E. Conclusions and Future Work

Because of external pressures like variable power prices and product demands, it can be profitable to vary operating conditions regularily, instead of operating at a fixed steady state. This paper presents a multiperiod formulation to determine optimal operating strategies for an energy-intensive air separation plant. In particular, the results demonstrate that a rigorous nonlinear model can be used in a mathematical programming formulation addressing both variability in inputs and uncertainty in desired product demands. The formulation contains a rigorous mathematical model for the highly-coupled air separation process including four coupled distillation columns, heat exchanges, compressors, and liquifiers. Transitions were not assumed to be instantaneous, but rather are assumed to be proportional to the required load change. Furthermore, the optimization variables include the operating conditions in each period as well as the start time for each of the transitions. Uncertainty is addressed through use of the loss function in both the objective function and in fill-rate constraints on supplied product. The loss function is used to express the expected value of the plant revenue, and provide a means to constrain customer satisfaction levels. Because uncertainty exists on the process outputs only, this approach allows a

probabilistic treatment without the need for a multiscenario formulation.

This formulation is used in several case studies to illustrate the effectiveness of the approach. As described in the first two case studies, the formulation can easily and rigorously determine the potential for improved profits comparing the optimal steady state case with the optimal multiperiod operating strategy. In the case study presented, multiperiod operation resulted in a five percent reduction in operating costs, however, increased savings are possible when power pricing variability is higher. The final four case studies consider uncertainty in product demands and, in particular, increased uncertainty in argon demand. These case studies illustrate that the approach can effectively handle this uncertainty, while providing management with valuable information regarding the tradeoff between profit and contractual obligations. It can be used to provide effective bounds on the level of uncertainty that can feasibly be addressed by the plant. Furthermore, since the formulation uses a rigorous process model, the approach provides facility specific operating strategies.

The multiperiod formulation presented in this paper uses a rigorous model of the air separation plant, however, modern nonlinear programming tools can obtain solutions very efficiently. The six case studies in the paper all contained over 3500 variables and solved in under ten seconds on a 3.2 GHz Intel Xeon processor.

Future work will include extending this formulation to include a rigorous dynamic model of the air separation process. We have previously developed a rigorous dynamic optimization formulation for optimal load changes in air separation processes [85]. This formulation can be extended to include variable power pricing and uncertainty in product demands. Furthermore, control strategies (e.g. model predictive control) could be included in the formulation to realistically describe the required switching time. Parallel nonlinear programming algorithms may be necessary to ensure efficient solution of these large-scale problems.

CHAPTER VI

DYNAMIC OPTIMIZATION UNDER UNCERTAINTY

A. Introduction

Optimal planning under uncertain product demands and different customer satisfaction levels is discussed in Chapter IV, while optimal operating strategies under varying power pricing are investigated in Chapter V. However, the models in these two chapters are steady state and not any dynamic. The assumption of instantaneous transient limits the performance of mulitperiod optimization in Chapter IV. Of course, it can provide rough forecast of long-term optimal planning and scheduling strategies while considering customer satisfactions. Since the assumption of instantaneous transient is not practical, Chapter V included a linear relationship between the load change and the transient time.

In this chapter, we want to adopt rigorous dynamic model of cryogenic air separation columns rather than the steady state models used in Chapter IV and Chapter V. We seek to find optimal control profiles to transition from one operating condition to another. This problem is challenging for these main reasons. First, the dynamic ASC process model is represented by a large set of differential constraints. Using the simultaneous discretization approach, the differential constraints are converted to a set of algebraic constraints, producing a very large nonlinear programming problem. Second, the air separation process contains significant mass and energy integration. The high and low pressure columns are directly heat integrated. Multiple Argon columns are increasingly used, introducing significant coupling through recycle flows. The behavior of these integrated systems is highly nonlinear. Third, uncertainties during transition also challenges optimal control strategies. Uncertainty is an inher-

ent characteristic of any process system. Many uncertainties are present in such large scale ASC process and have been classified in references [67]. These uncertainties always not only cause serious mismatch between the true process and the model but also have a large influence on optimal control strategies.

Therefore, it is necessary to design effective control strategies for dynamic transition of ASC systems under uncertainty. There are several publications on advanced control of air separation systems [83, 84, 78, 81, 80]. However, few of them consider uncertainty in their control system. By means of our parallel nonlinear algorithm discussed in Chapter II, this work focuses on obtaining dynamic open-loop optimal control trajectories for a load change with an uncertain pressure drop discussed in the LPC.

The structure of the air separation system is the same as the one in Chapter III and Chapter IV, with three high coupled distillation columns. More detailed information about this process can be found in Figure 3. Some nominal operation conditions of the ASC system under study are listed in Table IX.

B. Dynamic Model of the Cryogenic Air Separation Process

Our dynamic model for the air separation process builds off of previous research [83, 84, 89, 80]. Three assumptions are made in this study: 1. complete mixing on each tray and 100% tray efficiency; 2. Negligible heat losses in the tray; 3. Constant pressure drop on each try. The model is based on a first-principle approach including mass, energy balances coupled with the equilibrium relationships and hydraulic equations.

Table IX. Nominal Operation Conditions of Dynamic Optimization in Cryogenic ASC Systems

Process Variables	Values
Total air input, mol/s	2817
Waste Nitrogen stream, mol/s	471.05
Gas Oxygen product output, (VO2), mol/s	330.65
Liquid Oxygen product output, (LO2), mol/s	180.64
Oxygen product purity	$\geq$98%
Nitrogen product output, (VN2), mol/s	1820
Nitrogen product purity	$\geq$99.99%
Argon product output, (VAR), mol/s	14.66
Argon product purity	$\geq$97%
Pressure on the top of LPC, MPa	0.13
Pressure on the top of HPC, MPa	0.68
Pressure on the top of CAC, MPa	0.12

1. Mass Balances

$$\begin{aligned}
\frac{\mathrm{d}\left(M_j x_{i,j}\right)}{\mathrm{d}t} &= V_{j+1}y_{i,j+1} + L_{j-1}x_{i,j-1} + F_j^V z_{i,j}^V + F_j^L z_{i,j}^L \\
&- \left(V_j + S_j^V\right)y_{i,j} - \left(L_j + S_j^L\right)x_{i,j} - x_{i,j}\frac{\mathrm{d}M_j}{\mathrm{d}t} \qquad (6.1) \\
\frac{\mathrm{d}M_j}{\mathrm{d}t} &= V_{j+1} + L_{j-1} + F_j^V + F_j^L - \left(V_j + S_j^V\right) - \left(L_j + S_j^L\right) \qquad (6.2)
\end{aligned}$$

where j is the index of each tray from the top of each column, and $i \in \mathcal{P}$ is the index of the product set of Nitrogen, Argon, and Oxygen. F_j^V and F_j^L are the vapor and liquid molar feed flows entering into the j^{th} tray. S_j^V and S_j^L are the vapor and liquid

molar side flows out of the j^{th} tray. The vapor and liquid flow rates are given by V_j and L_j, respectively. The liquid and vapor compositions are given by $x_{i,j}$ and $y_{i,j}$ respectively. $z^V_{i,j}$ and $z^L_{i,j}$ are the vapor and liquid compositions of feed flows entering into the j^{th} tray. M_j is the liquid holdup. Note that if there are no feed or side flows to the j^{th}, the relevant terms must be removed.

2. Energy Balances

$$\begin{aligned} \frac{\mathrm{d}\left(M_j H^L_j\right)}{\mathrm{d}t} &= V_{j+1}H^V_{j+1} + L_{j-1}H^L_{j-1} + F^V_j H^{FV}_j \\ &+ F^L_j H^{FL}_j - \left(V_j + S^V_j\right)H^V_j - \left(L_j + S^L_j\right)H^L_j \end{aligned} \tag{6.3}$$

where H^{FV}_j and H^{FL}_j are the vapor and liquid enthalpies of feed flows entering into the the j^{th} tray. The vapor and liquid enthalpies of the j^{th} tray are given by H^V_j and H^L_j respectively. All above enthalpies are calculated based on relevant temperature, pressure, compressibility factors and binary interaction parameters. Note that the above differential energy equations make the DAE system index 2 which is not easily solved. Therefore, the same method as reported in references [83, 84] is adopted in order to reduce this system to index 1 by converting the above differential equation to an algebraic equation.

3. Hydraulic Equation

A Francis-weir relationship was utilized [89].

$$L_j = 11988 l_{w,j}\rho_{l,j}\left(h_{ow,j}\right)^{1.5} \tag{6.4}$$

$$h_{ow,j} = M_j/\left(\rho_{l,j}A_{act,j}\right) - h_{w,j} \tag{6.5}$$

where l_w is the weir length, ρl is the liquid molar density, h_{ow} is the height of the liquid over weir, A_{act} is the available area on the tray, and h_w is the weir height.

4. Summation Equation

$$\sum_{i \in \mathcal{P}} y_{i,j} = 1 \tag{6.6}$$

5. Vapor-liquid Equilibrium

$$y_{i,j} = \gamma_j K_{i,j} x_{i,j} \tag{6.7}$$

$$K_{i,j} = \exp\left[A_i - \left(B_i / \left(T_j + C_i\right)\right)\right] / P_j \tag{6.8}$$

$$\log \gamma_{1,j} = \left(\frac{A_{1,3} x_{3,j}^2 + A_{1,2} x_{2,j}^2 + \left(A_{1,3} + A_{1,2} - A_{2,3}\right) x_{3,j} x_{2,j}}{R T_j} \right) \tag{6.9}$$

$$\log \gamma_{2,j} = \left(\frac{A_{1,2} x_{1,j}^2 + A_{2,3} x_{3,j}^2 + \left(A_{1,2} + A_{2,3} - A_{1,3}\right) x_{1,j} x_{3,j}}{R T_j} \right) \tag{6.10}$$

$$\log \gamma_{3,j} = \left(\frac{A_{1,3} x_{1,j}^2 + A_{2,3} x_{2,j}^2 + \left(A_{1,3} + A_{2,3} - A_{1,2}\right) x_{1,j} x_{2,j}}{R T_j} \right) \tag{6.11}$$

The activity coefficients $\gamma_{i,j}$ are calculated using the Margules equations equation and $K_{i,j}$ is the ideal vapor-liquid equilibrium constant calculated by Antoine equation. T_j and P_j are the temperature and pressure of each tray in each column. The Margules and Antoine constants can be found in references [90].

6. Pressure Equation

$$\frac{\mathrm{d}P_{top}}{\mathrm{d}t} = \left(\frac{R T_{avg}}{V_{tot}} \right) \left(V_{top} - L_c - V_{draw}\right) \tag{6.12}$$

$$P_j = P_{j-1} + \Delta P \tag{6.13}$$

where P_{top} is the pressure at the top of each column. T_{avg} is the average column temperature. V_{tot} is the total column volume, V_{top} is the vapor flow rate from the top stage of the column. L_c is the condensation rate at the top of the column and V_{draw} is the product vapor draw rate from the top of the column. We assume that the feed flow rates of each column depend on the upstream pressure and the column pressure when these flows pass through the compressor, the expansion turbine, and the throttling valves. Opposed to previous research [84, 80] where pressure holdup is negligible, pressure dynamics are considered in this work to better capture the dynamic behavior. Here, the pressure at the top of the column is calculated from a differential equation. The remaining stage pressures are calculated using a constant pressure drop per stage [89]. Note that pressure drop across each tray, ΔP, is constant in the same column but differs between columns.

7. Heat Integration

The combined condenser/reboiler is assumed to be an additional normal tray for both the HPC and the LPC. In combined condenser/reboiler, the energy that is being transferred can be calculated by Equ. (6.14). This energy is extracted from the condensing vapor stream at the top of the HPC and is released into the vapor stream at the bottom of the LPC. Similarly, the condenser of the CAC is heat integrated with the oxygen-rich stream from the bottom of the HPC. The relevant energy transferred in the condenser of the CAC can be calculated by Equ.(6.15). This energy is extracted from the condensing vapor stream at the top of the CAC and released into a portion of liquid oxygen-rich stream from the HPC.

$$Q_1 = UA_1 \left(T_1^{HPC} - T_{70}^{LPC}\right) \tag{6.14}$$

$$Q_2 = UA_2 \left(T_1^{CAC} - T_{in}^{HPC}\right) \tag{6.15}$$

8. Safety Inequality Constraints

During operating changes, the main safety constraints are concentration and flow rate limits for normal operation of the CAC. As a result of the poor operation, significant quantities of nitrogen may enter the crude argon column. The nitrogen, being the more volatile of all the components, will concentrate at the top of column and form a non-condensible mixture, which disrupts the column operation [69]. Therefore, the nitrogen purity of feed flow from the LPC to the CAC is restricted to be less than 0.1%. The range of argon and oxygen purities for this feed flow are $8 - 10\%$ and $90 - 91\%$ respectively.

C. Simultaneous Dynamic Optimization Approach

In this case study, we focus on determining robust optimal control trajectories for a change in oxygen production from 100% to 70%, considering uncertain pressure drops. Nitrogen, argon and oxygen production rates are treated as controlled variables. There are five main manipulated variables are selected: the feed air stream of the HPC, U_1, the feed air stream of the LPC, U_2, the reflux flow from the HPC to the LPC, U_3, the waste nitrogen stream, U_4, and the side withdrawal from the LPC to the CAC, U_5. Given the specifications presented in the previous section, the

multi-scenario-based optimal control problem with uncertainty can be formulated as

$$
\begin{aligned}
\min_{U(t)} \quad & \sum_{q=1}^{NS} w_q \int_0^{t_f} \left(y\left(t\right) - y^S\right)^{\mathrm{T}} \mathrm{V}_y \left(y(t) - y^S\right) \\
& + \left(U\left(t\right) - U^S\right)^{\mathrm{T}} \mathrm{V}_u \left(U\left(t\right) - U^S\right) \mathrm{d}t \\
s.t. \quad & F_q(\frac{\mathrm{d}x_q(t)}{\mathrm{d}t}, x_q(t), y_q(t), z_q(t), U(t), m_q, p) = 0 \\
& G_q(x_q(t), y_q(t), z_q(t), U(t), m_q, p) = 0 \\
& x_q(0) = x^0 \\
& x^L \leq x_q(t) \leq x^U \\
& y^L \leq y_q(t) \leq y^U \\
& z^L \leq z_q(t) \leq z^U \\
& U^L \leq U(t) \leq U^U
\end{aligned} \tag{6.16}
$$

where $U\left(t\right)$ is a vector of manipulated variables. We wish to find a single control profile that is robust to the uncertainty in the pressure drop. Therefore, we seek a single control profile that is feasible over all scenarios. Once discretized, this discretized control profile becomes the common variables in the multiscenario formulation. The variable, $y_q\left(t\right)$ is a vector of controlled variables in scenario q, while y^S and U^S are the set-points for the controlled variables and manipulated variables respectively. F_q and G_q are differential and algebraic equation (DAE) constraints in each scenario including differential state vectors, $x_q(t)$, algebraic state vectors excluding controlled variables, $z_q(t)$, uncertain parameter vectors, m_q, and the time-independent parameter vector without uncertainty, p. The initial values of x_q in each scenario are given by x_0, and w_q is the weighting coefficient of each scenario. V_y and V_u denote diagonal weighting matrices.

Again, we selected the simultaneous discretization approach in which the state

and control variables are fully discretized using collocation techniques. In this work, the simultaneous orthogonal collocation-based discretization approach is adopted, using 20 finite element and Radau collocation points.

D. Optimal Control Results

In this study, the pressure drop of each tray in the LPC which may vary from 145 to 185 Pa is assumed to be uncertain. The range is discretized by selecting 8 points assuming uniform distribution. Five manipulated variable profiles are selected as the common variables. One processor is used for each scenario corresponding to each pressure drop value. There are 600 differential and 2800 algebraic equations in each scenario. In the whole large scale problem,there are approximately 1,120,000 total variables including 300 common variables. The optimal control trajectories with and without considering uncertain pressure drops are shown in the Figure 26.

In Figure 26, influences of uncertain pressure drop in the LPC on the optimal control profile can be seen. The profiles of the feed air stream of the LPC, U_2, and the reflux flow from the HPC to the LPC, U_3, and the Waste nitrogen stream, U_4 are significantly different from the nominal profiles, while the trajectories of the feed air stream of the HPC, U_1 and the side withdrawal from the LPC to the CAC have only small differences.

To demonstrate the scaleup efficiency of Schur-IPOPT in this case study, Figure 27 shows the computational timing results as a function of an increasing number of scenarios. As before, with the addition of each scenario, we allow use of another processor. It can be seen that the parallel approach significantly outperforms the serial approach. We can see that the scalability suffers as we approach 8 scenarios and processors. This is due to a bottleneck in memory bandwidth and much better

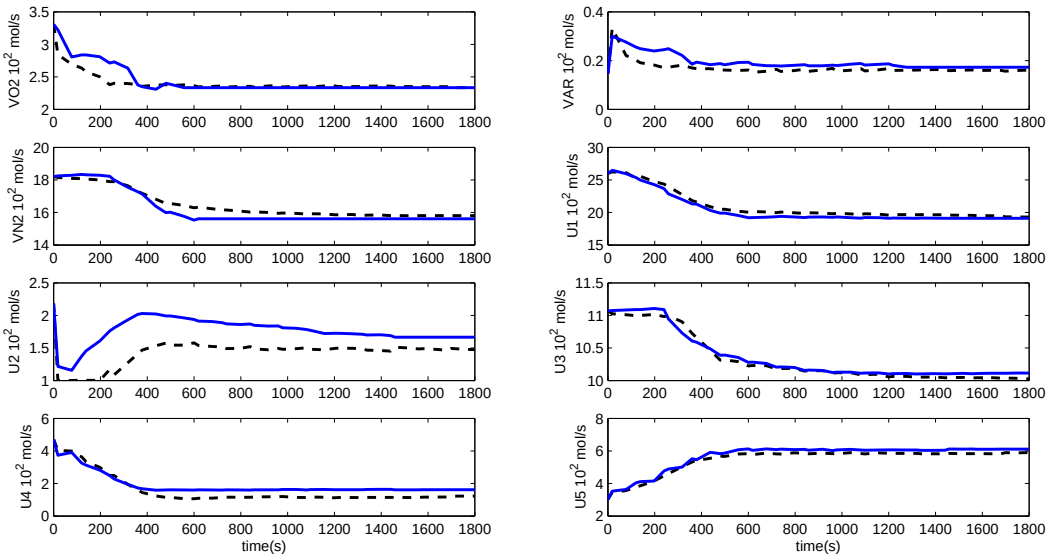

Fig. 26. Optimal Trajectories of Oxygen, Argon and Nitrogen Products, and Manipulated Variables under Nominal (Dashed) and Uncertain (Solid) Pressure Drops of the LPC.

scalability is expected on a distributed memory cluster.

The approach of this case study can be also extended for not only determining optimal shut-down and start-up strategies of air separation columns but also implementing effective and reliable nonlinear model predictive control.

E. Conclusions

Dynamic optimization under uncertainty using first-principle models for air separation units can provide more rigorous treatment of optimal operation when transient conditions occur. The optimal solution can be obtained quickly, meeting online requirements. Considering uncertain parameters can improve the actual optimal control performance.

Based on the parallel nonlinear programming algorithm proposed in Chapter II, large scale uncertain trajectory planning problem can be formulated as a multiscenario

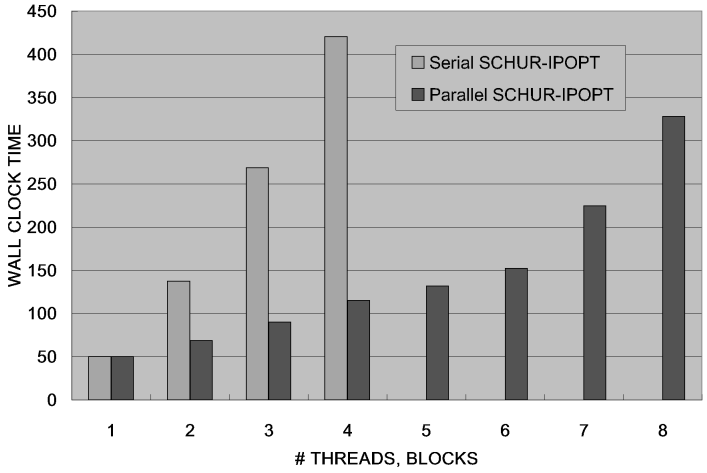

Fig. 27. Wall Clock Time per Iteration for Serial and Parallel Approaches of Optimal Control under Uncertainty

problem with common control profiles. The timing results also show the benefits of our parallel nonlinear algorithm in terms of computational efficiency.

CHAPTER VII

SPATIAL DECOMPOSITION OF CITY-WIDE PIPELINE NETWORK

The parallel nonlinear optimization algorithm proposed in Chapter II has been used in Chapter III, Chapter IV and Chapter VI, in order to solve steady state design, operation planning, and dynamic optimization under uncertainty. These applications identify the appropriateness of our approach for decomposing both multiscenario and multiperiod problems. Our parallel nonlinear optimization algorithm can be used under other problem decomposition methods as well. In this chapter, we focus on water demand estimation of a large scale network by adopting a spatial decomposition rather than a multiscenario or multiperiod decomposition.

A. Problem Description

As an important part of the water supply system, a water distribution network is a hydraulic infrastructure, including a set of pipes, pumps, and other hydraulic devices. There are significant challenges associated with successful operation of water distribution systems. Our problem is accurate characterization of real-time demands and network flow patterns. In this chapter, we focus on optimal demand estimation in a large-scale water distribution system using limited measurement information. In almost all cases, the number of uncertain demands greatly outnumbers the available measurement. As with most inverse formulation, the problem must be regularized. Every node in the network has an assumed demand based on historical monthly data and daily usage patterns. However, the true real-time demand will deviate from this value. Given spatially sparse measurements of flow and pressure, the goal is the estimate the real-time demand using the assume demands as regularization. This demand estimation can be formulated as a NLP problem. Nevertheless, efficient so-

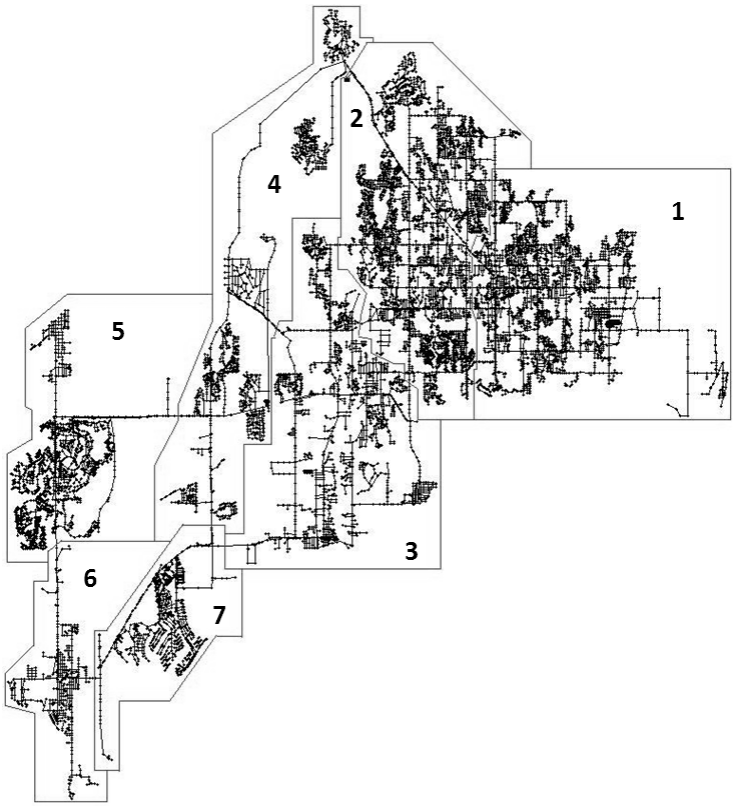

Fig. 28. Structure of Large Water Network with Seven Sub-parts

lution of this large scale estimation problem with a first-principle model is still quite challenging due to the large size of real municipal water networks.

In this section, we spatially decompose a real municipal water network into seven sub-networks and then adopt our proposed parallel NLP algorithm, to efficiently estimate water demands at each node. The network structure is shown in Figure 28. There are over 12500 nodes and 14800 pipelines in this water network.

B. Mathematical Formulation

The objective function minimizing the least-squares errors in measured flow and head, with a Tikhonov regularization. On the assumed demand as given by,

$$\min \alpha \sum_{i \in N_s} \left(d_i - d_i^B\right)^2 + \beta \sum_{j \in P_m} \left(f_j - f_j^M\right) + \gamma \sum_{i \in N_m} \left(h_i - h_i^M\right)^2, \tag{7.1}$$

where N_s is the set of all nodes, P_m is the set of all measured pipe flows, and N_m is the set of all measured node pressures. The variables d_i, f_j and h_j are the calculated demands, flows, and pressures respectively. the measured flows and pressures are given by f_j^M and h_i^M respectively, while d_i^B are the assumed values for the demands. The weights are assumed 10^2, 10^5, and 10^5, respectively.

For each junction node i, a continuity constraint should be met

$$\sum f_{j|\kappa_{j,i}=1} - \sum f_{j|\lambda_{i,j}=1} = d_i, \ \forall j \in P_s, \forall i \in N_s, \tag{7.2}$$

where $\kappa_{j,i}$ and $\lambda_{i,j}$ are the indices of connections between the j^{th} pipeline and the i^{th} node. When $\kappa_{j,i}$ equals to 1, the f_j is flow into the i^{th} junction. Similarly, when $\lambda_{i,j}$ equals to 1, the f_j is flow out of the i^{th} junction. P_s is the set of all pipes.

The head loss in each pipe is the head difference between connected nodes. The following Hazen-Williams equation is the most commonly used for hydraulics of head loss and adopted in this section.

$$\Delta H_j = \omega \frac{L_j \left(0.0022278|f_j|\right)^a}{\left(C_j\right)^a \left(D_j\right)^b}, \ \forall j \in P_s, \tag{7.3}$$

where ω is a coefficient assumed to be 4.727. C_j is Hazen-Williams roughness coefficient of the j^{th} pipe and a is a coefficient equal to 1.852. D_j is the j^{th} pipe diameter (ft) and b is a coefficient equal to 4.871. L_j is the j^{th} pipe length (ft).

The conservation of energy in each pipeline is given as

$$h^{in} - h^{out} = \Delta H_j, \tag{7.4}$$

where h^{in} and h^{out} are heads of the input and output nodes for any pipe, respectively.

The conservation of energy for pump is given by

$$h_P^{out} - h_P^{in} = \Delta E_P, \tag{7.5}$$

where h_P^{in} and h_P^{out} are heads of the input and output nodes for any pump, respectively. ΔE_P is the head increase through the pump and can be calculated by 7.6

$$\Delta E_P = \mu_1 + \mu_2 |f_P|^{\mu_3}, \tag{7.6}$$

where μ_1, μ_2 and μ_3 are coefficients equal to 46.7, -0.006212 and 1.31, respectively. f_P is the flow through the pump.

The minimum head constraint for each node is given as

$$h_i - e_i \geq h_i^{min}, \tag{7.7}$$

where h_i^{min} and e_i are the minimum required head and elevation of the i^{th} node.

C. Spatial Decomposition

In order to efficiently solve the above problem by our parallel NLP algorithm, the whole problem is spatially decomposed. Since some nodes have only one input and one output, we split the whole network by choosing such nodes.

Figure 29 shows how to split one-input-one-output node into different sub parts of network. In part (a), the pipelines $(j+1)^{th}$ and j^{th} are connected by the i^{th} node. The variables relative to the i^{th} node are head (h_i), demand (d_i), input (f_{j+1}) and

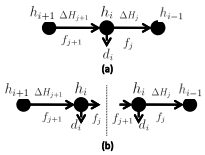

Fig. 29. Structure of Splitting Network by One-input-one-output Node: (a) Original Nodes Without Splitting; (b) Updated Nodes After Splitting

output (f_j) flow rates. In part (b), the left region does not have the information of the j^{th} pipeline, so needs output flow rate (f_j). Similarly, the right region needs input flow rate (f_{j+1}), while the h_i and d_i are commonly used by the left and right regions. Therefore, each split node leads to four common variables. In this work, 14 one-input-one-output nodes are selected to split the whole water network into 7 parts shown in Figure 28. Note that the sizes of sub-networks are different and 56 common variables are used to connect the sub-networks.

D. Numerical Results

EPANET [115] is adopted to build a simulation model for the above network in Figure 28. Parameter data and network structure are read from EPANET output files using Python and AMPL .dat files are written. The problem has 52,492 variables. Figure 30 shows the wall clock time per iteration for serial and parallel approaches. This problem requires 268 (s) of CPU time to solve using the serial approach, while the parallel approach with seven processors only requires 75 (s) of CPU time. These results clearly show the significant benefit provided by the parallel approach which saves 72% of the total calculation time.

Recall that the sizes of sub-networks are different. The largest sub-network has approximately 12,000 variables, while the smallest has approximately 4,500 variables. Therefore, the computational loads are different. It is possible that there is a better

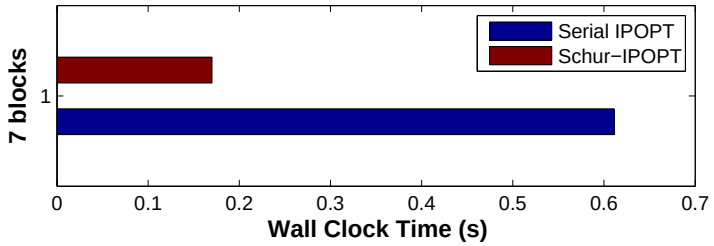

Fig. 30. Wall Clock Time per Iteration for Serial and Parallel Approaches

spatial separation which can provide improved load balancing, improving performance further.

This case study also demonstrates that our parallel nonlinear algorithm can be expected to effectively solve multi-unit problems based on spatial decomposition. In practical chemical processes, several units are always highly coupled together. Therefore, our proposed algorithm provides a feasible approach to decompose into individual units, while the linking information between units can be considered as common variables.

CHAPTER VIII

CONCLUSIONS

This dissertation was motivated by the need for effective problem formulation and efficient solutions of optimal design and operation problems with rigorous first-principle models under external disturbances and uncertain market factors. The incorporation of first-principle nonlinear models in process design and operation problem can reduce the mismatch between the true process and the model. Furthermore, a more rigorous and systematic treatment of uncertainty in process optimization can improve process profitability and flexibility.

However, the use of first-principle models in optimal process design and operations under uncertainty also results in several computational challenges. The objective of this dissertation has been to propose computational strategies including suitable model development, problem formulation and advanced numerical algorithms for overcoming some computational challenges. In this chapter, we summarize our contributions and present suggestions for future work.

A. Summary and Contributions

A brief description of motivation and challenges of nonlinear optimization with rigorous models is given in Chapter I. Some potential applications of large scale nonlinear optimization in the chemical engineering area are discussed according to the structure and relationship of process design and operations under uncertain and varying market demands. Nonlinear programming approaches can provide an effective tool to include information from both the process and the market simultaneously and obtain optimal reliable decisions in design and operation. Based on this structure, this dissertation focuses on conceptual design under uncertainty (Chapter III), mul-

tiperiod steady state optimal operating strategies with uncertainty and contractual constraints (Chapters IV and V), dynamic optimization under uncertainty (Chapter VI), and parameter estimation (Chapter VII) as case studies to demonstrate that effective formulation and advanced parallel algorithms can provide significant computational efficiency and handle the emerging challenges of NLP applications in the chemical engineering area.

In Chapter II, advances in interior-point NLP algorithms were compared with the classical SQP approach. The main computational cost of interior-point NLP algorithms, like IPOPT is the solution of large linear systems at each iteration arising from a Newton step on the primal-dual optimality conditions. We developed a parallel nonlinear programming algorithm based on general IPOPT package using an internal schur-complement decomposition. To illustrate the benefit of this proposed algorithm, we solved several different large-scale chemical process problems.

1. Summary of All Case Studies

As one important application of our parallel nonlinear algorithm, conceptual design under uncertainty is investigated in detail and we have presented the following contributions:

- A multiscenario problem formulation is developed to handle desire under uncertainty of a highly coupled air separation process and a heat-integrated distillation column. To our knowledge, this is the most rigorous air separation model that has ever been used for design under uncertainty in a simultaneous NLP framework. Improved model rigor levels to reduce mismatch between the process plant and the model.

- In addition to the treatment of uncertainty we have demonstrated that modern nonlinear programming tools can address complex design problems including constants a controllability by adopting RGA and condition number methods.

- We have develop a parallel nonlinear programming approach that can effectively tackle these large scale multiscenario problems (We have shown oven 1500 scenario for the heat-integrated distillation column.) Scalability is excellent for these problem classes.

In Chapters IV and V, we have seen that optimal operating single and multiperiod strategies of cryogenic air separation units can be obtained by solving large scale NLP problems. Compared with previous research on this area, we adopt a rigorous nonlinear model with three highly coupled distillation columns rather than a simplified linear model. Furthermore, the the Type 2 service level is adopted as a measure of the customer satisfaction levels, and contractual constraints are integrated into the optimization. Such integration provides an effective tool to consider the trade-off between profitability and customer satisfaction levels. In additions, the following contributions have been made:

- Based on contractual constraints, a formulation and solution procedure has been developed to identify different operating regions and visibly select suitable contractual obligations. Optimal operating conditions within the Profit Defined Region (PDR) are determined by profit considerations alone, and customer satisfaction constraints do not dictate operation. In the Fill-rate Constrained Region (FCR), the contractual constraints become active and profits begin to suffer. The Infeasible Region (IR) space can help the management identify the capacity limitations of a plant under increasing customer satisfaction levels where inventory and other resources should be considered and used.

- This formulation simultaneously considers contractual constants on multiple interesting products. Inventory control is investigated and optimal operating policies are developed to handle uncertain product demands.

- The Schur-complement decomposition approach provides an efficient parallel computing strategy. Rather than the multi-scenario method used by design under uncertainty in Chapter III, the problem is decomposed into different time periods. The production rates, feed rates, and inventory information are selected as the common variables to link the different sub-problems (time periods). It has been demonstrated that this parallel NLP algorithm has very good scalability as the size of the problem increases.

Chapter V focuses on optimal operation among different operating conditions considering variability in electrical prices and uncertain product demands. In this chapter, we have presented the following contributions:

- Both constant and uncertain product demands are studied in detail. It has been demonstrated that suitable switching operating conditions can have higher energy efficiency compared with a fixed steady state operation.

- Peak and Off-peak power pricing is considered in this chapter to get optimal daily operating strategies including feed load, production rates and inventory levels of three different products, as well as starting and ending time of process transitions. A linear relationship between load changes and transient time is adopted and formulated to replace instantaneous switching assumption.

- A rigorous model, safety constraints, and economic evaluation, are included within this multiperiod formulation.

Parameter uncertainty has a significant impact on the performance of large scale dynamic processes. Chapter VI is motivated by the desire for improving the performance of dynamic optimization of operating strategies under uncertainty. Contributions of this chapter include:

- A rigorous dynamic model of a highly integrated air separation process has been developed, including **600** differential and **2800** algebraic equations. To our knowledge, this the largest dynamic model of an air separation process that has been optimized using the simultaneous approach while considering uncertainty.

- Uncertainty is handled with a multiscenario approach where control profiles are selected as common variables across scenarios. Our parallel NLP algorithm is able to efficiently solve this extremely complex dynamic control problem including **1,120,000** variables.

Chapter VII focuses on the parameter estimation of unknown water demand in a city-wide water distribution network. In this chapter, we have presented the following contributions:

- We have built a first-principle hydraulic model of a large water distribution system. To our knowledge, this is the largest water network model that has been optimized using a simultaneous framework.

- In this chapter, we demonstrate that our parallel approach is effective for spatial decomposition of large networks. This approach is expected to handle plant-wide problems, decomposing at the unit level.

2. Challenges and Experience

In this subsection, we are interested in discussing some challenges we need to pay much attention to in future large scale NLP problems with rigorous models while providing some experiences on handling these challenges.

- Initial guess values: Initialization of nonlinear optimization problems is a delicate issue for both SQP and Interior point methods. Bad initial values can lead to convergence failure. Different initial values for the same optimization problem can produce totally different solutions. It is necessary to understand the fundamental process principles completely to provide reasonable initial values. Simulation models should be used to provide good initial values for optimization problems.

- Model development: When we need to develop a large scale NLP problem that includes several chemical units, it is dangerous to formulate all equations from all units into one problem before testing. Even if we have a simulation model of the whole plant, it is better to build independent optimization models of different units. In order to check these independent optimization models, we can regard input variables as degrees of freedom formulated into an objective function that pushes input variables to get close to specified values provided by simulation models as much as possible. In addition, when we adopt modeling languages (e.g. AMPL and GAMS) that can provide detailed information of Jacobian and Hessian, reasonable substitution can reduce the number of intermediate variables arising from complex thermodynamic and kinetic equations. Correspondingly, the time used for evaluation of Jacobian and Hessian can decrease and the size of problem can be also reduced. Of course, such substitution also leads to a denser augmented matrix in each Newton iteration and may in-

crease the time used for solving the linear dense augmented matrix.

- Model reduction: This dissertation adopts a parallel NLP algorithm to efficiently solve several design and operating problems in the chemical engineering area. However, it does not mean that parallel NLP algorithm can solve any large scale NLP problems without any trouble. Model reduction can be considered in order to obtain further computational efficiency. In general, model reduction, used in process industry, can be classified into two main categories: mathematical and physical approaches. Mathematical approaches (e.g. Empirical Gramians and Proper orthogonal decomposition) transform original variables to new variables by projection. These models can be applied in different plants with similar fundamental mathematical principles. The large disadvantage of these mathematical methods is that the new variables do not have any physical meaning. Physical approaches depend on adding new physical assumptions in the models or replacing complex equations with simpler parameterized equations. For example, a cubic equation of state method may be replaced by much simpler relative volatility method. Physical reduction does not require additional mathematical theories so it is preferred in most practical applications. Model reduction can improve the computational efficiency of large-scale optimization problems. However, reduction level should be considered carefully in order to keep reasonable accuracy and avoid large mismatch between processes and models.

3. Parallel Computing

The purpose of parallel NLP algorithms is to solve problems that serial algorithms can not solve or to solve problems faster than serial algorithms. In this dissertation,

several case studies are studied in order to demonstrate the excellent scalability and computational efficiency of our proposed parallel NLP algorithm.

a. Scalability

In this dissertation, we have shown the scalability of our parallel algorithm on multi-core shared memory machines. On these architecture, our parallel approach can solve large problems significantly faster than the serial algorithm. However, on the shared memory architecture, we can observe a memory bottleneck as we scale to more processors. While not discussed in this dissertation, other research from our group indicates that distributed memory architecture scale much more effectively for these problems.

b. Distributed and Multi-core Architectures

There are a number of emerging architectures for parallel scientific computing:

- *Distributed Architecture:* Beowulf clusters are an example of a distributed-memory parallel processor architecture. The cluster is built by networking affordable desktop computers through standard Ethernet or specialized networking technologies. The system consists of a primary computer functioning as a master node, controlling access to the compute nodes. Each compute node has its own local RAM. Since the memory is not shared with other nodes, communication among nodes occurs over the network. This is typically done via a Message-Passing Interface (MPI) although other technologies and paradigms exist. Communication via Ethernet is the biggest cause of latency, so for a program to run efficiently, this communication and the need for synchronization must be kept to a minimum. These architectures are most appropriate

for coarse-grained problems that require limited communication, and our work has demonstrated that this architecture is highly appropriate for parallel solution of large-scale structured nonlinear programs. Grid computing represents an extreme case of a distributed memory architecture where compute nodes are typically heterogeneous and geographically distributed, with communication over the internet.

- *Multi-core Architecture:* Multi-core architectures allow for shared-memory and parallel computation within a single node. Each of the processing cores has access to the same local memory and these architectures promise significantly faster communication among processes (or threads) through local RAM. Nevertheless, in most multi-core systems access to local RAM is shared through a common memory bus, and the performance of individual processes may deteriorate as each process competes for access to the local memory it needs. Even with a sufficient number of processors, the memory bandwidth can become a bottleneck and deteriorate the expected benefits from parallel computing. In this dissertation, we also demonstrate that multi-core architectures are also appropriate for parallel solution of large-scale structured optimization problems, however, they do not scale as well as distributed architectures for the class of problems studied in Chapter III.

B. Future Work

In order to think further about our research, here, we are interested in discussing potential research work in future. The future work includes the NLP applications we focus on in this dissertation and the potential development of parallel NLP algorithms.

1. NLP Application

Challenging industrial applications like cryogenic air separation columns, internal heat-integrated distillation columns, and city-wide water networks still motivate further development in terms of process and algorithm.

a. Integration of IPOPT with Other Software

All the problems in this dissertation are formulated by using AMPL Modeling language which can effectively provide good information of Jacobian and Hessian. However, it also limits the application of our parallel NLP algorithm because of modeling limitation in AMPL. For example, AMPL does not have constructs for representing differential equations and all discretization must be done manually.

Here, we give a potential platform called JModelica which can found in http://jmodelica.org. This platform supports IPOPT by using CppAD to provide Jacobian information and the BFGS method to approximate the Hessian information. The big advantage of using JModelica is that it allows users develop their simulation models in the Modelica language [116] and convert their simulation into an optimization formulation.

Also, the Python based modeling language PYOMO shows significant promise. Since it is based on a complete object-oriented scripting language, it allows for advanced modeling and the development of additional package for high-level modeling constructs.

b. Air Separation Units

Cryogenic air separation units are studied widely in this dissertation which includes design under uncertainty, planning and operation under uncertain product demands

and varying power pricing, as well as dynamic optimization. However, there are still possible improvements and future developments:

- **Integration of RTO and MPC**. Dynamic optimization under uncertainty is investigated in Chapter VI. However, this does not optimize the economic performance directly because the set-point trajectory is not given by the RTO layer. In Figure 1, design and long-term planning are always done off-line while both RTO and MPC should be calculated on-line with high frequency. Future work should integrate these two with rigorous models while focusing on efficiency and reliability.

- **Development of suitable thermodynamic dynamic models**. The dynamic model used in this dissertation depends on an activity coefficient approach to describe the Gas-Liquid equilibrium. However, it is still very difficult to solve. Model reduction is expected to contribute better computational efficiency. The wave model is built by Bian et. al. [83] however this method is more suitable for a binary-component system, while air separation columns have a triple-component system. Compartmental modeling is also studied in [117]. However, this method, which is a physical model reduction approach, aims at the special plant and it can not be used as a general approach. Therefore, mathematical model reduction methods, like Proper Orthogonal Decomposition, can be tried in order to further improve computational efficiency.

- **Network Optimization**. We have applied our block-structured nonlinear algorithm to a large-scale water network problem. Gas products of air separation units are also delivered by pipelines in large scale networks. Such networks include not only one single air separation unit, but also multiple units at the different nodes in order to satisfy different customers' demands. Therefore, one

candidate research topic is to focus on large scale gas networks under uncertain factors such as uncertain demand and time delay. Another choice is dynamic optimization and simulation for pipeline network under uncertain output pressure and demand. Research will include the development of effective techniques to determine appropriate sub-systems from the whole network.

2. Parallel Computing Development

Here, we focus on introducing some potential architectures for further development of parallel scientific computing algorithms:

- GPU Architecture: Graphics Processing Units (GPUs) are another type of multi-core processor that has recently emerged within the scientific computing community. GPUs typically contain several hundred basic processing cores, however, these cores are not general purpose CPU cores. Therefore, while these systems may give access to many hundreds of cores at an affordable price, these cores are limited in their capability. For example, the general GPU architecture is modeled after the NVidia Tesla GPU units for scientific computing. Here, each GPU device contains a number of multiprocessors, each with a number of single-instruction-multiple-data (SIMD) stream processors. These architectures have complicated memory structures that must be considered. The different types of memory in a GPU can be grouped into categories based on their scope. Registers serve individual processors; shared memory, constant cache, and texture cache serve multiprocessors; global device memory serves all cores [118]. While this memory hierarchy allows for very low latency at the processor level, access to global device memory has high latency. Thus, the problem must be highly parallel so that the program can break it into enough threads to keep the

individual processors busy [119]. In spite of these and other drawbacks, there is significant potential for these architectures in certain scientific computing tasks and examples of their success are numerous. Current efforts indicate significant potential for efficient parallel solution of linear systems. With regards to parallel nonlinear optimization, this provides a promising avenue for immediate use of these architectures since most NLP algorithms require the solution of a large linear system at each iteration.

- CELL Architecture: The Cell (Cell Broadband Engine Architecture) is similar to the architecture of the GPU systems in that there are a number of non-general purpose processing cores that have shared access to various levels of memory. The Cell processor contains eight Synergistic Processing Elements (SPEs). Each SPE contains a Synergistic Processing Unit (SPU) that operates using an SIMD architecture. Processors are mated closely to their own independent memory allowing for very low latencies between the processor and memory. However, this is a distributed memory system [120]. The Cell system has gained popularity, as it is available rather inexpensively and fully supports the Linux operating system. As with the GPU architectures, there have been significant efforts towards efficient parallel solution of linear systems on the Cell processor [120], and the use of parallel linear solvers provides potential for parallel nonlinear optimization.

- Cray XMT Architecture: The Cray XMT system is designed to give a relatively inexpensive, scalable multithreading, shared-memory supercomputing platform. It is built with up to 96 processors per cabinet. Each processor accommodates 128 fine-grained hardware streams and is associated with its own memory system. Since these memory systems are linked together the system can function

as a shared-memory computer. The latency associated with shared-memory systems is masked in this supercomputer through multithreading. Multiple threads give processing efficiency by skipping threads that are waiting for data from memory and running threads that have data available This is ideal for data-intensive applications requiring irregular memory access.

In addition, while our proposed schur-complement parallel NLP algorithm has already solved several large scale nonlinear optimization problems with high computational efficiency, one potential limitation of this parallel NLP algorithm is that the number of backsolves increases linearly with the number of coupling (common) variables. In order to further improve computational performance of our algorithm, a new approach including PCG and BFGS can be taken into account.

Instead of explicitly forming the Schur-Complement which is used in this dissertation, PCG solver is used to solve Equ. (2.37) according to $Ax = b$ form. The inverse of the schur-complement, $\left[\delta_1 I - \sum_{q \in Q} A_q^T K_q^{-1} A_q\right]^{-1}$, can be approximated by using a BFGS update to provide the preconditioner. This method requires only one backsolve of K_q for each PCG iteration.

REFERENCES

[1] R. Smith, *Chemical Process Design and Integration*, London: John Wiley & Sons, Ltd, 2^{nd} ed., 2005.

[2] S. Engell, "Feedback control for optimal process operation," *Journal of Process Control*, vol. 17, pp. 203–219, 2007.

[3] D. M. Prett, B. L. Ramaker, and C. R. Cutler, *Dynamic Matrix Control Method*, Houston, United States Patent, Sept. 1982.

[4] S. J. Qin, and T. A. Badgwell, "A survey of industrial model predictive control technology," *Control Engineering Practice*, vol. 11, pp. 733–764, 2003.

[5] J. Van Dan Berg, "Model reduction for dynamic real-time optimization of chemical processes, " Ph.D dissertation, Technische Universiteit Delft, Rotterdam, The Netherlands, 2005.

[6] I. E. Grossmann, "Challenges in the new millennium: Product discovery and design, enterprise and supply chain optimization, global life cycle assessment," *Computers and Chemical Engineering*, vol. 29, pp. 29–39, 2005.

[7] R. B. Wilson, "A simplicial method for convex programming," Ph.D dissertation, Harvard University, Cambridge, MA, 1963.

[8] M. C. Biggs, "Constrained minimization using recursive equality quadratic programming," in *Numerical Methods for Nonlinear Optimization,* F. A. Lootsma, ed., Academic Press, New York: pp. 411–428, 1972.

[9] S. P. Han, "Super linearly convergent variable metric algorithms for general nonlinear programming problems," *Math. Program.*, vol. 11, pp. 263–282, 1976.

[10] M. J. D. Powell, "A Fast Algorithm for Nonlinearly Constrained Optimization Calculations," Technical Report NA 77, Department of Applied Mathematics and Theoretical Physics, University of Cambridge, England, 1977.

[11] P. E. Gill, W. Murray, and M. A. Saunders, "SNOPT: An SQP algorithm for large-scale constrained optimization," *SIAM Journal of Optimization*, vol. 12, pp. 979–1006, 2002.

[12] R. Fletcher and S. Leyffer, "User Manual for filterSQP," Numerical Analysis Report NA 181, Department of Mathematics, University of Dundee, Dundee, April 1998.

[13] K. Schittkowski, "NLPQL: A Fortran subroutine for solving constrained nonlinear programming problems, " *Ann. Op er. Res.,* vol. 11, pp. 485–500, 1986.

[14] P. E. Gill, W. Murray, M. A. Saunders, and M. H. Wright, "Users Guide for NPSOL (Version 4.0): A Fortran Package for Nonlinear Programming, " Report 86-2, Department of Operations Research, Stanford University, Stanford, CA, 1986.

[15] P. Spellucci, An SQP method for general nonlinear programs using only equality constrained subproblems, *Math. Program.,* vol. 82, pp. 413–448, 1998.

[16] A. V. Fiacco and G. P. McCormick, *Nonlinear Programming: Sequential Unconstrained Minimization Techniques*, New York, John Wiley, 1968. Reprinted by SIAM Publications, 1990.

[17] R. H. Byrd, M.E. Hribar, and J. Nocedal, J., "An interior point algorithm for large-scale nonlinear programming," *SIAM Journal of Optimization*, vol. 9, pp. 877–900, 1999.

[18] S. A. El-Bakry, and A. R. Tapia, "On the formulation and theory of the newton interior-point method for nonlinear programming," *Journal of Optimization Theory Application*, vol. 89, pp. 507–541, 1996.

[19] R. J. Vanderbei, and D. F. Shanno, "An interior point method for nonconvex nonlinear programming," *Comput. Optim. Appl*, vol. 13, pp. 232, 1999.

[20] A. Wächter, and L. T. Biegler, "On the implementation of an interior-point filter line-search algorithm for large-scale nonlinear programming," *Mathematical Programming,* vol. 106, pp. 25–57, 2006.

[21] R. A. Waltz, J. L. Morales, J. Nocedal, and D. Orban, "An interior algorithm for nonlinear optimization that combines line search and trust region steps," *Mathematical Programming*, vol. 107, pp. 391–408, 2006.

[22] R. H. Byrd, J. Gilbert, and J. Nocedal, "A trust region method based on interior point techniques for nonlinear programming," *Mathematical Programming*, vol. 89, pp. 149–185, 2000.

[23] J. Nocedal, and S. J. Wright, *Numerical Optimization*, New York: Springer Verlag New York Inc, 2^{nd} ed., 2006.

[24] O. Schenk, M. Manguoglu, A. Sameh, M. Christen, and M. Sathe, "Parallel scalable PDE-constrained optimization: Antenna identification in hyperthermia cancer treatment planning," *Computer Science - Research and Development*, vol. 23, pp. 177–183, 2009.

[25] J.A. Vegeais, and M.A. Stadtherr, "Vector processing strategies for chemical process flowsheeting," *AICHE Journal*, vol. 36, pp. 1687–1696, 1990.

[26] J.U. Mallya, S. E. Zitney, S. Choudhary, and M. A. Stadtherr, "A parallel block frontal solver for large scale process simulation: Reordering effects," *Computers and Chemical Engineering*, vol. 21, pp. 439–444, 1997.

[27] J. U. Mallya, S. E. Zitney, S. Choudhary, and M. A. Stadtherr, "Matrix reordering effects on a parallel frontal solver for large scale process simulation," *Computers and Chemical Engineering*, vol. 23, pp. 585–593, 1999.

[28] J.R. Paloshi, "Testing a new parallel preconditioner on linear systems arising from flowsheeting simulation," *Computers and Chemical Engineering*, vol. 21, pp. 433–438, 1997.

[29] J.R. Paloshi, "Steps towards steady-state process simulation on mimd machines: Implementation in the speedup simulator," *Computers and Chemical Engineering*, vol. 22, pp. 745–755, 1998.

[30] J. Borchardt, "Newton-type decomposition methods in large-scale dynamic process simulation," *Computers and Chemical Engineering*, vol. 25, pp. 951–961, 2001.

[31] F. A. Lootsma, and K. M. Ragsdell, "State-of-the-art in parallel nonlinear optimization," *Parallel Computing*, vol. 6, no. 2, pp. 133–155, 1988.

[32] A. Migdalas, G. Toraldo, and V. Kumar, "Nonlinear optimization and parallel computing," *Parallel Computing*, vol. 29, no. 4, pp. 375–391, 2003.

[33] P.K.H. Phua, W. Fan, and Y. Zeng, "Parallel algorithms for large-scale nonlinear optimization," *International Transactions in Operational Research*, vol. 5, no. 1, pp. 67–77, 1998.

[34] R.B. Schnabel, "A view of the limitations, opportunities, and challenges in parallel nonlinear optimization," *Parallel Computing*, vol. 21, no. 6, pp. 875–905, 1995.

[35] Y. Censor, and S. A. Zenios, *Parallel Optimization: Theory, Algorithm, and Applications*, New York: Oxford University Press, Inc. 1997.

[36] C. Zhong, and F. Pusheng, "A parallel algorithm for constrained optimization problems," *Journal of Computational and Applied Mathematics*, vol. 61, no. 2, pp. 225–230, 1995.

[37] L.T. Biegler, and I. Tjoa, "A parallel implementation for parameter estimation with implicit models," *Annals of Operations Research*, vol. 42, pp. 1–23, 1993.

[38] L. Jiang, L. T. Biegler, and V. G. Fox, "Design and optimization of pressure swing adsorption systems with parallel implementation," *Computers and Chemical Engineering*, vol. 29, pp. 393–399, 2005.

[39] V. M. Zavala, C. D. Laird, and L. T. Biegler, "Interior-point decomposition approaches for parallel solution of large-scale nonlinear parameter estimation problems," *Chemical Engineering Science*, vol. 63, no. 19, pp. 4834–4845, 2008.

[40] J. Gondzio, and A. Grothey, "Exploiting structure in parallel implementation of interior point methods for optimization," technical report MS-04-004, School of Mathematics, The University of Edinburgh, Edinburgh, Scotland, July 2005.

[41] J. F. Benders, "Partitioning procedures for solving mixed-variables programming problems," *Numerische Mathematik*, vol. 4, pp. 238–252, 1962.

[42] A. M. Geoffrion, "Generalized benders decomposition," *Journal of Optimization Theory and Applications*, vol. 10, no. 4, pp. 237–260, 1972.

[43] A. M. Geoffrion, "Duality in nonlinear programming: A simplified applications-oriented development," *SIAM Review*, vol. 13, no. 1, pp. 1–37, 1971.

[44] A.J. Conejo, F. J. Nogales, and F.J. Prieto, " A decomposition procedure based on approximate Newton directions," *Mathematical Programming*, vol. 93, no. 3, pp. 495–515, 2002.

[45] P. R. Amestoy, I. S. Duff, J. -Y. L'Excellent, and J. Koster, "A fully asynchronous multifrontal solver using distributed dynamic scheduling," *SIAM J. Matrix Anal. Appl.*, vol. 23, no. 1, pp. 15–41, 2001.

[46] O. Schenk, O. A. Wächter, and M. Hagemann, "Matching-based preprocessing algorithms to the solution of saddle-point problems in large-scale nonconvex interior-point optimization," *Journal of Computational Optimization and Applications*, vol. 36, pp. 321–341, 2007.

[47] A. Gupta, "Recent advances in direct methods for solving unsymmetric sparse systems of linear equations," *ACM Transactions on Mathematical Software*, vol. 28, no. 3, pp. 301–324, 2002.

[48] E. Polizzi, and A. H. Sameh, "A parallel hybrid banded system solver: The spike algorithm," *Parallel Computing*, vol. 32, no. 2, pp. 177–194, 2006.

[49] I. E. Grossmann, and R. Sargent, "Optimum design of chemical plants with uncertain parameters," *AICHE Journal*, vol. 24, pp. 1021–1028, 1978.

[50] K. Halemane, and I. E. Grossmann, "Optimal process design under uncertainty," *AICHE Journal*, vol. 29, pp. 425–433, 1983.

[51] I.E. Grossmann, and Guillén-Gosálbez, "Scope for the application of mathematical programming techniques in the synthesis and planning of sustainable pro-

cesses," *in Proc. of 7th International Conference on Foundations of Computer-Aided Process Design, FOCAPD 2009*, Breckenridge, June, 2009, pp. 55–73.

[52] J. R. Birge, and F. Louveaux, *Introduction to Stochastic Programming*, New York: Springer Verlag New York Inc, 2000.

[53] G. Paules, and C. Floudas, "Stochastic programming in process synthesis: A two stage model with MINLP recourse for multiperiod heat-integrated distillation sequences," *Computers and Chemical Engineering*, vol. 16, pp. 189, 1992.

[54] E. Pistikopoulos, and I. Grossmann, "Optimal retrofit design for improving process flexibility in linear systems," Computers and Chemical Engineering, vol. 12, pp. 719, 1988.

[55] E. Pistikopoulos, and I. Grossmann, "Stochastic optimization of flexibility in retrofit design of linear systems," *Computers and Chemical Engineering*, vol. 12, pp. 1215, 1988.

[56] E. Pistikopoulos, and M. Ierapetritou, "Novel approach for optimal process design under uncertainty," *Computers and Chemical Engineering*, vol. 19, pp. 1089, 1995.

[57] C. Raspanti, J. Bandoni, and L. T. Bielger, "New strategies for flexibility analysis and design under uncertainty," *Computers and Chemical Engineering*, vol. 24, pp. 2193, 2000.

[58] W. Rooney, and L. T. Biegler, "Incorporating joint confidence regions in to design under uncertainty," *Computers and Chemical Engineering*, vol. 23, pp. 1563.

[59] W. Rooney, and L. T. Biegler, "Design for model parameter uncertainty using nonlinear confidence regions ," *AICHE Journal*, vol. 47, pp. 1794-1804, 2001.

[60] W. Rooney, and L. T. Biegler, "Optimal process design with model parameter uncertainty and process variability," *AICHE Journal*, vol. 49, pp. 438, 2003.

[61] D. Varvarezos, L. Biegler, and I. Grossmann, "Multiperiod design optimization with SQP decomposition," *Computers and Chemical Engineering*, vol. 18, pp. 579, 1994.

[62] L. Biegler, I. Grossmann, and A. Westerberg, *Systematic methods of chemical process design*, New Jersey: Prentice Hall, 1997.

[63] E. Pistikopoulos, "Uncertainty in process under uncertainty," *Computers and Chemical Engineering*, vol. 19, pp. 553, 1995.

[64] N. Sahinidis, "Optimization under uncertainty: State-of-the-art and opportunities," *Computers and Chemical Engineering*, vol. 28, pp. 971, 2004.

[65] J. Luedtke, and S. Ahmed, S. "A sample approximation approach for optimization with probabilistic constraints," *SIAM Journal on Optimization*, vol. 19, no. 2, pp. 674–699, 2008.

[66] A. Nemirovski, and A. Shapiro, "Scenario approximations of chance constraints," *Probabilistic and Randomized Methods for Design Under Uncertainty*, pp. 3–47, 2006.

[67] Y. Zhu, S. Legg, and C.D. Laird, "Optimal design of cryogenic air separation columns under uncertainty," *Computers and Chemical Engineering*, vol. 34, no. 9, pp. 1377–1384, 2010.

[68] W. Castle, "Air separation and liquefaction: Recent developments and prospects for the beginning of the new millennium," *International Journal of Refrigeration*, vol. 25, pp. 158–172, 2002.

[69] C. E. Baukal, *Oxygen-enhanced combustion*' New York: CRC Press, 1998.

[70] S. Bian, M. Henson, P. Belanger, and L. Megan, "Nonlinear state estimation and model predictive control of nitrogen purification columns," *Industrial and Engineering Chemistry Research*, vol. 44, pp. 153–167, 2005.

[71] M.H. Karwan, M. Keblis, "Operations planning with real time pricing of a primary input," *Computers and Operation Research*, vol. 34, pp. 848–867, 2007.

[72] Energy information association. Manufacturing energy consumption survey, 2002, http://www.eia.doe.gov/emeu/mecs/mecs2002/data02/shelltables.html

[73] R. Agrawal, and T. Yee, "Heat pumps for thermally linked distillation columns: An exercise for argon production from air," *Industrial Engineering Chemistry Research*, vol. 33, pp. 2717, 1994.

[74] R. Agrawal, R. Woodward, K. Ludwig, and D. Bennett, "Impact of low pressure drop structure packing on air distillation," *IChemE Symposium Series*, vol. 128, pp. A125, 1993.

[75] R. Agrawal, "Production of ultrahigh-purity oxygen: A distillation method for the coproduction of the heavy key component stream free of heavier impurities," *Industrial Engineering Chemistry Research*, vol. 34, pp. 3947, 1995.

[76] R. Agrawal, "Synthesis of distillation column configurations for a multicomponent separation," *Industrial Engineering Chemistry Research*, vol. 35, pp. 1059, 1996.

[77] N. Egoshi, H. Kawakami, and K. Asano, K. "Heat and mass transfer model approach to optimum design of cryogenic air separation plant by packed columns

with structured packing," *Separation and Purification Technology*, vol. 29, pp. 141, 2002.

[78] V. White, J. Perkins, and D. Espie, "Switchability analysis," *Computers and Chemical Engineering*, vol. 20, no. 4, pp. 469–474, 1996.

[79] G. Zhu, M. A. Henson, and L. Megan, "Low-order dynamic modeling of cryogenic distillation columns based on nonlinear wave phenomenon," *Separation and Purification Technology*, vol. 24, pp. 467–487, 2001.

[80] B. Roffel, B. H. L. Betlem, and J. Ruijter, "First principles dynamic modeling and multivariable control of a cryogenic distillation process," *Computers and Chemical Engineering*, vol. 24, pp. 111–123, 2000.

[81] J. Trierweiler, and S. Engell, "A case study for control structure selection: Air separation plant," *Journal of Process Control*, vol. 10, pp. 237–243, 2000.

[82] B. Seliger, R. Hanke, F. Hannemann, and K. Sundmacher, "Modelling and dynamics of an air separation rectification column as part of an IGCC power plant," *Separation and Purification Technology*, vol. 49, pp. 136–148, 2006.

[83] S. Bian, M. A. Henson, P. Belanger, and L. Megan, "Nonlinear state estimation and model predictive control of nitrogen purification columns," *Industrial and Engineering Chemistry Research*, vol. 44, pp. 153–167, 2005.

[84] R. Huang, V. Zavala, and L. T. Biegler, "Advanced step nonlinear model predictive control for air separation units," *Journal of Process Control*, vol. 9, pp. 678–685, 2009.

[85] Y. Zhu, and C. Laird, "A parallel algorithm for structured nonlinear programming," in *Proc. of 5th International Conference on Foundations of Computer-*

Aided Process Operation, FOCAPO 2008, Cambridge, Massachusetts, July, 2008, pp. 345–348.

[86] B. Daryanian, R. E. Boln, and R. D. Tabors, "Optimal demand-side response to electricity spot prices for storage-type customers," *IEEE Transactions on Power Systems*, vol. 4, pp. 897–903, 1989.

[87] M. G. Ierapetritou, D. Wu, J. Vin, P. Sweeney, and M. Chigirinskiy, "Cost minimization in an energy-intensive plant using mathematical programming approaches," *Industrial and Engineering Chemistry Research*, vol. 41, pp. 5262–5277, 2002.

[88] A. R. Sirdeshpande, and M. G. Ierapetritou, "Process synthesis optimization and flexibility evaluation of air separation cycles," *AICHE Journal*, vol. 51, pp. 1190–1200, 2005.

[89] J. Miller, W. Luyben, and S. Blouin, "Economic incentive for intermittent operation of air separation plants with variable power costs," *Industrial and Engineering Chemistry Research*, vol. 47, pp. 1132–1139, 2008.

[90] A. Harmens, "Vapour–liquid equilibrium N2–Ar–O2 for lower argon concentrations," *Cryogenics*, vol. 6, pp. 406, 1970.

[91] J. Douglas, *Conceptual Design of Chemical Processes*, New York: McGraw-Hill, 1988.

[92] M. Peters, K. Timmerhaus, R. West, *Plant Design and Economics for Chemical Engineers*. New York: McGraw-Hill, 2002.

[93] C. D. Laird, and L. T. Biegler, "Large-scale nonlinear programming for multi-scenario optimization," in *Proc. of the International Conference on High Perfor-*

mance Computing, Hanoi, Vietnam, 2006, pp. 323–336.

[94] X. Liu, and J. Qian, "Modeling, control and optimization of ideal internal thermally coupled distillation columns," *Chem. Eng. Technol*, vol. 23, no. 3, pp. 235–241, 2000.

[95] Z. Olujic, F. Fkhnri, A. Rijke, J. Graauw, and P. Jansens, "Internal heat integration-the key to energy-conserving distillation column," *J. Chem. Technol. Biotechnol*, vol. 78, pp. 241–248, 2003.

[96] M. Nakaiwa, K. Huang, A. Endo, T. Ohmori, T. Akiya, and T. Takamatsu, "Internally heat-integrated distillation columns: A review," *Trans. Inst. Chem. Eng.*, vol. 81, pp. 162–176, 2003.

[97] K. Huang, L. Shan, Q. Zhu, and J. Qian, "Design and control of an ideal heat-integrated distillation column(ideal HIDiC) system separating a close-boiling ternary mixture," *Energy*, vol. 32, pp. 2148–2156, 2007.

[98] A.K. Jana, "Heat integrated distillation operation," *Applied Energy*, vol. 87, pp. 1477–1494, 2010.

[99] Z. Olujic, L. Sun, A. Rijke, and P. J. Jansens, "Conceptual design of an internally heat integrated propylene-propane splitter," *Energy*, vol. 31, pp. 3083, 2006.

[100] Y. Zhu, and X. Liu, "Dynamics and control of high purity heat integrated distillation columns," *Industrial and Engineering Chemistry Research*, vol. 44, no. 23, pp. 8806–8814, 2005.

[101] Y. Zhu, and X. Liu, "Investigating control schemes for an ideal thermally coupled distillation column (ITCDIC)," *Chemical Engineering and Technology*, vol. 28, no. 9, pp. 1048–1055, 2005.

[102] V. Zavala, and L. Biegler, "The advanced step NMPC controller: Optimality, stability and robustness," *Automatica*, vol. 45, no. 1, pp. 86–93, 2009.

[103] W. Li, C. Hui, P. Li, and A. Li, "Refinery planning under uncertainty," *Industrial and Engineering Chemistry Research*, vol. 43, pp. 6742–6755, 2004.

[104] S. Nahmias, *Production and Operation Analysis*, Singapore: McGraw-Hill Press, 5^{th} ed., 2005.

[105] P. Li, H. G. Arellano, and G. Wonzy, "Chance constrained programming approach to process optimization under uncertainty," *Computers and Chemical Engineering*, vol. 32, pp. 25–45, 2008.

[106] M. Wendt, P. Li, and G. Wonzy, "Nonlinear chance-constrained process optimization under uncertainty," *Industrial and Engineering Chemistry Research*, vol. 41, pp. 3621–3629, 2002.

[107] L.J. Salerno, J. Gaby, R. Johnson, P. Kittel, and E. D. Marqurdt, "Terrestrial applications of zero-boil-off cryogen Storage," *Cryocoolers*, edited by R. G. Ross, Jr. vol. 11, pp. 809–816, 2000.

[108] F. G. Kerry, *Industrial gas handbook: Gas separation and purification*, New York: Taylor & Francis Press, 2006.

[109] F. P. Bernardo, and P. Saraiva, "Robust optimization framework for process parameter and tolerance Design," *AICHE, J.*, vol. 44, no. 9, pp. 2007–2017, 1998.

[110] F. P. Bernardo, E. N. Pistikopoulos, and P. Saraiva, "Robustness criteria in process design optimization under uncertainty," *Computers and Chemical Engineering*, vol. 23, no. 1, pp.S459–S462, 1999.

[111] M. C. Gerogiadis, and E.N. Pistikopoulos, "An integrated framework for robust and flexible process systems," *Industrial and Engineering Chemistry Research*, vol. 38, pp. 133–143, 1999.

[112] M. L. Liu, and N. V. Sahinidis, "Optimization in process planning under uncertainty," *Industrial and Engineering Chemistry Research*, vol. 35, pp. 4154–4165, 1996.

[113] P. Li, M. Wendt, and G. Wozny, "Optimal operations planning under uncertainty by using probabilistic programming," *in Proc. of FOCAPO Conference*, Coral Springs, FL, Jan. 2003, pp. 289–292.

[114] R. Fourer, D. M. Gay, and B. W. Kernighan, *AMPL: A Modeling Language for Mathematical Programming*. Belmont, CA: Duxbury Press, 1992.

[115] L. A. Rossman, *EPANET 2 Users Manual*. Cincinnati, Ohio, US Environmental Protection Agency, 2000.

[116] M. Tiller, *Introduction to Physical Modeling with Modelica*, London: Kluwer Academic Publishers, 2001.

[117] S. Bian, S. Khowinij, M. A. Henson, P. Belanger and L. Megan, "Compartmental modeling of high purity air separation columns," *Computers and Chemical Engineering*, vol. 29, pp. 2096–2109, 2005.

[118] A. Richardson, and A. Gray, "Utilisation of the GPU architecture for HPC," *HPCx Consortium*, 2008.

[119] M. Wolfe, " Compilers and more: GPU architecture and applications," HPCwire, September, pp. 1–3, 2008.

[120] J. Kurak, A. Buttari, P. Luszczek, and J. Dongarra, "The playStation 3 for high-performance scientific computing," *Computing in Science & Engineering*, vol. 10, no. 3, pp. 84–87, 2008.

VITA

Yu Zhu received his B.S. degree and M.S. degree in control science and engineering from Zhejiang University, China, in 2003 and 2006 respectively. Since the fall of 2006, he has been working with Dr. Carl Laird towards his Doctoral degree in chemical engineering and a M.Eng degree in industrial engineering at the Texas A&M University. During his Ph.D. education, he served as a committee member for Graduate Student Council in the Artie McFerrin Department of chemical engineering at Texas A&M University.

From September 2010 to November 2010, he worked for Modelon AB in Lund, Sweden as a research intern. At the summer of 2010, he had the opportunity to work for Bayer AG, in Baytown, USA as an intern in the Process Dynamics and Optimization Group. During the summer of 2009, he was a research intern in the Core Process Control Department of ExxonMobil Chemicals in Baytown, USA.

His dissertation title was " Efficient Nonlinear Optimization with Rigorous Models for Large Scale Industrial Chemical Processes" including nonlinear modeling, optimal design, and operations under uncertainty. His work on parallel computing received a best poster award in PSE′09 (Brazil). He defended his dissertation on December 2010. He obtained his Ph.D. in chemical engineering in May 2011 and his M.Eng in industrial engineering in May 2010, respectively.

Address: Artie McFerrin Department of Chemical Engineering, c/o Dr. Carl Laird, TAMU 3122, College Station, TX 77843.

The typist for this dissertation was Yu Zhu.